

ITP-SB-96-4
January, 1996
hep-ph/9606312

PARTONS, FACTORIZATION AND RESUMMATION TASI 95 ¹

GEORGE STERMAN

Institute for Theoretical Physics
State University of New York at Stony Brook
Stony Brook, NY 11794-3840, USA

Abstract

I review the treatment of high-energy QCD in Minkowski space, with an emphasis on factorization theorems as extensions of the operator product expansion. I discuss how the factorization properties of high-energy cross sections and amplitudes lead to evolution equations that resum large logarithms for two-scale problems.

¹Based on seven lectures at the Theoretical Advanced Study Institute, *QCD and Beyond*, Boulder, Colorado, June 1995.

Contents

1	Introduction: Fundamental Issues and Problems	3
1.1	A Prehistory of QCD	4
1.2	Deeply inelastic scattering and the parton model	6
1.3	QCD, asymptotic freedom and the running mass	11
1.4	Wick rotation	13
1.5	Infrared safety	16
1.6	QCD in the n plane	17
2	Long and Short Distances in Minkowski Space	18
2.1	Example: IR and CO divergences in the massless vertex function	18
2.2	Analytic structure and IR divergences: Landau equations and physical pictures .	20
2.3	Power counting and pinch surfaces	23
2.4	Pinch surfaces for the all-order EM form factor	25
3	Short Distance Cross Sections and Unitarity	28
3.1	Cut diagrams and generalized unitarity	28
3.2	Infrared safety for inclusive annihilation and decay	29
3.3	Jet and weighted cross sections	30
4	Factorization and Evolution in DIS	33
4.1	Venturing out on the light cone	33
4.2	Gauge invariant distributions; schemes	36
4.3	One-loop distributions and coefficient functions	38
4.4	Evolution	40
4.5	The light-cone expansion	42
4.6	Hard hadron-hadron scattering	44
4.7	Jet-soft analysis	46

5 Two-scale problems I: Sudakov resummation	50
5.1 Sudakov double logarithms	51
5.2 Factorization for $T \rightarrow 1$	51
5.3 Resummation for $T \rightarrow 1$	53
5.4 k_T -factorization for the Drell-Yan cross section	56
6 Two-Scale Problems II: Small x and the BFKL equation	58
6.1 $x \rightarrow 0$ for DGLAP evolution	58
6.2 k_T -factorization for DIS; the BFKL equation	59
6.3 Solution of the BFKL equation	63
7 High Orders in Perturbation Theory	66

1 Introduction: Fundamental Issues and Problems

Many of the fundamental properties of field theory, such as the operator product expansion, are best developed in Euclidean space. The very nature of space-time, however, dictates that an understanding of field theory directly in Minkowski space is also indispensable. I hope these lectures will arm the reader with general insights into how perturbative quantum chromodynamics (QCD) manifests itself at high energy in Minkowski space. I will discuss the calculational challenges that result from singularities on the light cone, and develop some of the methods that we currently possess to deal with them.

The unifying thread that runs through these lectures is factorization [1], the systematic separation of dynamics associated with short and long distance scales [2, 3]. This is a recurring theme in modern theoretical physics, which can also be found as a central idea, sometimes under the names effective actions or field theories, in other lecture series in this school. One aim of these lectures is to identify quantities in QCD that are genuinely short-distance dominated, which will lead us to the concept of infrared safety, and the ubiquity of jet cross sections [4]. Another is to show how one of the great phenomenological successes of high energy physics, the parton model [5, 6], emerges as a consequence of the factorization properties of QCD in Minkowski space, which lead as well to its systematic improvement, including evolution [7].

Resummation refers below to the summation of enhancements (usually logarithmic) in ratios of kinematic variables, such as energy and momentum transfer, to all orders in field-theoretic perturbation theory. Rather than try to review all recent progress in this large and growing field, I will emphasize two representative and classic examples, Sudakov [8] resummation in e^+e^- annihilation and BFKL [9] resummation in deeply inelastic scattering, stressing

how they may be regarded as consequences of the underlying factorization properties of field theory.

These lectures are concerned primarily with the theoretical foundation of perturbative QCD. Of necessity, much introductory material involves quite general properties of quantum field theory. Much of this material may be found in field theory textbooks [10, 11], as well as in the books by Yndur  in and Muta on QCD [12], although some developments are given below which may be less widely familiar [11, 13]. In particular, I have tried to outline a general analysis of long-distance behavior in perturbation theory, based upon the analytic structure of Feynman diagrams [14] and on an infrared power-counting procedure. The reader will find many points of contact, but many differences in emphasis, with my TASI 91 lectures [15].

Many of the important and innovative calculational techniques and the phenomenological analyses that realize the program described here, as well as other equally important aspects of the theory, are treated in other lectures at this school. Very useful recent reviews that treat these topics in a more directly phenomenological manner include the TASI 94 lectures of Ellis [16], and a “Handbook” by the CTEQ Collaboration [17]. As a review of perturbative QCD, the collection of monographs edited by Mueller [18] is extremely helpful, and introduces and reviews subjects, particularly elastic scattering [19] and QCD coherence [20, 21], that are closely connected to the discussion in these lectures. Finally, for a theoretical introduction from a complementary point of view, see the book of Dokshitser, Khoze, Mueller and Troian [22].

So much of the terminology of QCD is intertwined with its sources in experiment and theory, that it seems appropriate to begin with a very brief review of the strong interaction physics that led to QCD. This will be followed by an introduction to deeply inelastic scattering, the pivotal experiments whose outcome made it possible to identify quantum chromodynamics as a promising theory of the strong interactions over twenty years ago. The balance of these lectures will discuss how this promise has been realized.

1.1 A Prehistory of QCD

It is plausible to identify the birth of strong interaction physics with the discovery of the neutron, which along with its beta decay, signaled the existence of two new interactions, the strong and weak. From this slender thread, physicists suspended the four-fermion theory of weak interactions, and the concepts of (strong) isospin, the S-matrix, and the Yukawa theory, in which the strong interaction is mediated by the exchange of scalar particles, now identified as pions, between nucleons. Beyond this, through the thirties and forties into the fifties, strong interaction physics remained for the most part nuclear physics, with many well-known successes and consequences [23].

With the discovery of the pion and then other mesons, around 1950, and the development of high energy accelerators, the substructure of nucleons became for the first time an object

of study. The earliest information was on the excited states of mesons and baryons, and the discovery of the Δ in pion-nucleon scattering ushered in a bewildering array of resonances. Order was imposed on this chaos through symmetry principles, leading eventually to the concept of quarks as the building blocks of hadrons; three quarks for baryons and a quark-antiquark pair for mesons. This “constituent” quark model still successfully describes most of the qualitative features of baryon spectroscopy [24, 25]. It was thus natural to try and “see” the quarks in experiments with momentum transfers large enough to resolve the internal structure of the nucleon, and to explore the possibility that forces between quarks are mediated by a field, dubbed, perhaps for want of a better name, the gluon.

At this time it was by no means obvious, or universally recognized, that such a picture of strong interactions would or could succeed. Indeed, it was a widely held view that the idea of elementary particles was inappropriate for the strong interactions altogether, and that theories, particularly those involving perturbative methods, could serve only as guides to suggest the mathematical properties of the S-matrix [14].

The deeply inelastic scattering experiments, which we shall discuss shortly, changed all that. They showed unequivocally that the proton possessed charged substructure of a spatial size much smaller than the proton itself. Indeed, the experiments also suggested spin one-half for these particles. At the same time, it was recognized that the constituent-quark model seemed to require a new quantum number for the quarks, “color”. Color, although originally introduced to solve the problem of Fermi statistics for the spin-1/2 quarks, provided a natural set of currents to which the gluons might couple. A three-color model of quarks has a global $SU(3)$ symmetry, with currents reflecting its group structure. This suggested a local nonabelian gauge theory of the type originally introduced by Yang and Mills many years before [26].

In a relatively few months [27] this theory was recognized to possess a number of important properties. At lowest order, it produces attractive forces in the three-quark and quark-antiquark systems, and repulsive forces for a quark-quark system. It automatically incorporated the well-established successes of current algebra ². Perhaps its characteristic and most crucial property, however, is *asymptotic freedom*, according to which its coupling decreases with decreases in the distance scale over which it is measured [28]. The need for asymptotic freedom was signalled by the very experiments designed to detect point-like structure in the nucleon. These are the deeply inelastic scattering (DIS) experiments, initiated at SLAC in the late sixties, to which we now turn.

²In essence, current algebra follows from the assumption that the electromagnetic and weak interactions couple to hadrons via point-like operators (the currents) which are then assumed to obey commutation relations consistent with the symmetries of these interactions (the algebra). In QCD, this algebra follows automatically by identifying the currents with operators $\bar{q}_i \gamma_\mu q_j$, with q_i quarks of differing flavors.

1.2 Deeply inelastic scattering and the parton model

In deeply inelastic (deep-inelastic) scattering, a massive hadronic state X of invariant mass $M_X^2 \gg m_N^2$ is produced by the scattering of a lepton (for instance, an electron) on a nucleon (or other hadron),

$$e(k) + N(p) \rightarrow e(k') + X_{\text{hadronic}}. \quad (1)$$

This process is illustrated in fig. 1.

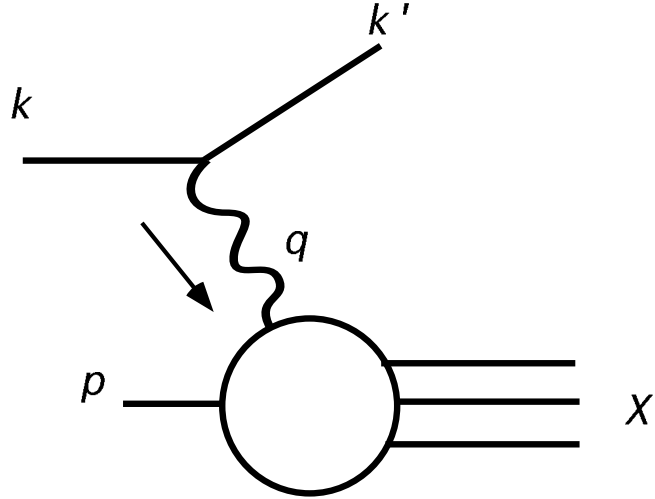


Figure 1: Deeply inelastic scattering.

Kinematics. Because the lepton interacts with the nucleon only through the exchange of a photon, W or Z , with relatively small electroweak corrections, the cross section for this process factors into leptonic and hadronic tensors,

$$d\sigma = \frac{d^3 k'}{2s|\vec{k}'|} \frac{1}{(q^2)^2} L^{\mu\nu}(k, q) W_{\mu\nu}(p, q), \quad (2)$$

where we have taken the example of photon exchange. The leptonic tensor $L^{\mu\nu}$ is known from the electroweak Lagrangian, while the hadronic tensor may be expressed in terms of matrix elements of the electroweak currents to which the vector bosons couple,

$$\begin{aligned} L^{\mu\nu} &\equiv \frac{e^2}{8\pi^2} \text{tr} [k^\mu k'^\nu] \\ W_{\mu\nu} &\equiv \frac{1}{8\pi} \sum_{\text{spins}} \sum_{\sigma} \langle N(p, \sigma) | J_\mu(0) | X \rangle \langle X | J_\nu(0) | N(p, \sigma) \rangle \\ &\quad \times (2\pi)^4 \delta^4(p_X - q - p). \end{aligned} \quad (3)$$

The expression for $L^{\mu\nu}$ is elementary, and the expression for $W_{\mu\nu}$ is quite general, depending only on the assumption that the electroweak interactions couple to the hadron via local currents³.

³This assumption, we have observed above, had considerable experimental and theoretical support by the late sixties. Nevertheless, it is itself a nontrivial assertion.

The matrix elements in $W_{\mu\nu}$ include the strong interactions only, and they hence satisfy symmetry properties of the strong interactions. For instance, both electromagnetic and strong interactions enjoy invariance under parity and time reversal. This leads to a symmetric $W_{\mu\nu}$ when the hadron is unpolarized, while time reversal invariance of the strong interactions leads to a real hadronic tensor,

$$W_{\mu\nu}^{(\text{em})} = W_{\nu\mu}^{(\text{em})} \quad (\text{spin-averaged}), \quad W_{\mu\nu} = W_{\mu\nu}^*. \quad (4)$$

Along with Lorentz invariance, and electromagnetic current conservation,

$$q^\mu W_{\mu\nu} = 0, \quad (5)$$

these constraints may easily be used to show that the sixteen components of the hadronic tensor are determined by two independent *structure functions*, W_1 and W_2 ,

$$\begin{aligned} W_{\mu\nu}^{(\text{em})} &= - \left(g_{\mu\nu} - \frac{q_\mu q_\nu}{q^2} \right) W_1(x, q^2) \\ &\quad + \left(p_\mu + q_\mu \left(\frac{1}{2x} \right) \right) \left(p_\nu + q_\nu \left(\frac{1}{2x} \right) \right) W_2(x, q^2). \end{aligned} \quad (6)$$

The W 's are functions of Q^2 and the dimensionless ratio,

$$x = -\frac{q^2}{2p \cdot q} \equiv \frac{Q^2}{2p \cdot q}. \quad (7)$$

For reasons which will become clear in a moment, it is also convenient to introduce dimensionless structure functions,

$$F_1 \equiv W_1, \quad F_2 = p \cdot q W_2. \quad (8)$$

It is worth noting that in the literature many definitions are given for the W 's (usually differing by factors of target mass), while definitions of the F 's are much more standardized.

Scaling. The striking result of the early deeply inelastic scattering experiments was that, for $Q^2 \geq 1 \text{ GeV}^2$, the structure functions $F(x, Q^2)$ become functions of x only, nearly independent of Q^2 . This property is called *scaling* [29, 30]. In its importance, it is (and should be) compared to the experiments of Rutherford and collaborators, who discovered the atomic nucleus in the wide-angle scattering of alpha particles. In deeply inelastic scattering, the wide-angle scattering of the electron serves to detect point-like structure in the nucleon through scaling. If electric charge were uniformly distributed within the nucleon, we would expect wide-angle scattering to be very rare, giving structure functions that decrease rapidly with Q^2 . To see how point charges produce scaling, we shall review the parton model.

The parton model. In the parton model [5, 6], we imagine the proton, or any other hadron, to be made of point-like constituents, the partons, through which it couples to the electroweak interactions, and eventually to the strong interactions as well. Deeply inelastic scattering will give information on the spin of these partons, which, in anticipation, we take to be one-half.

The fundamental relation of the parton model for deeply inelastic scattering may be written

$$d\sigma^{(\ell N)}(p, q) = \sum_f \int_0^1 d\xi \, d\sigma_{\text{Born}}^{(f)}(\xi p, q) \phi_{f/N}(\xi), \quad (9)$$

where $d\sigma^{(\ell N)}(p, q)$ is the *inclusive* cross section for nucleon-electron scattering, while $d\sigma_{\text{Born}}(\xi p, q)$ is the *lowest-order, elastic* parton-electron cross section, with the parton's momentum given by ξp , ξ between zero and one. The functions $\phi_{f/N}(\xi)$ are *parton distributions*, which describe the probability of finding a parton (of “flavor” f) in the “target” hadron N . There is assumed to be no interference, either between different flavors or between different fractions ξ . This “incoherence” is a hallmark of the parton model and its extension to QCD. An important consequence is that the parton distributions are universal, in the sense that, since they describe processes that do not interfere with the hard scattering, they are the same for all inclusive hard scattering processes, not only for electromagnetic DIS. The most obvious extension is to neutrino DIS, but there are many others. Eq. (9) is illustrated by fig. 2, in which the hadronic interaction of fig. 1 is broken up into a parton distribution and parton-electron scattering.

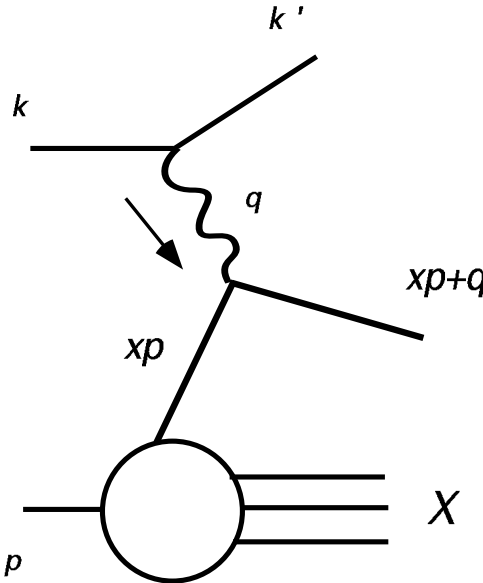


Figure 2: Deeply inelastic scattering in the parton model.

Scaling and spin in the parton model. Both the inclusive hadronic cross section and the elastic (exclusive) partonic cross section may be factored into leptonic and hadronic tensors as in eq. (2). The hadronic tensor at Born level is given explicitly by

$$W_{\mu\nu}^{(f)} = \frac{1}{8\pi} \int \frac{d^3 p'}{(2\pi)^3 2\omega_{p'}} Q_f^2 \text{tr}[\gamma_\mu p'^\nu \gamma_\nu p'] (2\pi)^4 \delta^4(p' - \xi p - q), \quad (10)$$

with Q_f the electromagnetic charge of quark flavor f . Substituting (10) into (9), and using the definitions (6) and (8), we find the following simple relations between hadronic and partonic

structure functions,

$$\begin{aligned} F_2^{(N)}(x) &= \sum_f \int_0^1 d\xi F_2^{(f)}(x/\xi) \phi_{f/N}(\xi) \\ F_1^{(N)}(x) &= \sum_f \int_0^1 \frac{d\xi}{\xi} F_1^{(f)}(x/\xi) \phi_{f/N}(\xi), \end{aligned} \quad (11)$$

from which we can read off the partonic structure functions,

$$2F_1^{(f)}(z) = F_2^{(f)}(z) = Q_f^2 \delta(1-z). \quad (12)$$

Note the minor difference in the powers of ξ in the convolutions (11), which is a reflection of the tensor structure of $W^{\mu\nu}$.

Turning again to the general relation eq. (9), we derive nucleon structure functions in the parton model

$$F_2^{(N)}(x) = \sum_f Q_f^2 x \phi_{f/N}(x) = 2x F_1^{(N)}(x). \quad (13)$$

The relation $F_2 = 2x F_1$ is a direct consequence of the spin of the partons. This result [31], known as the “Callan-Gross relation” is important evidence that the partons detected in deeply inelastic scattering are indeed the quarks of hadron spectroscopy.

A crucial feature of eq. (13) is that the structure functions F_i are independent of Q^2 . This is the *scaling* of experiment, and is a direct result of the assumed point-like nature of the partons. In summary, the parton model serves both to explain scaling and to identify partons as quarks.

Heuristic justification and requirements on a field theory. The ultimate justification of the parton model must be in quantum field theory, but many of its features can be understood on the basis of compelling heuristic arguments. Fig. 3 illustrates the time development of a deeply inelastic scattering event. Fig. 3a shows the system before the collision, as seen in the center of mass. The isolated electron approaches from the left, and from the right the nucleon, of momentum p . The nucleon is pictured as a set of partons, spread out more-or-less evenly in the transverse direction. The nucleon is highly Lorentz contracted in the longitudinal direction. We must first justify why the nucleon may be treated as a “pure” state with a definite number of partons. For this, we imagine that the wave function of these partons is formed by interactions which occur on time scales of the order of 1 GeV^{-1} . Such scales are long compared with the time it takes the electron to traverse the nucleon, and hence remain uncorrelated with hard processes that the electron may initiate in that time. During that short time, each of the partons may be thought of as possessing a definite fraction of the nucleon’s momentum, denoted ξp in the figure.

To initiate a hard scattering, the electron should pass very close to one of the partons, *i.e.* at $O(Q^{-1})$, close enough so that they may exchange a photon with an invariant mass Q^2 . Such

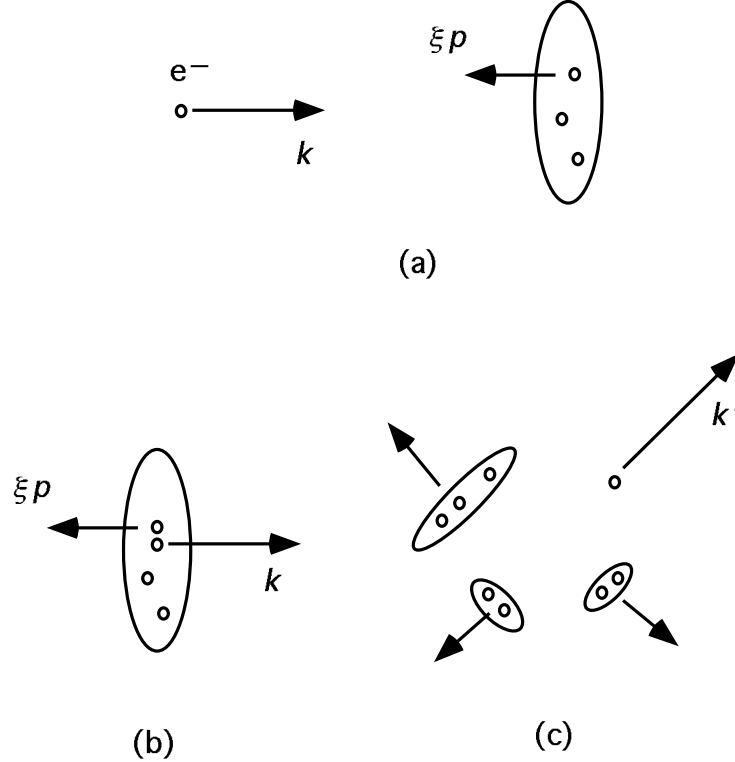


Figure 3: Heuristic picture of parton model DIS.

a collision is shown in fig. 3b. Actually, in most cases the electron will miss the highly localized partons altogether, and if it does come close to one, it is highly unlikely to hit another. Indeed, the probability for encountering n partons at a distance of Q^{-1} behaves as

$$P_{n \text{ partons}} \sim \left(\frac{1}{R_0^2 Q^2} \right)^n, \quad (14)$$

with R_0 the nucleon radius. Multi-parton events are thus power-suppressed in the parton model, a feature that will turn out to have a natural field-theoretic analog. Fig. 3c shows the results of the collision. Long-distance forces produce the observed hadrons from the fragments of the struck nucleon. These forces, however, are again on the scale of hadronic internal interactions, and hence cannot interfere with the short-distance scattering of fig. 3b. In a rough summary, deeply inelastic scattering shows incoherence because initial-state interactions (which bind the proton) are too early, and final-state interactions (which produce final-state hadrons) are too late relative to the short time scale of the hard scattering.

The above arguments rely on very general features of relativity and quantum mechanics. To justify their application within a specific quantum field theory, however, is highly nontrivial. The particular challenge concerns the separation of short and long time scales. We have assumed that at short scales the “strong” interactions, which evidently produce confinement, are weak enough to be neglected compared to the single, electroweak interaction. As we have seen in Collins’ lectures at this school, interaction strengths that change with distance scales are the

rule in quantum field theory. It is clear, however, that the successes of the parton model, and their consistency with long-distance strong interactions, requires an asymptotically free theory. Thus, we are ready to review elements of the asymptotically free theory of the strong interactions, quantum chromodynamics.

1.3 QCD, asymptotic freedom and the running mass

Quantum chromodynamics is specified by its Lagrange density, as a nonabelian $SU(3)$ gauge theory for Dirac spinors. Including gauge fixing and ghost terms the density for an $SU(N)$ theory may be written as

$$\begin{aligned}\mathcal{L} = & \sum_f \bar{q}_{f,i} (i\partial^\mu \delta_{ij} + ig A_a (T_a^{(F)})_{ij} - M_f \delta_{ij}) q_{f,j} \\ & - \frac{1}{2} \text{tr}(F_{\mu\nu} F^{\mu\nu}) - \frac{\lambda}{2} (\eta \cdot A_a)^2 \\ & + \eta_\mu \bar{c}_a (\partial^\mu \delta_{ad} - g C_{abd} A_b^\mu) c_d.\end{aligned}\quad (15)$$

Here the (Dirac spinor) quark fields are q_f of mass M_f ($f = 1, \dots, n_f$ labels flavor) with color index i , where $i = 1 \dots N$ for an $SU(N)$ theory. The gluon fields are A_a^μ , $a = 1 \dots N^2 - 1$, and ghost fields c_a (and antighost \bar{c}_a), $a = 1 \dots N^2 - 1$. The $T_a^{(F)}$ are $SU(N)$ generators in the N -dimensional defining representation. In matrix notation, the nonabelian “field strengths” $F_{\mu\nu} \equiv F_{\mu\nu,a} T_a^{(F)}$ are given by

$$F^{\mu\nu} = \partial^\mu A^\nu - \partial^\nu A^\mu + ig[A^\mu, A^\nu], \quad (16)$$

where the commutator is in terms of the color matrices. A number of useful identities and other properties of the color generators are listed in Appendix A.

In the gauge-fixing term $(\lambda/2)(\eta \cdot A)^2$, η is typically chosen as the gradient ∂ (covariant gauge) or as a fixed vector n . For the latter choice, it is sometimes convenient to distinguish the possibilities $n^2 > 0$ (temporal gauge), $n^2 < 0$ (axial) and $n^2 = 0$ (light-cone). In the limit $\lambda \rightarrow \infty$, the condition $\eta \cdot A = 0$ is enforced, and the gluon decouples from the ghost.

The diagrammatic rules for perturbation theory that follow from Eq. (15) are derived by standard techniques [10, 11, 12]. Their most characteristic feature is the self-interaction of the massless gluons and, in covariant gauges, the necessity of ghost fields.

The theory, of course, must be renormalized, and the strength of its coupling therefore depends upon (“runs with”) the momentum scale at which it is defined, according to

$$\frac{\partial}{\partial \ln \mu} g(\mu) |_{g_0} = \beta(g(\mu)), \quad (17)$$

where the bare coupling g_0 held fixed. The beta function $\beta(g)$ is determined to one loop from the coupling renormalization constant Z_g by

$$\beta(g) = -g \left(b_2 \frac{\alpha}{4\pi} + b_3 \left(\frac{\alpha}{4\pi} \right)^2 + \dots \right)$$

$$\begin{aligned}
&= \frac{\partial}{\partial \ln \mu} (Z_g^{-1} g_0) \\
&= \frac{\partial}{\partial \ln \mu} \left(g_0 - \ln(\mu^2/M^2) \left\{ \frac{g_0^3}{8\pi^2} \left[\frac{11N}{3} - \frac{2n_f}{3} \right] \right\} + \dots \right) \\
&= -\frac{g^3}{16\pi^2} \left(\frac{11}{3} N - \frac{2}{3} n_f \right), \tag{18}
\end{aligned}$$

where M^2 is an ultraviolet cutoff, and where in the final line we have used $g = g_0$ to lowest order. The solution to (17) is then the familiar

$$\begin{aligned}
g^2(\mu) &= \frac{g^2(\mu_0)}{1 + \frac{g^2(\mu_0)}{16\pi^2} b_2 \ln \frac{\mu^2}{\mu_0^2}} \\
&\equiv \frac{16\pi^2}{b_2 \ln(\mu^2/\Lambda^2)}, \tag{19}
\end{aligned}$$

with $b_2 = 11 - 2n_f/3$ for QCD and where in the second form we define

$$\Lambda = \mu_0 e^{-8\pi^2/2b_2 g^2(\mu_0)}, \tag{20}$$

independent of μ_0 . Evidently, the coupling $g(\mu)$, or equivalently “alpha-strong”,

$$\alpha_s(\mu^2) \equiv \frac{g^2(\mu)}{4\pi} = \frac{4\pi}{b_2 \ln(\mu^2/\Lambda^2)}, \tag{21}$$

decreases for large momenta, or short distances (with corrections due to higher terms in $\beta(g)$). At the same time, as the momentum scale decreases, and distances correspondingly increase, the perturbative coupling grows. This is just what we needed for the parton model. It is, however, still a long way from this observation to a phenomenology of deeply inelastic and other hard-scattering processes. Nevertheless, it is with asymptotic freedom that everything begins. Without it, there is no natural explanation in field theory of the successes of the parton model.

The last item in this synopsis of QCD and asymptotic freedom is a brief discussion of quark masses. Unlike quantum electrodynamics, where the physical mass of the electron is directly observable, the masses of the quarks must remain to a large extent theoretical constructs, which may be determined from experiment once a scheme for doing so is defined, but for which there is no unique scheme. In this sense, quark masses are much like the gauge coupling itself, and for many purposes it is useful to define a running quark mass,

$$\begin{aligned}
m(\mu^2) &= m(\mu_0^2) \exp \left\{ - \int_{\mu_0}^{\mu} \frac{d\lambda}{\lambda} [1 + \gamma_m(g(\lambda))] \right\}, \\
\frac{m(\mu^2)}{\mu^2} \mu &\xrightarrow{\rightarrow \infty} 0. \tag{22}
\end{aligned}$$

Here $\gamma_m(g)$ is a perturbative quantity, much like $\beta(g)$, which therefore vanishes as μ increases and $g(\mu)$ decreases. Thus, as indicated, the effective mass vanishes compared to the renormalization scale when that scale diverges, and the perturbative theory becomes, effectively, a massless theory.

An important point for the phenomenology of QCD [32] is that the “light” u and d quarks have masses of just a few MeV at scales of $\mu \sim 1$ GeV, so that

$$m_{u,d}(\mu) \ll \Lambda \quad (23)$$

for any scale μ , right down to μ ’s characteristic of strong coupling. For any but the longest scales, the same holds for the s quark. Thus, for these quarks, QCD is effectively a theory of massless particles at any scale where we can hope to do perturbation theory. The other three, “heavy” quarks, c, b and t have masses whose running must be taken into account. Depending on the quantity being considered, each requires special treatment, and correspondingly offers a rich variety of theoretical and experimental challenges and opportunities. For the most part here, however, we shall concentrate on QCD as a theory of massless quarks, and try to address the question of how to use its asymptotic freedom in the “real world” of Minkowski space.

1.4 Wick rotation

By itself, asymptotic freedom is a striking result, and very supportive of the partonic picture of scaling in deeply inelastic scattering. But the problem arises of how to separate short distances, represented by the Born cross section in the parton model, from long, represented by the parton distributions. How can we increase our confidence in the heuristic arguments given above? The operator product expansion is designed to organize the relationship between short distances and long, and indeed, it will play an important role in our analysis. This analysis, however, now will be somewhat more complicated, just because we want to discuss cross sections in Minkowski space, rather than Green functions in Euclidean space.

Since our aim is to use asymptotic freedom in Minkowski space, it is worthwhile to recall the method of Wick rotation, which is used to define Green functions as they approach physical regions in external momenta. This technique is a very general one, which applies to any relativistic field theory. For simplicity, consider a self-interacting scalar field. The generating functional for its Green functions may be defined in Euclidean space as the path integral

$$Z_E[J] = \int [d\phi] \exp \left[- \int d^4x \left(\frac{1}{2} \left[\sum_{i=1}^4 (\partial_i \phi)^2 + m^2 \phi^2 \right] + V(\phi) + J\phi \right) \right], \quad (24)$$

where $V(\phi)$ is a potential.

Formulating the field theory in Euclidean space has a number of advantages. The path integral rapidly damps contributions from large values of the field. Correspondingly, the perturbative Green functions found from $Z_E[J]$ are real functions, free of singularities for real external momenta. In perturbation theory, their internal propagators are of the negative definite form

$$\Delta(k) = \frac{1}{k_E^2 - m^2}, \quad k_E^2 = - \sum_{i=1}^4 k_i^2. \quad (25)$$

Such Green functions, however, cannot describe physical processes. Indeed, the S-matrix elements necessary to define cross sections are themselves found from singularities in Green functions when external momenta approach the mass shell, $p_i^2 = m^2$. Wick rotation makes the connection between these two regions. We analytically continue Z_E by replacing the real “time” component x_4 by a complex number τ in terms of two real parameters x_0 and θ as follows:

$$-ix_4 \rightarrow \tau \equiv x_\theta e^{-i\theta}. \quad (26)$$

For arbitrary values of θ we *define* a new generating functional Z_θ by replacing dx_4 by $idx_0 e^{-i\theta}$,

$$Z_\theta[J] \equiv \int [d\phi] \exp \left[-ie^{-i\theta} \int dx_\theta d^3x \left(\frac{1}{2} \left[-e^{2i\theta} \left(\frac{\partial\phi}{\partial x_\theta} \right)^2 + (\nabla\phi)^2 + m^2\phi^2 \right] + V(\phi) + J\phi \right) \right]. \quad (27)$$

Note that (26) is not a change of variables, and that Z_θ is not equal to Z_E except for $\theta = \pi/2$; rather, we regard it as an analytic continuation of Z_E in τ . We must assume that such a continuation is possible for the full generating functional, as turns out to be the case for its perturbative expansion, for which the propagator is given at arbitrary θ by

$$\Delta(k, \theta) = \frac{e^{-i\theta}}{-k_\theta^2 e^{-2i\theta} - \sum_{i=1}^3 k_i^2 - m^2}. \quad (28)$$

This expression has no singularities for real k_θ, k_i , so long as θ remains finite.

The physical field theory is generated by the limit $\theta \rightarrow 0^+$, in which θ approaches zero from above,

$$Z_0[J] = \int [d\phi] \exp \left[i \int dx_0 d^3x \left(\frac{1}{2} \left((\partial_0\phi)^2 - (\vec{\nabla}\phi)^2 - m^2\phi^2 + i\epsilon\phi^2 \right) - V(\phi) - J\phi \right) \right]. \quad (29)$$

In this limit $\Delta(k, 0^+)$ becomes precisely the normal Feynman propagator,

$$\Delta(k, 0^+) = \frac{1}{k_0^2 - \sum_{i=1}^3 k_i^2 - m^2 + i\epsilon}, \quad (30)$$

whose singularities are regulated by an “ $i\epsilon$ prescription”.

Wick rotation for a two-point function. As a practical example in perturbation theory, let's consider the scalar equal-mass two point function at one loop, fig. 4, directly in Minkowski space. Working in n dimensions, combining denominators by Feynman parameterization and

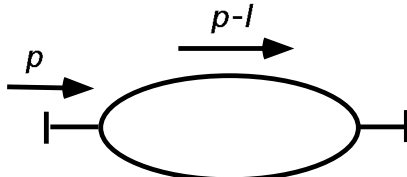


Figure 4: Scalar two-point function.

completing the square in the loop momentum, we find

$$\begin{aligned}
I(p^2) &= \int \frac{d^n \ell}{(2\pi)^n} \frac{g^2 \mu^{2\epsilon}}{(\ell^2 - m^2 + i\epsilon)((p - \ell)^2 - m^2 + i\epsilon)} \\
&= g^2 \mu^{2\epsilon} \int \frac{d^n \ell}{(2\pi)^n} \int_0^1 \frac{dx}{(\ell^2 - 2xp \cdot \ell + xp^2 - m^2 + i\epsilon)^2} \\
&= g^2 \mu^{2\epsilon} \int_0^1 dx \int \frac{d^n \ell'}{(2\pi)^n} \frac{1}{(\ell'^2 + x(1-x)p^2 - m^2 + i\epsilon)^2}.
\end{aligned} \tag{31}$$

The factor $\mu^{2\epsilon}$ keeps the coupling dimensionless in n dimensions.

In Minkowski space, with $\ell'^2 = \ell_0'^2 - \vec{\ell}'^2$, the integrand in (31) has poles at

$$\ell_0' = \pm \sqrt{\vec{\ell}'^2 + m^2 - x(1-x)p^2} \mp i\epsilon. \tag{32}$$

The integral, however, is defined by the $i\epsilon$ prescription, which keeps the poles off the real axis, so long as $p^2 < 4m^2$. For these values of p^2 , the poles are in the standard arrangement shown in fig. 5, and the ℓ_0' integration contour may be rotated to the vertical (imaginary) axis, according to

$$\ell_\theta' = \ell_0' e^{i\theta} \quad 0 \leq \theta \leq \pi/2, \tag{33}$$

where $i\ell_n' \equiv \ell_{\pi/2}'$ is the imaginary energy along the vertical axis in the ℓ_0' plane. This rotation

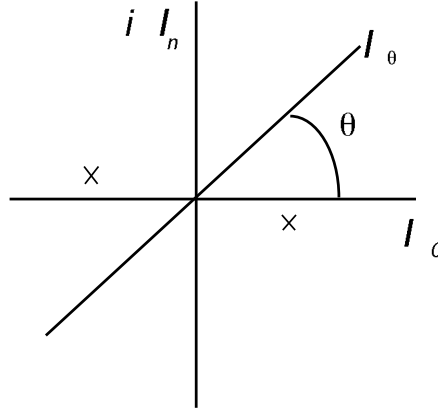


Figure 5: Wick rotation in the energy plane.

is in just the opposite sense from the rotation of time in eq. (26). For $p^2 = -Q^2 < 0$ (in fact, for $p^2 < 4m^2$), the integral may be rotated as an analytic continuation into a purely Euclidean integral,

$$\begin{aligned}
I(-Q^2) &= g^2 \mu^{2\epsilon} \int_0^1 dx \int \frac{id^n \ell'}{(2\pi)^n} \frac{1}{(\ell_E'^2 - x(1-x)Q^2 - m^2)} \\
&= g^2 \mu^{2\epsilon} i \Gamma(2 - \frac{n}{2}) \frac{\pi^{n/2}}{(2\pi)^n} \int_0^1 \frac{dx}{(x(1-x)Q^2 + m^2)^{2-n/2}},
\end{aligned} \tag{34}$$

where $d^n \ell' = d\ell_n' d^3 \ell'$. Exanding around $n = 4$, and defining ⁴,

$$\epsilon = 2 - n/2, \tag{35}$$

⁴This ϵ is one-half of the convention used by Collins in his lectures.

we find

$$I(p^2) = \frac{i}{\epsilon} \frac{g^2}{(4\pi)^2} [1 - \epsilon(\gamma_E - \ln 4\pi)] - \frac{ig^2}{(4\pi)^2} \int_0^1 dx \ln \left[(m^2 - x(1-x)p^2)/\mu^2 \right] + \mathcal{O}(\epsilon). \quad (36)$$

In the full theory, the pole term is removed by ultraviolet renormalization. We are interested, rather, in the finite, momentum-dependent remainder. It is real for $p^2 < 4m^2$ and is defined by analytic continuation for $p^2 \geq 4m^2$, where, on the real axis, it is complex but finite, as long as $m^2 > 0$. Real, negative p^2 is equivalent to Euclidean space in which, as observed above, all Green functions are (relatively) real, analytic functions of their external momenta. Our example shows how branch points develop in their analytic continuation. Note in particular that the branch point occurs at “threshold” for the production of two on-shell particles. This correspondence of singularities to physical processes is quite general, as we shall see presently.

Recalling that in QCD light quark masses are small compared to the natural scale of the coupling, we may take a special interest in the $m^2 \rightarrow 0$ limit of (36). The branch point moves to the origin in the p^2 plane, where the function $I(p^2)$ diverges logarithmically. This divergence has quite different interpretations in Euclidean space, where it occurs at a single point, $p^\mu = 0$, and in Minkowski space, where it is on an entire two-dimensional subspace, the light-cone $p_0^2 = \vec{p}^2$. Such divergences in Green functions will recur in QCD, and get worse at higher order. This is a clear difficulty for any program to exploit asymptotic freedom - since it indicates that Green functions have, in general, divergent sensitivity to low-momentum, long-distance physics. In fact, since in Minkowski space, small invariant mass does not necessarily mean small energy, the situation is much more complicated than in Euclidean space. It is this long-distance behavior whose analysis, which is still an ongoing topic of research, we shall describe in the following. Before we do so, however, it will be useful to introduce a simple rule for identifying quantities that are *not* sensitive to long-distance, nonperturbative physics.

1.5 Infrared safety

Asymptotic freedom is useful for quantities that are dominated by the short-distance behavior of the theory [4]. Such quantities, which are termed *infrared safe*, cannot depend sensitively on the masses of quarks, nor can they suffer from infrared divergences of the sort identified in the example above. Infrared safety is one of the fundamental concepts of perturbative QCD, and it makes essential use of the renormalization group. To see how, and to see further why an analysis of infrared divergences is necessary, we consider a generic physical quantity (say, a cross section) $\tau(Q^2/\mu^2, \alpha_s(\mu^2), m^2/\mu^2)$, where Q represents “large” invariants, much greater than Λ , m represents light quark masses (and the vanishing gluon mass), and μ the renormalization scale. We assume that τ has been scaled by an overall factor of Q , to make it dimensionless. Now because τ is physical, it cannot depend on μ ,

$$\tau \left(\frac{Q^2}{\mu^2}, \alpha_s(\mu^2), \frac{m^2(\mu^2)}{\mu^2} \right) = \tau \left(1, \alpha_s(Q^2), \frac{m^2(Q^2)}{Q^2} \right). \quad (37)$$

This just says that we may, if we like, expand in the coupling at the scale of the large momenta of the problem, and use asymptotic freedom. In general, however, we pay the price of introducing dependence on the large ratio Q/m , which typically occurs in powers of logarithms. The presence of such logarithms (an example of which was illustrated above) can make the perturbative expansion unusable. On the other hand, perturbation theory *can* be used if τ happens to be infrared safe. To be specific, we shall demand that τ behave in the large μ limit as

$$\tau \left(\frac{Q^2}{\mu^2}, \alpha_s(\mu^2), \frac{m^2(\mu^2)}{\mu^2} \right) \mu \xrightarrow{\mu \rightarrow \infty} \hat{\tau} \left(\frac{Q^2}{\mu^2}, \alpha_s(\mu^2) \right) + \mathcal{O} \left(\left(\frac{m^2}{\mu^2} \right)^a \right), \quad a > 0. \quad (38)$$

That is, τ should approach a limit as $m/\mu \rightarrow 0$, with Q/μ held fixed, with corrections that vanish as a power of m . Again, $I(p^2)$ discussed above, is an example of an infrared safe quantity so long as $p^2 \sim Q^2 \neq 0$.

Much of the remaining discussion will center on identifying infrared safe quantities, and separating them from long-distance dependence. Indeed, this is the essence of the QCD justification of the parton model. In this connection we note that infrared safety can apply not only to cross sections and other direct physical observables, but also to renormalization-group invariant quantities that obey equations of the form

$$\left(\mu \frac{d}{d\mu} - \gamma_\Gamma \right) \Gamma = 0, \quad (39)$$

with γ_Γ an anomalous dimension.

1.6 QCD in the n plane

We'll end this introductory section with a few comments on the double role of dimensional regularization in perturbative QCD. Dimensional continuation serves to regulate both ultraviolet ($n < 4, \epsilon > 0$) and infrared ($n > 4, \epsilon < 0$) divergences. When the number of dimensions is less than four, the volume of phase space is decreased. Because ultraviolet divergences result from the large number of states at high energy, they are softened as the number of dimensions is decreased. In contrast, infrared divergences result from singularities in the integrands of momentum space integrals, and when these singularities are spread out over a larger phase space at higher dimension, they are softened. The question arises, however, how dimensional continuation can handle both problems at the same time.

To see how it works, we recall the basic path from a Lagrangian to cross sections and other physical quantities. This is illustrated by the sequence below:

$$\begin{aligned} \mathcal{L}_{QCD} &\rightarrow G^{(reg)}(p_1, \dots, p_n), \quad n < 4 \\ &\rightarrow G^{(ren)}(p_1, \dots, p_n), \quad n < 4 + \Delta \\ &\rightarrow S^{(unphys)}(p_1, \dots, p_n), \quad 4 < n < 4 + \Delta \\ &\rightarrow \tau^{(unphys)}(p_1, \dots, p_n), \quad 4 < n < 4 + \Delta \\ &\rightarrow \tau^{(phys)}(p_1, \dots, p_n), \quad n = 4. \end{aligned} \quad (40)$$

The first step is to generate regularized off-shell Green functions, denoted $G^{(reg)}$ from the Feynman rules of the theory. As we shall see, these Green functions are free of infrared divergences, and so are rendered completely finite for $n < 4$. Here is where the theory is renormalized, producing a set of renormalized Green functions, $G^{(ren)}$ which are now analytic functions of n , treated as a complex number, in some strip in the n -plane, $4 - \Delta' \leq n \leq 4 + \Delta$, with $\Delta, \Delta' > 0$. It is thus possible to analytically continue the renormalized Green functions to n slightly greater than four. Because the *infrared* divergences of the theory are regulated in this region of n , we can now define S-matrix elements, $S^{(unphys)}$ for the renormalized theory. These S-matrix elements, although fully renormalized are nevertheless unphysical, because they are only infrared finite for $n > 4$. That is, they are not infrared safe. They can, however, be used to compute infrared safe quantities in $n > 4$, $\tau^{(unphys)}$, which, finally, may be continued to $n = 4$ to derive finite, physical predictions, $\tau^{(phys)}$ from the theory. It is important to stress that QCD for $n > 4$ is not physical QCD, and cannot be used to compute physical quantities unless they are infrared safe, and thus have finite limits for $n \rightarrow 4$. Having made these observations, we are ready to begin our analysis of infrared divergences in field theory.

2 Long and Short Distances in Minkowski Space

In this section we shall discuss how to analyze and classify sources of long-distance behavior in perturbation theory. We do so not because we expect perturbation theory to be correct at long distances, but rather to identify and eventually calculate short-distance (infrared safe) quantities for which perturbation theory may reasonably be trusted.

2.1 Example: IR and CO divergences in the massless vertex function

A very informative example, which already illustrates many of the general properties we will identify below, is the fully massless three-point function at one loop, with two on-shell external lines. We shall start, as above, with this vertex in a scalar theory, shown in fig. 6a,

$$I_\Delta = g^3 \mu^{3\epsilon} \int \frac{d^n k}{(2\pi)^n} \frac{1}{(k^2 + i\epsilon)((p_1 - k)^2 + i\epsilon)((p_2 + k)^2 + i\epsilon)}. \quad (41)$$

This integral may be evaluated just as the two-point integral above, by Feynman parameterization and n -dimensional integration. The resulting (two) parametric integrals can then be done in terms of Euler beta functions, with the result,

$$I_\Delta = (-ig\mu^\epsilon) \frac{1}{q^2} \frac{g^2}{(4\pi)^2} \left(\frac{4\pi\mu^2}{-q^2 - i\epsilon} \right)^\epsilon \Gamma(1 + \epsilon) \frac{B(-\epsilon, 1 - \epsilon)}{-\epsilon}, \quad (42)$$

with $q^2 = 2p_1 \cdot p_2$, and where again, $\epsilon = 2 - n/2$. This scalar integral is ultraviolet-finite, so the double pole in ϵ is entirely infrared in origin. Before discussing it further, we may exhibit the

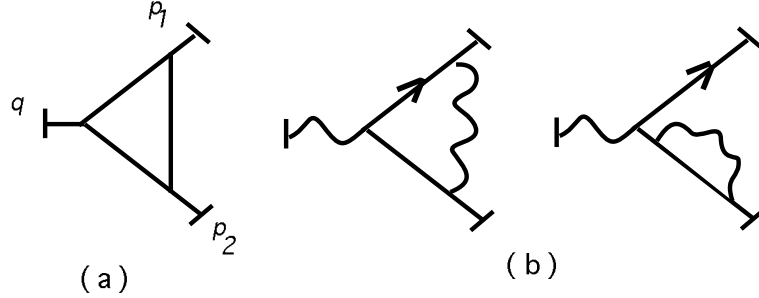


Figure 6: (a) scalar vertex and (b) gauge theory electromagnetic vertex.

corresponding result for the electromagnetic vertex function in a massless gauge theory, found from the diagrams of fig. 6b.

For zero-mass fermions (quarks) the electromagnetic vertex is given in terms of a single form factor. For example, in a quark-antiquark production process we have

$$\Gamma_\mu(q^2, \epsilon) = -ie\mu^\epsilon \bar{u}(p_1)\gamma_\mu v(p_2) \rho(q^2, \epsilon). \quad (43)$$

At one loop the form factor is given by

$$\rho(q^2, \epsilon) = -\frac{\alpha_s}{2\pi} C_F \left(\frac{4\pi\mu^2}{-q^2 - i\epsilon} \right)^\epsilon \frac{\Gamma^2(1-\epsilon)\Gamma(1+\epsilon)}{\Gamma(1-2\epsilon)} \left\{ \frac{1}{(-\epsilon)^2} - \frac{3}{2(-\epsilon)} + 4 \right\}, \quad (44)$$

where $C_F = (N^2 - 1)/2N$ (see Appendix A). Up to this group factor, the leading, double pole term is essentially the same as in the scalar case, eq. (42). These double poles are common in dimensionally regulated massless integrals. To understand their origin, we may return to the scalar case.

Consider the integral I_Δ over a region of momentum space where the loop momentum k is small enough that $k^2 \ll p_1 \cdot k, p_2 \cdot k$. Neglecting the k^2 terms compared to $p_i \cdot k$ is called the “eikonal” approximation. It is a subtle approximation in Minkowski space, where $p_i \cdot k$ small does not necessarily imply that k^2 is smaller. Accepting that we shall have to return to this point later, we work in the eikonal approximation in a frame where

$$p_1 = (p_1^+, 0^-, \mathbf{0}_\perp), \quad p_2 = (0, p_2^-, \mathbf{0}_\perp), \quad (45)$$

and where plus and minus components are defined by $v^\pm = 2^{-1/2}(v^0 \pm v^3)$, so that $v^2 = 2v^+v^- - \mathbf{v}_\perp^2$.

The integral becomes

$$I_\Delta^{(\text{eik})} \sim \frac{1}{2q^2} \int \frac{dk^+ dk^- d^2 k_\perp}{(-k^- + i\epsilon)(k^+ + i\epsilon)(2k^+k^- - k_\perp^2 + i\epsilon)}. \quad (46)$$

In this integral we easily identify three limiting regions which lead to logarithmic divergence. In the first, all four components of k^μ vanish together; this we shall call the “soft” region. In the

other two, the component of k^μ parallel to either p_1 or p_2 remains finite, while the remaining components vanish in such a way that $k^+k^- \sim k_\perp^2$; these we refer to as “collinear” regions. Momentum components in these regions are of the order of $\sqrt{q^2}$ times powers of a “scaling” variable λ , which vanishes at the points in momentum space where I_Δ is singular,

1. $k^\mu \sim \lambda \sqrt{q^2}$ “soft”
2. $k^\pm \sim \sqrt{q^2}$
 $k^\mp \sim \lambda^2 \sqrt{q^2}$ “collinear”
 $k_\perp^2 \sim \lambda \sqrt{q^2}$.

(47)

The logarithmic divergences in I_Δ may be made explicit by changing variables in each of these regions to λ and a set of scaled momenta $\tilde{k}^\mu = k^\mu / \lambda^a$, with a the power appearing in eq. (47).

The collinear singularities of (47) are *the* characteristic feature of infrared sensitivity in Minkowski space, in which on-shell lines need not have vanishing momenta. Clearly, this complicates the situation relative to Euclidean space.

While soft and collinear divergences were relatively easy to identify in the simple example above, it is still natural to ask how to identify infrared sensitivity at higher orders, and in other processes. To answer these questions requires a more general analysis, to which we now turn.

2.2 Analytic structure and IR divergences: Landau equations and physical pictures

Our aim in this section is to systematize infrared analysis in Minkowski space [11, 13]. In this way, we shall find it possible to separate differing momentum scales and to apply the operator product expansion in the presence of light-cone singularities.

Let us return to the massless scalar triangle again, treating it this time from a more general point of view. Introducing Feynman parameters, the scalar triangle is given by (suppressing the coupling),

$$I_\Delta = 2 \int \frac{d^n k}{(2\pi)^n} \int_0^1 \frac{d\alpha_1 d\alpha_2 d\alpha_3 \delta(1 - \sum_{i=1}^3 \alpha_i)}{D^3}, \quad (48)$$

where the new denominator is

$$D = \alpha_1 k^2 + \alpha_2 (p_1 - k)^2 + \alpha_3 (p_2 + k)^2 + i\epsilon. \quad (49)$$

Again, the scalar integral in eq. (48) is ultraviolet finite, so the poles in (42) at $\epsilon = 0$ must come from infrared sensitivity due to the vanishing of D .

We shall make strong use of the analytic structure of the integral I_Δ , which is defined in terms of integrals in the complex k^μ and α_i planes, and whose singularity structure is defined by the “ $i\epsilon$ ” in eq. (49). Since D is quadratic in the momenta, it has no more than two poles in any

momentum component, when the others are held fixed. When these poles are at real values, D vanishes at two points along the contour. Now we recall that by Cauchy's theorem such a contour integral may be deformed between any pair of paths so long as this deformation crosses no singularity, in this case no point $D = 0$. Therefore, so long as the solutions to $D = 0$ are separated, the relevant contour may be deformed to make the integrand bounded at all points, leading to a finite result. On the other hand, if the poles coalesce (they are automatically in opposite half-planes), the contour can no longer be deformed, and the result may be singular. This is called a “pinch” of the contour. Because D is quadratic in momenta, this is equivalent to the condition

$$\frac{\partial}{\partial k^\mu} D(\alpha_i, k^\mu, p_a) = 0, \quad (50)$$

at $D = 0$. Assuming that we may choose to do any of the momentum integrals first, a *necessary* condition for a singularity is to have a pinch in every loop momentum component.

Similar considerations apply to each of the α_i 's. In this case, however, D is linear in each α_i , so there are never two poles to pinch, and the α_i contour may always be deformed away from a pole, except at the origin, since this is where its integral originates. A pole may, however, migrate to an end-point $\alpha_i = 0$, or it may be that at $D = 0$, $\ell_i^2 - m_i^2 = 0$ on the line corresponding to α_i , so that D is independent of α_i

These requirements apply equally to any diagram at any order, with line momenta ℓ_i and loop momenta k_s , and may be summarized as

$$\begin{aligned} & \text{either } \ell_i^2 = m_i^2, \text{ or } \alpha_i = 0, \\ & \text{and } \sum_{i \in \text{loop } s} \alpha_i \ell_i \epsilon_{is} = 0, \end{aligned} \quad (51)$$

for all i and s . Here ϵ_{is} is an “incidence matrix”, which takes the values $+1$ and -1 when line momentum ℓ_i flows in the same direction or opposite direction as loop momentum k_s , respectively, and is zero otherwise. Eqs. (51) are commonly known as the Landau equations [33, 14].

For the three-point vertex functions of fig. 6, the Landau equations are simply

$$\alpha_1 k^\mu - \alpha_2 (p_1 - k)^\mu + \alpha_3 (p_2 + k)^\mu = 0. \quad (52)$$

One solution to these equations corresponds to the soft limit of vanishing gluon momentum,

$$k^\mu = 0, \quad (\alpha_2/\alpha_1) = (\alpha_3/\alpha_1) = 0. \quad (53)$$

Another set of solutions correspond to the collinear limits, where k becomes proportional to p_1 or p_2 ,

$$\begin{aligned} k &= \zeta p_1, \quad \alpha_3 = 0, \quad \alpha_1 \zeta = \alpha_2 (1 - \zeta) \\ k &= -\zeta' p_2, \quad \alpha_2 = 0, \quad \alpha_1 \zeta' = \alpha_3 (1 - \zeta'). \end{aligned} \quad (54)$$

Are these the only solutions? The task of tracking down pinches is greatly simplified by an observation due to Coleman and Norton [34]. We begin by identifying the products $\alpha_i \ell_i$ for each on-shell line with a space-time vector,

$$\alpha_i \ell_i^\mu = \Delta x_i^\mu. \quad (55)$$

Suppose we identify further $\alpha_i = \Delta x_i^0 / \ell_i^0$ as the ratio of the time component of Δx_i to the energy ℓ_i^0 . Then

$$\Delta x_i^\mu = \Delta x_i^0 v_i^\mu, \quad (56)$$

with

$$v_i^\mu = \left(1, \frac{\vec{\ell}_i}{\ell_i^0} \right), \quad (57)$$

the four-velocity of a particle of momentum ℓ^μ . With this interpretation, Δx_i may be thought of as the four-vector describing the free propagation of a classical on-shell particle with momentum ℓ_i . In an alternate derivation of the Landau equations, based on time-ordered perturbation theory, this physical picture emerges automatically. This derivation is given in Appendix B.

Let us apply this analysis to the collinear pinch of the triangle diagram, eq. (54), where k becomes collinear with p_1 . Consider the vectors associated with the two on-shell lines at this pinch,

$$\Delta x_{p_1 - k}^\mu = \alpha_2(p_1 - k)^\mu = \alpha_1 k^\mu = \Delta x_k^\mu. \quad (58)$$

They are equal. Now consider the diagram shown in fig. 7, We have contracted the single off-shell line $p_2 + k$ to a point, corresponding to $\alpha_3 = 0$, i.e., no propagation for this line. Any

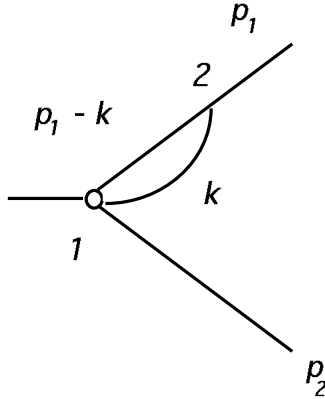


Figure 7: Reduced diagram corresponding to a collinear pinch surface.

such diagram, in which off-shell lines are contracted to points, is called a “reduced diagram”. The reduced diagram for this pinch describes a physical process, in which two on-shell massless particles, of momenta k and $p_1 - k$, are created at vertex 1, and propagate freely to vertex 2, where they combine to form the outgoing massless particle p_1 . This is kinematically possible only because the lines are massless. We have found that this collinear pinch surface describes a

physical process, in which vertices may be identified with points in space-time, between which particles propagate on the mass shell.

The generalization of this result to a completely arbitrary diagram is quite straightforward, and only requires the schematic subdiagram shown in fig. 8, in which a loop of n lines is shown. For this loop to describe a portion of a physical picture, the four-vector separation across any

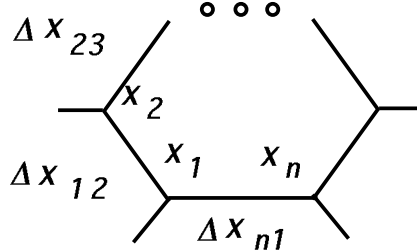


Figure 8: Schematic loop in an arbitrary reduced diagram.

line must equal the separation derived by going around the other $n - 1$ lines on the loop,

$$\Delta x_{12} + \Delta x_{23} + \dots + \Delta x_{n1} = 0. \quad (59)$$

Given the identification in eq. (55), we see that this requirement is identical to the Landau equations, (51).

2.3 Power counting and pinch surfaces

In the Landau equations and the physical picture analysis, we have powerful tools for the identification of sources of long-distance sensitivity in perturbation theory. But even a pinch is only a necessary condition for infrared divergences. In many circumstances, the perturbative integration contour may pass through a pinch surface without producing a singularity. The contributions from such regions may be vanishingly small in the limit of large momentum transfer, consistent with the requirements of infrared safety. When summing perturbation theory to high order, such regions may again become important, but for the present we shall look for a further necessary condition for infrared divergences at finite order. To find it, we shall study how to bound integrals near pinch surfaces. We refer to this process as “infrared power counting”, in analogy to the ultraviolet power counting employed in perturbative renormalization [11].

A general pinch surface is depicted schematically in fig. 9. At each point on a pinch surface S , we identify coordinates that lie in the surface, which we refer to as “intrinsic”, and those that parameterize directions out of the surface, which we call “normal”. By construction, the integrand is a singular function of the normal coordinates only.

It is possible to bound the integral near S using the power counting technique illustrated in Sec. 2.1 for the triangle diagram, fig. 6. We put bounds on the ratio of the volume of normal

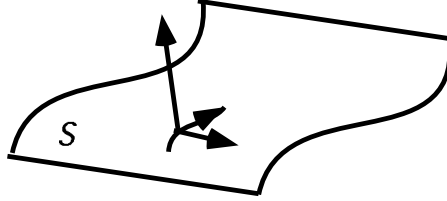


Figure 9: Schematic pinch surface S with one normal and two intrinsic coordinates.

coordinates to the magnitude of the integrand at the pinch surface. In general, the larger the volume of the normal space, the less singular the integral. This power counting will have a dual purpose. First, it is used to put bound on integrals, and hence to identify infrared safe quantities, and by the same token it may also be used to identify regions in momentum space that may give rise to infrared divergences.

- i. We redefine each of the normal variables κ_j in terms of a scaling variable λ according to

$$\kappa_j = \lambda^{a_j} \kappa'_j. \quad (60)$$

We will determine the behavior of the integral when λ vanishes for fixed values of the ratios $\kappa'_j/\kappa'_{j'}$. For instance, in the triangle diagram, eq. (41), the scalings of eq. (47) specify that the the propagators $(p_1 - k)^2$ and k^2 are linear in λ , while $(p_2 + k)^2$ is zeroth order in λ in the collinear region where k is in the p_1 direction. Similarly k^2 is quadratic, and both $(p_1 - k)^2$ and $(p_2 + k)^2$ are linear, for the soft scaling of eq. (47).

- ii. Given a set of powers a_j , we retain only terms of lowest power λ^{A_i} in λ for each perturbative denominator $k_i^2(\kappa_j, \lambda) - m_i^2$,

$$k_i^2(\kappa_j, \lambda) - m_i^2 = \lambda^{A_i} f(\kappa'_j) + \dots. \quad (61)$$

We call the resulting integral over the normal variables κ'_j the *homogeneous* integral. If the homogeneous integral is independent of any normal variable κ'_j , its scaling power a_j may be reduced until that variable appears in the homogeneous integral [11].

- iii. The homogeneous integral for pinch surface S is proportional to λ^{n_S} , with n_S given by

$$n_S = \sum_j a_j - \sum_i A_i + s_I, \quad (62)$$

where s_I represents the (possible) power of λ from momentum factors in the integrand (these will be important for QCD). If $n_S > 0$, the integral is finite when all of the normal variables vanish according to the scaling (61). If $n_S = 0$, the integrand may diverge logarithmically, while if $n_S < 0$, it may diverge as a power.

- iv. Finally, check for pinch surfaces in the homogeneous integral. If the only pinch surface is the original one, at which all normal variables vanish, the bound is complete for the singular surface S . Should the homogeneous integral have further pinch surfaces, however, bounds must be found for these special regions as well. These will correspond to subsurfaces of S where subsets of the normal variables vanish faster than others [11].

2.4 Pinch surfaces for the all-order EM form factor

We can now apply the Landau equations and power counting to identify the sources of infrared divergence in the electromagnetic form factor to *all* orders. Consider pair creation, in which a vector particle of momentum q , $q^2 > 0$ (Z or virtual photon), decays into a massless quark and antiquark with no radiation. The possible reduced diagrams associated with pinch surfaces are remarkably simple, and are all of the form shown in fig. 10. The general reduced diagram

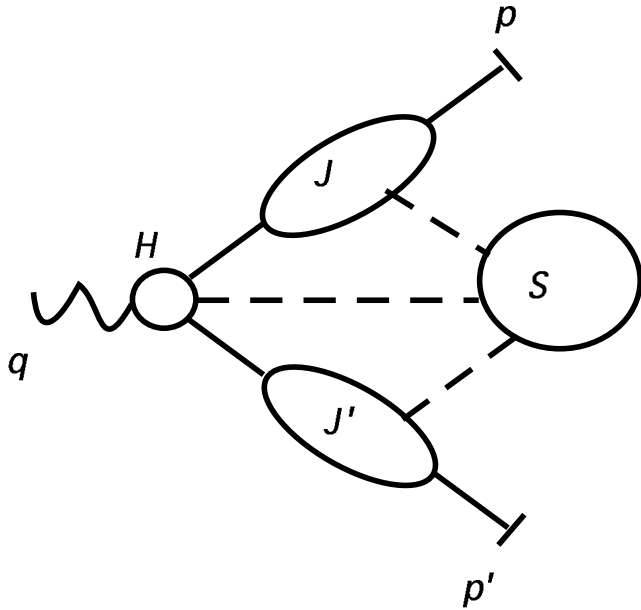


Figure 10: General reduced diagram for pair creation.

corresponds to a set of physical processes in which the decay of the vector is followed by the formation of two “jets”, labelled J and J' in the figure, of virtual particles in the same direction, and with the same total momenta, p and p' , as the two final state particles. The only interaction between the two jets is via zero-momentum “soft” particles, labelled S . Higher-order off-shell, short-distance, contributions reside in subdiagram H , adjacent to the decay vertex. No other physical processes, in particular no finite momentum transfers between the two jets, can be realized, because once the jets are formed at the point represented by H , they travel apart at the speed of light and can never meet again at a point in space-time.

Power counting for the pinch surfaces corresponding to the reduced diagrams of fig. 10

is straightforward. A natural choice of normal variables is (i) all four components k^μ of each loop momentum internal to the soft subdiagram S , and of each loop momentum that links the soft subdiagram with the jets; (ii) the total invariant mass ℓ^2 and the scalar product $\ell \cdot p$ for each loop ℓ in J , and similarly for J' . All of these variables may be scaled with $a_i = 1$ in eq. (60). The resulting homogeneous integral has no pinch surfaces, except those that correspond to reduced diagrams of the same form as fig. 10 [1, 11]. The scaling powers of lines are $A_j = 1$ for lines internal to J and J' , and $A_j = 2$ for soft lines in S . Self-energies on jet lines need not be considered explicitly, because each full two-point function $G_2(k)$ has only a single pole at $k^2 = 0$.

Consider an arbitrary pinch surface T with N_J lines and L_J loops in J , and similarly for J' and S . We assume in addition that M_J soft lines attach S to J , and $M_{J'}$ soft lines attach it to J' . The power counting measure is then, according to eq. (62),

$$n_T = 4(L_S + M_J + M_{J'} - 1) + 2L_J + 2L_{J'} - 2N_S - N_J - N_{J'} + s_T, \quad (63)$$

with s_T the numerator suppression factor. The contribution of all soft lines, loops and numerator momenta internal to S is just the dimension of S . For technical simplicity, we shall assume that the jets attach to H each by a single line, and that the soft lines are all gluons, attached to the jets only at three-point vertices. The dimension of S , including its external lines, is then $4 - 3M_J - 3M_{J'}$, and

$$n_T = M_J + M_{J'} + 2L_J + 2L_{J'} - N_J - N_{J'} + s'_T, \quad (64)$$

where s'_T measures the power associated with numerator factors that come from jet lines and vertices.

It is not difficult to find a lower bound for the numerator suppression factor s'_T . We note that there is a factor of numerator momentum for each three-point vertex in the jets, and that each of these momentum factors will have to combine to form an invariant. Each such invariant will scale as λ if it is the scalar product of two momenta within a jet, but as λ^0 if it involves momenta from different jets. On the other hand, the only way the latter may occur is if each factor of momentum is contracted with the spin tensor of one of the soft gluons. We conclude that

$$s'_T \geq \frac{1}{2}(V_{3,J} + V_{3,J'} - M_J - M_{J'}), \quad (65)$$

where $V_{3,J}$ is the number of three-point vertices internal to jet J . Substituting (65) into (64) we have

$$n_T \geq \frac{1}{2}(M_J + M_{J'}) + 2L_J + 2L_{J'} - N_J - N_{J'} + \frac{1}{2}(V_{3,J} + V_{3,J'}). \quad (66)$$

Now for each jet we have the Euler identity

$$L_J = N_J - \sum_i V_{i,J} + 1, \quad (67)$$

where V_i is the number of i -point vertices in the jet (counting the hard part H as a one-point vertex for each jet), as well as the relation

$$2N_J + M_J + 1 = \sum_i i V_i, \quad (68)$$

which takes into account the two external lines in each jet, one attached to H , and one in the final state. It is now a rather straightforward exercise to show that

$$n_T \geq 0, \quad (69)$$

which shows that at pinch surfaces like fig. 10, the integral is at worst logarithmically divergent.

In addition, a closer look, using the same reasoning, shows that $n_T = 0$, corresponding to logarithmic divergence, can occur only when the reduced diagrams for each jet are themselves of the forms of standard perturbative diagrams, with only three- and four-point vertices internal to the jets. A five- or higher-point vertex in a reduced diagram always leads to suppression in the infrared. In addition, we also find that S is connected to the jets by soft gluons only; the interaction of soft quark lines with jet lines is similarly suppressed, although soft quark loops are possible internal to S . It is clear that attachments of soft lines of any flavor to H will be suppressed relative to diagrams where they are attached only to jets.

In the above, we assumed that the jets attach to H by a single line. This assumption depends on the choice of gauge. In an axial gauge $n \cdot A = 0$, the form of the propagator

$$G_{\mu\nu}(k, n) = \left(-g_{\mu\nu} + \frac{k_\mu n_\nu}{n \cdot k} + \frac{n_\mu k_\nu}{n \cdot k} - \frac{k_\mu k_\nu n^2}{(n \cdot k)^2} \right) \frac{1}{k^2 + i\epsilon}, \quad (70)$$

leads to a suppression whenever it is contracted with the momentum of the gluon itself. That is, the combination

$$k^\mu G_{\mu\nu}(k, n) = \frac{n_\nu}{k \cdot n} - \frac{k_\nu n^2}{(k \cdot n)^2}, \quad (71)$$

has no pole at $k^2 = 0$, and hence does vanish except at $k = 0$. This leads to a contribution to s'_T of $1/2$ in (65) whenever k is a jet line, even if the line k attaches a jet to the hard part H . Then it is easy to verify that in an axial (or other physical) gauge, reduced diagrams that give infrared divergences have only a single line connecting each jet to H , as assumed above.

In covariant gauges, such as the Feynman gauge, there is no such suppression, and multiple collinear gluons may attach J or J' to H . This is not quite the complication it appears to be, however, for the following reason. At the pinch surface, we can have $n_T = 0$ only when each of these gluons appears in the combination

$$k^\mu G_{\mu\nu}(k) = \frac{-k^\nu}{k^2}, \quad (72)$$

in which the gluon propagator is replaced by an unphysical “polarization” vector k^ν , equal to the gluon’s momentum. Such gluons are sometimes described as “scalar-polarized”. As we shall see, scalar-polarized gluons decouple from the hard scattering [1].

In summary, reduced diagrams associated with logarithmic divergence in the electromagnetic (or other electroweak) vertex are characterized by a simple two-jet structure, with a single hard-scattering function, in which the jets are connected to the hard part by single lines in physical gauges, and in which the soft part is connected to the jets by soft gluons only, and not to the hard part.

Most of these observations are much more general than the electromagnetic form factor from which they have been derived. In the following, we shall apply the tools we have developed to a wide set of processes.

3 Short Distance Cross Sections and Unitarity

We are now ready to discuss a class of physical quantities that can be proved infrared safe by a combined analysis of their analytic structure and power counting. They are primarily cross sections initiated by timelike electroweak currents, the prime examples being the total and jet cross sections in e^+e^- annihilation [4]. Other examples include the decay width of the Z and W, and various event shapes defined to describe cross sections and decay rates of this type. The analysis of these cross sections is related to the operator product expansion, but gives many results that cannot be derived directly from the operator product expansion.

3.1 Cut diagrams and generalized unitarity

To discuss cross sections of this type, we introduce the “cut diagram” notation shown on the left-hand side of fig. 11. This diagram represents the amplitude for a process in which a set

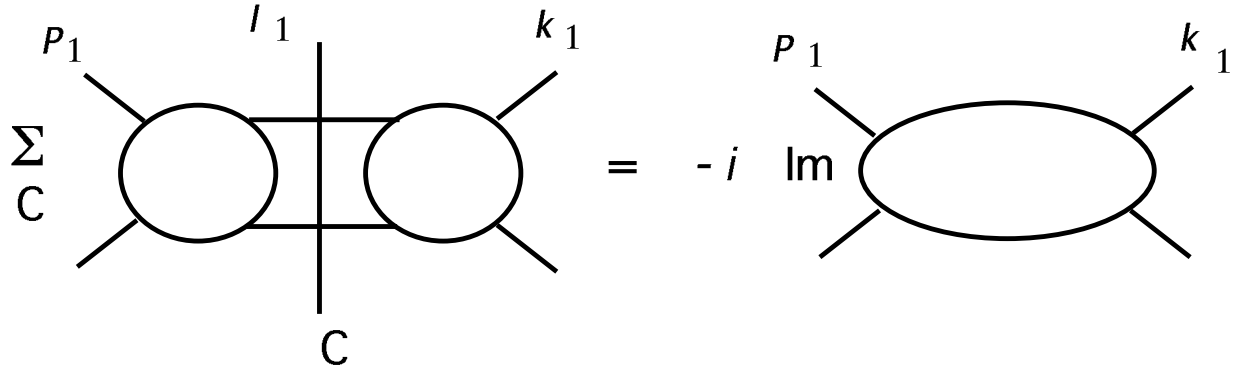


Figure 11: Cut diagram and unitarity.

of particles with momenta p_1, \dots, p_n scatter into a set ℓ_1, \dots, ℓ_m , times the complex conjugate amplitude for the latter to scatter into a third set $k_1, \dots, k_{n'}$, integrated over part or all of the phase space of the intermediate set. Perturbation theory rules to the left of the cut are the

usual ones, those to the right their complex conjugates. Each such cut, which we label C in fig. 11, specifies a distinct intermediate state. We shall denote a particular cut diagram found from uncut diagram G by cut C as G_C .

Fig. 11 as a whole states a very useful theorem satisfied by cut diagrams. The sum over all cuts with fixed external momenta p_1, \dots, p_n and $k_1, \dots, k_{n'}$ is given by twice the imaginary part of $(-iG)$, the uncut diagram,

$$\sum_{\text{all } C} G_C(p_i, k_j) = 2 \text{Im} \ (-iG(p_i, k_j)) . \quad (73)$$

This result is a generalization of unitarity expressed in terms of the T matrix, $T = -i(S - 1)$, with S the scattering matrix,

$$TT^\dagger = -i(T - T^\dagger) . \quad (74)$$

It is, however, more general, because it applies for *fixed spatial momenta*, in both the external *and* internal loops of the overall diagram G . This result is proved in Appendix B by use of time-ordered perturbation theory.

3.2 Infrared safety for inclusive annihilation and decay

The simplest physical application of the analyticity/power counting analysis is to the total cross section for e^+e^- annihilation or Z decay, fig. 12. By the optical theorem, a special case of

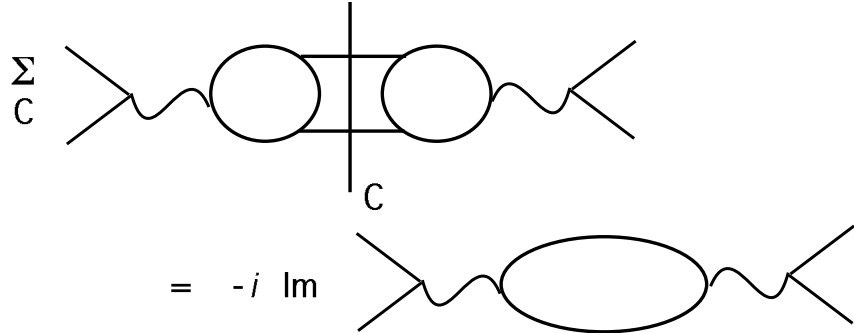


Figure 12: Unitarity applied to the total annihilation cross section.

generalized unitarity, eq. (73), the total cross section is proportional to the vacuum expectation value of the time-ordered product of two currents,

$$\sigma_{e^+e^-}^{(\text{tot})}(q^2) = \frac{e^2}{q^2} \text{Im} \pi(q^2) , \quad (75)$$

where the function π is defined in terms of the two-point correlation function of the relevant electroweak currents J_μ (with their couplings included) as

$$\pi(q^2)(q_\mu q_\nu - q^2 g_{\mu\nu}) = i \int d^4x e^{iqx} \langle 0 | T J_\mu(x) J_\nu(0) | 0 \rangle . \quad (76)$$

The proof that $\pi(q^2)$, and hence its imaginary part, and therefore the total cross section, is infrared safe requires only that we recognize that π represents a forward scattering process. There are no physical processes in which an off-shell photon (or on-shell Z) can decay into a set of on-shell particles that propagate freely and then annihilate to form another photon of the same invariant mass. The set of particles originating from a point will recede in different directions, and can never meet again by physical propagation. This eliminates pinch surfaces with finite momentum particles, and hence any infrared divergences associated with decay processes. This is a particular example of the famous Kinoshita-Lee-Nauenberg (KLN) theorem [35].

It is still possible to have pinch surfaces involving only massless particles, coupled to a single hard-scattering, as in fig. 13. Dimensional counting shows that such pinch surfaces are finite order-by-order in perturbation theory. They will, however, lead to an important connec-

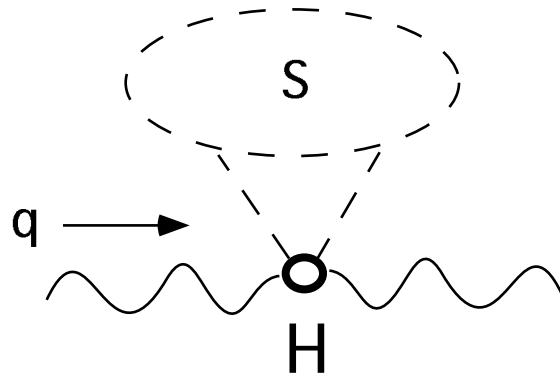


Figure 13: Pinch surface with only zero-momentum lines (subdiagram S) coupled to a point-like hard part H .

tion of perturbation theory, even without explicit masses, to the operator product expansion, as we shall see in Section 7 below.

3.3 Jet and weighted cross sections

The class of infrared safe cross sections is by no means exhausted by the totally inclusive processes above. More detailed information on final states is available in jet and other “weighted” cross sections.

Jet cross sections measure the probability of producing states that are identified as jet-like, according to infrared safe criteria. The simplest of these [4] is illustrated by fig. 14, which are defined by the energies e_i flowing into each of two cones, δ , back-to-back along a fixed axis, at angle θ from the beam direction. We may define a two-jet cross section in e^+e^- annihilation as one for which

$$\frac{e_1 + e_2}{\sqrt{s}} \geq 1 - \epsilon, \quad (77)$$

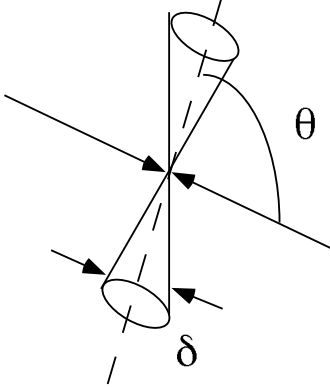


Figure 14: Cones for a two-jet cross section.

that is, for which all the energy, up to a fraction ϵ , is emitted into the two back-to-back cones. If the cones are sufficiently small, the event will “look like” two jets of nearly collinear particles. Such a cross section is infrared safe, and the proof is a variation of the proof of infrared finiteness of the total annihilation cross section.

Consider for simplicity a two-jet cross section. The relevant pinch surfaces of cut diagrams are shown in fig. 15. Each cut C of the diagram has a final state that contributes to the jet cross section, with one jet in each of the cones of fig. 14, for instance. The pinch surfaces associated with long-distance behavior are easily verified to be of exactly the same form as those for quark-antiquark production, fig. 10, except that now there may be any number of particles from each jet in the final state. At the pinch surface, if cut C of reduced diagram R contributes to the two-jet cross section, then *every* cut of R contributes to the same cross section. The sum over cuts, however, may then be carried out using the generalized form of unitarity, fig. 11, to derive an integral which has no pinch surface at all corresponding to the two-jet configuration, by exactly the same reasoning as for the total cross section.

The difference between total and jet cross sections is that momentum integrals for jet cross sections encounter boundaries between two- and three-jet events (for instance), which are absent in the total cross section. At such points, the phase space is discontinuous, and integrals may not be deformed after the sum over cuts. Manifolds of such points are of reduced dimension, however, compared to the general pinch surfaces of cut diagrams, which produce at worst logarithmic divergences [13, 36]. This reduced dimension weakens their power-counting, and they do not give rise to infrared singularities order-by-order in perturbation theory. Similar considerations apply to pinch surfaces with more than two jets.

In weighted cross sections, final states are weighted according to “shape variables”, $\mathcal{S}_n(p_1 \dots p_n)$, which are functions of the momenta of particles in the final state. The shape variables may or may not be chosen to enhance jet-like configurations. A general cross section

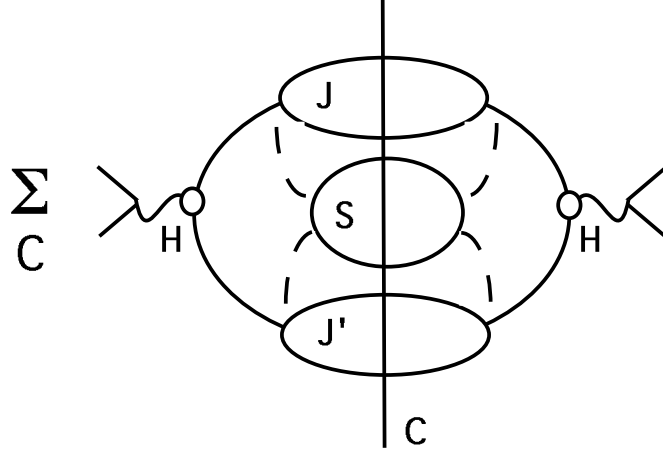


Figure 15: Cut reduced diagram for two-jet configuration.

at fixed shape variable \mathcal{S} is of the form

$$\sigma_{\mathcal{S}} = \sum_n \int d\tau_n \frac{d\sigma}{d\tau_n} \mathcal{S}_n(p_1 \dots p_n), \quad (78)$$

where the \mathcal{S}_n are functions of the momenta in an n -particle final-state, whose phase space is denoted by $d\tau_n$. A weighted cross section is infrared safe whenever the same mechanism that produces infrared safety for jet cross sections applies to them as well. That is, it is infrared safe if, whenever a pinch surface of a cut reduced diagram like fig. 15 contributes to the weighted cross section, the weight is the same for every possible cut of the reduced diagram at the pinch surface. If this holds, the divergences of individual cuts cancel, since the sum over cuts produces an integral without the corresponding pinch surface. This condition will be satisfied so long as the weight function does not distinguish between states in which one set of collinear particles is substituted for another set with the same total momentum, or when zero-momentum particles are absorbed or emitted. Quantitatively, these requirements may be summarized by the conditions

$$\mathcal{S}_n(p_1 \dots p_i \dots p_{n-1}, \lambda p_i) = \mathcal{S}_{n-1}(p_1 \dots p_i + \lambda p_i \dots p_{n-1}). \quad (79)$$

Perhaps the best known weight is the “thrust”, defined [37] for an event with n particles of momenta \vec{p}_i by

$$T = \frac{1}{\sum_i |\vec{p}_i|} \max_{\hat{n}} \sum_{i=1}^n |\vec{p}_i \cdot \hat{n}|, \quad (80)$$

with the maximum taken over all unit vectors \hat{n} . The direction of \hat{n} that produces the maximum is known as the “thrust axis”.

Other important weighted cross sections iteratively assign particles into jets of momenta P_j . The algorithm begins with each particle defined as a separate jet. At each stage in the iterative process, a set of variables y_{jk} ,

$$y_{jk} = \frac{1}{s} f(P_j, P_k) \quad (81)$$

are computed for each pair of jets. The function f is chosen to be consistent with infrared safety. An influential choice [38] defines the “ k_T algorithm”, based on

$$y_{jk} = \min (E_j^2, E_k^2)(1 - \cos \theta_{jk}), \quad (82)$$

where E_j and E_k are the energies of jets j and k in the overall center-of-mass frame, and θ_{jk} is the angle between them. For this, and other such variables, if one or more of the y_{jk} are smaller than a fixed value y_{cut} , the pair whose value is minimum is combined to form a single jet and the process is repeated. The number of jets left when all y_{jk} are larger than y_{cut} defines the number of jets in the event, which may be plotted against y_{cut} and compared to perturbative or event-generator predictions.

4 Factorization and Evolution in DIS

4.1 Venturing out on the light cone

Although the set of infrared safe cross sections is large, it is a small subset of interesting scattering experiments. In particular, QCD cross sections in which one or more of the incoming particles is a hadron are never fully infrared safe. For DIS, this is already clear in the parton model, in which parton distributions must be taken from experiment. This will remain the case in field theory, where we shall discover how to extract infrared safe quantities from many (not all!) cross sections, a process known as *factorization* [1].

Factorization, as mentioned at the outset, is a realization of the separation of long- and short-distance dynamics in the presence of massless particles in Minkowski space. In this context, we shall derive a generalization of the parton model in QCD, and a field-theoretic definition for parton distributions [39, 40]. Let us begin with dimensionally regularized deeply inelastic scattering of a light-like parton. Now our initial state is fixed on-shell, and is sure to include singularities in Feynman integrals associated with the light cone.

Amplitudes for DIS are full of collinear singularities; to analyze them we turn again to a pinch surface analysis via physical pictures. That is, we look for the most general physical process in which a single incoming parton absorbs a spacelike photon to form a final state. The result, analogous to fig. 15 for e^+e^- annihilation, is shown in fig. 16. In this process, the incoming particle of momentum p produces a jet of collinear lines $J(\xi)$, one of which, a parton of flavor i with momentum ξp , absorbs the virtual photon (or other electroweak boson) of momentum q at H , producing a set of outgoing jets. All jets, including the remains of the incoming jet of lines collinear to p , propagate into the final state. The jets may interact mutually only through the exchange of soft particles. Because all particles in the physical picture must have positive energy, we find that

$$1 > \xi > x. \quad (83)$$

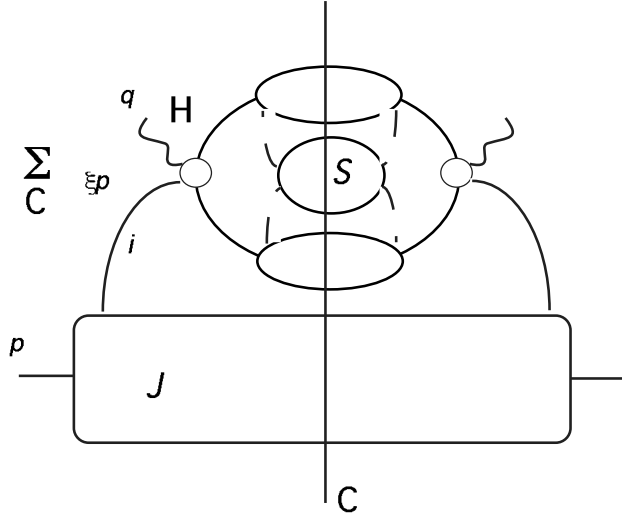


Figure 16: Pinch surface for DIS.

Thus, the struck particle is a parton of the incoming particle, with a proper fractional momentum. That there is only one struck parton, at least in a physical gauge, follows the power counting of Sec. 2.4, especially the discussion of eq. (71). An exception is that in covariant gauges the physical parton may share its momentum with unphysical, scalar-polarized gluons. We shall incorporate this possibility below.

Next, if we sum over all final states at fixed q , soft and collinear divergences associated with the final-state jets and their interactions cancel, by the same unitarity arguments as for e^+e^- annihilation. This may be verified by using the relation of the hadronic tensor $W_{\mu\nu}$ to the forward Compton amplitude $T_{\mu\nu}$,

$$W_{\mu\nu} = 2 \operatorname{Im} T_{\mu\nu} \quad (84)$$

with

$$T_{\mu\nu} = \frac{i}{8\pi} \int d^4x e^{iq \cdot x} \langle h(p) | T J_\mu(x) J_\nu(0) | h(p) \rangle. \quad (85)$$

The absence of pinch surfaces involving final-state jets in the forward-scattering amplitude follows easily from the much simpler physical pictures for $T_{\mu\nu}$, which involve the incoming jet only, as in fig. 17. Note that, as in e^+e^- , this result, and the cancellation of infrared sensitivity to the final state, applies to any weighted DIS cross section consistent with eq. (79), and not only to fully inclusive DIS. Infrared sensitivity from the incoming jet remains in all these cases, of course.

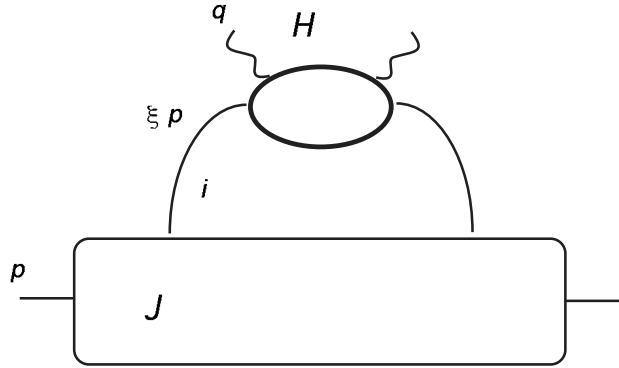


Figure 17: Pinch surface for forward Compton scattering.

In summary, in the neighborhood of *any* of its pinch surfaces, the DIS hadronic tensor takes a form that is very suggestive of the parton model,

$$W^{\mu\nu} = \sum_i \int_x^1 d\xi H_{i,\beta\alpha}^{\mu\nu}(q, \xi p) J_{i,\alpha\beta}(\xi). \quad (86)$$

The strategy of factorization is to separate the long-distance contributions from the hard-scattering part. Unlike the operator product expansion in Euclidean space, however, such a factorization cannot be expressed as a finite sum of coefficient functions times matrix elements, even to the leading power in Q^2 . This is because the short-distance part and the incoming jet remain in convolution form, tied together by the fractional momentum ξ of the struck parton. The finite sum, therefore, is replaced by a convolution of functions.

As in the operator product expansion, however, we can express the long-distance function in terms of the matrix elements of partons that connect the incoming hadron to the hard scattering. Thus, the long-distance contributions of all diagrams with pinch surfaces like those in fig. 16, when the scattered parton i is a quark are summarized by matrix elements of the form

$$J_{q,\alpha\beta} = \frac{1}{2} \sum_{\substack{\text{spin} \\ \sigma}} \int_{-\infty}^{\infty} \frac{dy^-}{2\pi} e^{-i\xi p^+ y^-} \langle h(p, \sigma) | \bar{q}_\alpha(0^+, y^-, \mathbf{0}_\perp) q_\beta(0) | h(p, \sigma) \rangle, \quad (87)$$

with α and β Dirac indices. Instead of a local composite operator, we find a product of operators separated by a light-like distance y^- . In this fashion, the plus momentum of the parton is fixed, although its remaining components, to which H is insensitive, are integrated over. As we shall see shortly, the matrix elements of such composite operators are ultraviolet divergent in perturbation theory, and require renormalization. This is similar to the local composite

operators of the OPE. The effective ultraviolet cutoff for the matrix element is referred to as the “factorization scale”, separating the short-distance from the jet functions.

A Fierz projection between the hard and jet functions, followed by some power counting, shows that the leading Dirac structure may be projected out by the trace of $J_{\alpha\beta}$ with a single Dirac matrix, for unpolarized scattering. This results in the following definition for the quark distribution [39],

$$\phi_{q/h}(\xi, \mu^2) = \frac{1}{2} \sum_{\sigma} \int_{-\infty}^{\infty} \frac{dy^-}{2\pi} e^{-i\xi p^+ y^-} \langle h(p, \sigma) | \bar{q}(0^+, y^-, \mathbf{0}_\perp) \frac{1}{2} n \cdot \gamma q(0) | h(p, \sigma) \rangle, \quad (88)$$

where n^μ is the lightlike vector directed oppositely to the incoming momentum p , $n^\mu = \delta_{\mu-}$. Similarly, when the scattered parton is a gluon, we encounter the distribution

$$\phi_{G/h}(\xi, \mu^2) = \frac{1}{4\pi\xi p^+} \int dy^- e^{-i\xi p^+ y^-} \sum_{\sigma} \sum_{\mu=1}^2 \langle h(p, \sigma) | F^+_\mu(0, y^-, \mathbf{0}) F^{\mu+}(0) | h(p, \sigma) \rangle, \quad (89)$$

now a matrix element of the field strengths $F_{\mu\nu}$. These matrix elements are illustrated in fig. 18a.

In summary, the inclusive DIS hadronic tensor, and hence its structure functions, may be written in the following factorized form, which generalizes the OPE and which is clearly a justification of the use of the parton model in this process,

$$\begin{aligned} F_2^{(h)}(x, Q^2) &= \sum_{i=f, \bar{f}, G} \int_x^1 d\xi C_2^{(i)} \left(\frac{x}{\xi}, \frac{Q^2}{\mu^2}, \alpha_s(\mu^2) \right) \phi_{i/h}(\xi, \mu^2) \\ F_1^{(h)}(x, Q^2) &= \sum_{i=f, \bar{f}, G} \int_x^1 \frac{d\xi}{\xi} C_1^{(i)} \left(\frac{x}{\xi}, \frac{Q^2}{\mu^2}, \alpha_s(\mu^2) \right) \phi_{i/h}(\xi, \mu^2). \end{aligned} \quad (90)$$

Compared to the parton model, the coefficient functions are now expansions in the strong coupling, and the parton distributions have become functions of the factorization scale.

4.2 Gauge invariant distributions; schemes

The distributions, (88) for the quark, and (89) for the gluon, have been justified so far only in physical gauges, where only a single, physical parton connects the hard scattering and the p -jet on either side of the cut in fig. 16. At the same time, these distributions are not gauge invariant. Their gauge variations, however may be absorbed in the hard scattering functions. This is because a change in the gauge of the matrix elements (88) or (89) is equivalent to a phase acting on the quark or gluon operators only.

Alternately, we may define gauge-invariant distributions by connecting the physical quark and gluon fields in the matrix elements with ordered exponentials (Wilson lines) along the n^μ -light cone between the fields [39],

$$\bar{q}(y^-) n \cdot \gamma q(0) \rightarrow \bar{q}(y^-) P \exp \left[-ig \int_0^{y^-} d\lambda n \cdot A(\lambda n^\mu) \right] n \cdot \gamma q(0)$$

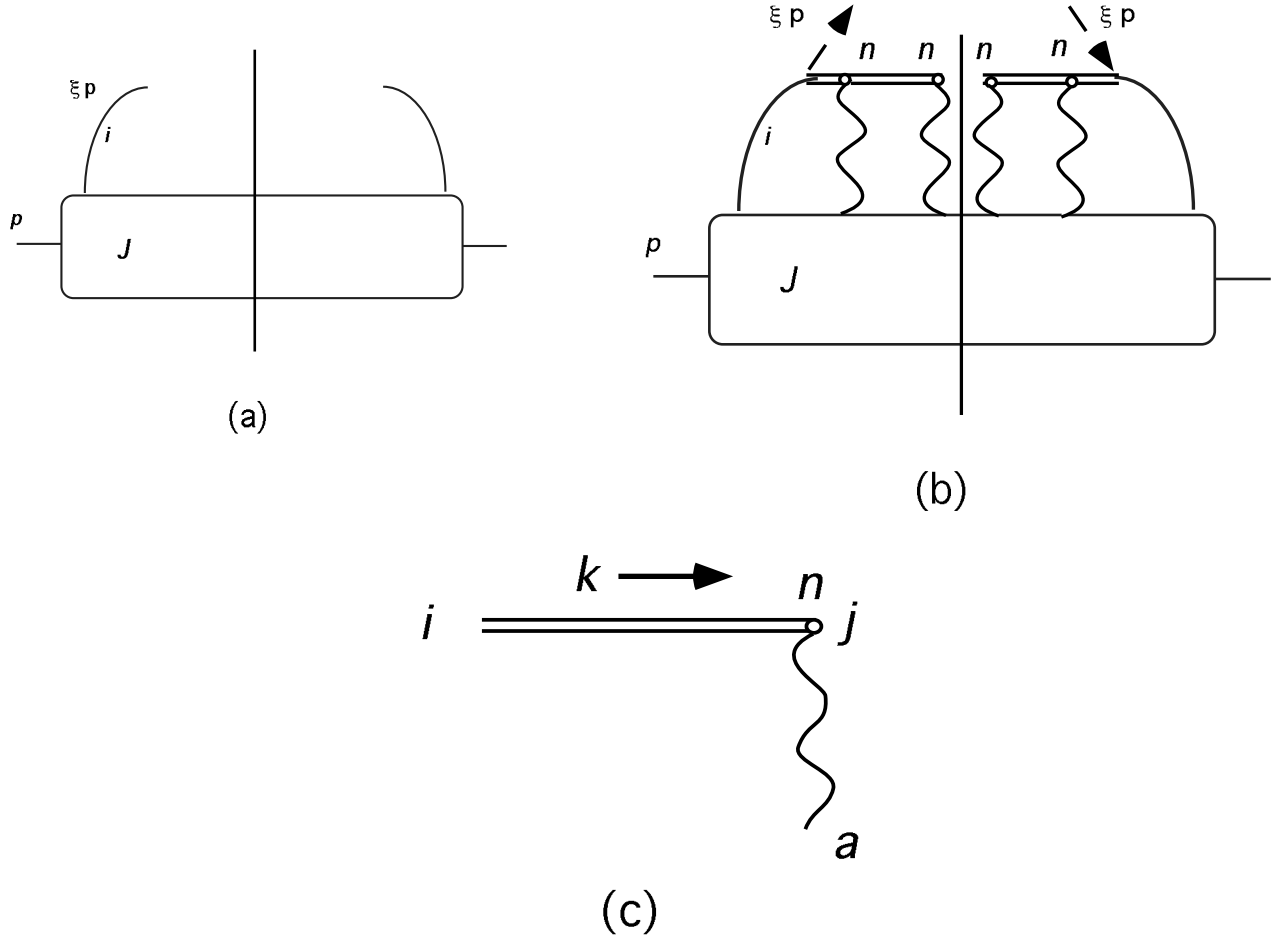


Figure 18: (a) Gauge-variant parton distribution (flavor i). (b) Gauge-invariant parton distribution with ordered exponential in the n directions. (c) Graphical representation of the ‘eikonal’ propagator and vertex.

$$\sum_{\mu=1}^2 F^+_{\mu}(y^-) F^{\mu+}(0) \rightarrow \sum_{\mu=1}^2 F^+_{\mu}(y^-) P \exp \left[-ig \int_0^{y^-} d\lambda n \cdot A(\lambda n^{\mu}) \right] F^{\mu+}, \quad (91)$$

where $n \cdot A$ in the quark distribution is in the fundamental (quark) representation, and $n \cdot A$ in the gluon distribution is in adjoint representation. The gauge invariant distributions reduce to (88) and (89) in $n \cdot A = 0$ (often identified as $A^+ = 0$) gauge. Again, any of these definitions require renormalization. They are commonly defined by $\overline{\text{MS}}$ prescriptions, and are referred to as $\overline{\text{MS}}$ distributions.

Gauge-invariant parton distributions have perturbative expansions, defined by the diagrams of fig. 18b, which include propagators and vertices generated by the ordered exponentials of eq. (91). The combination of a propagator and a vertex, illustrated by fig. 18c, is given by the expression

$$\frac{i}{n \cdot k + i\epsilon} \left(-ign^{\mu} (T_a^{(R)})_{ji} \right), \quad (92)$$

where $R = F$ for the quark distribution and A for the gluon. The linear propagator is sometimes referred to as an “eikonal line”.

The $\overline{\text{MS}}$ matrix elements just defined are not the only possible choices for the distributions. Other choices may be defined by convolution with any IR safe distribution D , as

$$\phi_{i/h}^{(D)}(\xi, \mu^2) = \int_{\xi}^1 \frac{d\eta}{\eta} D_{ij} \left(\xi/\eta, \alpha_s(\mu^2) \right) \phi_j^{(\overline{\text{MS}})}(\eta, \mu^2), \quad (93)$$

which preserves the factorization (90). Of particular interest is a choice that absorbs the full $\overline{\text{MS}}$ F_2 DIS coefficient function C_2 . Defining $C_2^{(j, \overline{\text{MS}})}(z) = \sum_f Q_f^2 \bar{c}_{fj}(z)$, we take

$$D_{fj}(\xi/\eta) = (\eta/\xi)(\bar{c})_{fj}(\xi/\eta). \quad (94)$$

In this “DIS scheme”, the parton model relation

$$\sum_f Q_f^2 x \phi_{f/n}^{(\text{DIS})}(x, \mu^2) = F_2^{(h)}(x, \mu^2), \quad (95)$$

in eq. (13), holds by construction to all orders in perturbation theory. Note, however, that the Callan-Gross relation in (13), which involves F_1 as well as F_2 , cannot be exact at the same time, and so inherits corrections even in DIS scheme.

4.3 One-loop distributions and coefficient functions

We are now in a position to compute corrections to parton model relations such as (13) in QCD. The complexity of these calculations increases precipitously with order, but the pattern is well illustrated by one-loop considerations.

The first goal is to compute infrared safe coefficient functions $C_a^{(i)}$, in a given factorization scheme, by comparing *perturbative* expressions for structure functions $F_a^{(f)}$ of partons of flavor f with the distributions $\phi_{i/f}$ of parton i in parton f , using the factorized expressions eq. (90), expanded to the appropriate order in α_s . Neither $F_a^{(f)}$ nor $\phi_{i/f}$ is infrared safe, and must be defined through dimensional (or some other) regularization, but the resulting coefficient functions are infrared safe. Once the coefficient functions are determined to some order, the same factorized expressions, (90), may be applied to experimental measurements of the $F_a^{(h)}$ to determine the physical values of parton distributions in hadrons h . This process is similar to the parton model, and as in the parton model, many predictions result by using the parton distributions in different processes.

The one-loop corrections to quark DIS are given by the cuts of the graphs in fig. 19a. The one-loop corrections of the perturbative distribution $\phi_{f/f}$ of a quark in a quark (flavor f) are given in fig. 19b for $A^+ = 0$ gauge. A short calculation shows that the gluon emission diagram in 19b is given in n dimensions by

$$\phi_{f/f}^{(1)}(\xi, \mu^2) = \alpha_s \mu^{2\epsilon} \frac{C_F}{(2\pi)^{n-2}} \frac{2(1+\xi^2)}{1-\xi} \int \frac{d^{n-2}k_T}{k_T^2}. \quad (96)$$

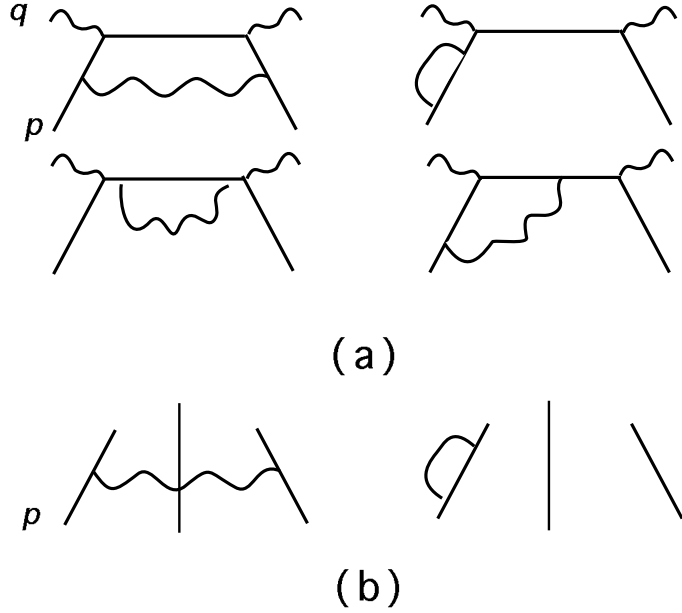


Figure 19: (a) Uncut corrections to quark DIS. (b) One-loop corrections to distribution of a quark in a quark in $A^+ = 0$ gauge.

The phase space of the gluon is reduced to a transverse momentum integral by fixing the longitudinal momentum carried by the upper quark line to ξp . The remaining integral is, as expected, divergent at $k_T = 0$, corresponding to a collinear divergence from gluon emission. As anticipated above, it is also ultraviolet divergent. Such a scaleless integral must be defined to vanish in dimensional regularization. This does not mean that the distribution is zero, however. Rather, the scaleless k_T integral is replaced by a ξ -dependent ultraviolet counterterm, which removes the unphysical contribution of transverse momenta much larger than the factorization scale [39]. In this manner, we define the $\overline{\text{MS}}$ distribution at one loop as a “pure counterterm”. Adding the contribution of the virtual diagram, which is proportional to $\delta(1 - \xi)$, we find the explicit expression

$$\phi_{f/f}^{(1)}(\xi, \mu^2) = \frac{\alpha_s}{2\pi} \left(\frac{1}{-\epsilon} + \gamma_E - \ln 4\pi \right) P_{q/q}^{(1)}(\xi), \quad (97)$$

where the distribution $P_{q/q}^{(1)}$ is given by

$$P_{q/q}^{(1)}(\xi) \equiv C_F \left\{ (1 + \xi^2) \left[\frac{1}{1 - \xi} \right]_+ + \frac{3}{2} \delta(1 - \xi) \right\}. \quad (98)$$

For reasons that will become clear shortly, $P_{q/q}^{(1)}$ is referred to as an “evolution kernel”. The “plus distribution” is defined through its integrals with smooth functions $f(\xi)$ by

$$\int_x^1 d\xi f(\xi) \left[\frac{1}{1 - \xi} \right]_+ = \int_0^1 d\xi \left(\frac{f(\xi) - f(1)}{1 - \xi} \right) - \int_0^x d\xi \frac{f(\xi)}{1 - \xi}. \quad (99)$$

Other distributions $\phi_{i/j}(\xi)$ of parton i in parton j at one loop have exactly the form (97),

$$\phi_{i/j}(\xi, \epsilon) = \frac{\alpha_s}{2\pi} \left(\frac{1}{-\epsilon} + \gamma_E - \ln 4\pi \right) P_{i/j}^{(1)}(\xi) + \dots. \quad (100)$$

Each $P_{i/j}^{(1)}$ is one of the set of evolution kernels,

$$\begin{aligned}
P_{q/q}^{(1)}(\xi) &= C_F [2D(\xi) - 1 - \xi + \frac{3}{2}\delta(1-x)] \\
P_{q/G}^{(1)}(\xi) &= T_F [(1-\xi)^2 + \xi^2] \\
P_{G/q}^{(1)}(\xi) &= C_F \left[\frac{(1-\xi)^2 + 1}{\xi} \right] \\
P_{G/G}^{(1)}(\xi) &= 2C_A [\xi D(\xi) + \left(\frac{1}{\xi} + \xi \right) (1-\xi) + \frac{11}{12} \delta(1-\xi)] - \frac{1}{3} n_f \delta(1-\xi), \quad (101)
\end{aligned}$$

where $D(\xi) \equiv [1/(1-x)]_+$.

At zeroth order in the strong coupling, we have

$$\phi_{f'/f}^{(0)}(\xi) = \delta_{f'f} \delta(1-\xi), \quad (102)$$

for any flavors f and f' , which simply states that without interaction parton f remains itself. Then, at lowest order in (90) we recover the partonic results

$$F_2^{(f)}(x) = Q_f^2 \delta(1-x) = C_2^{(f)}(x). \quad (103)$$

Finally, the perturbative coefficient functions may be determined from the one-loop expansion of eq. (90). For instance, at one loop, we have (using (102) and (103)),

$$F_2^{(f,1)}(x, Q^2) - \sum_{f'} Q_{f'}^2 x \phi_{f'/f}^{(1)}(x) = C_2^{(f,1)} \left(x, \frac{Q^2}{\mu^2}, \alpha_s(\mu^2) \right). \quad (104)$$

At one loop, the electromagnetic structure functions of fig. 19a are (for details of the calculation, see [41, 11])

$$\begin{aligned}
F_2^{(f,1)} &= Q_f^2 x \left[\frac{\alpha_s}{2\pi} \frac{1}{(-\epsilon)} P_{q/q}^{(1)} \left(1 - \epsilon \gamma_E + \epsilon \ln \frac{4\pi\mu^2}{Q^2} \right) \right. \\
&\quad + C_F \left\{ (1-x^2) \left(\frac{\ln(1-x)}{1-x} \right)_+ - \frac{3}{2} \frac{1}{(1-x)_+} \right. \\
&\quad \left. \left. - \left(\frac{9}{2} + \frac{\pi^2}{3} \right) \delta(1-x) - (1+x^2) \frac{\ln x}{1-x} + 3 + 2x \right\} \right] \\
F_1^{(f,1)} &= \frac{1}{2x} F_2^{(f,1)} - Q_f^2 C_F \frac{\alpha_s}{2\pi} x. \quad (105)
\end{aligned}$$

The determination of one-loop quark coefficient functions in the $\overline{\text{MS}}$ and DIS schemes is now a matter of subtraction, using (97) and (105) in (104) for $\overline{\text{MS}}$, and then (93)-(95) for the DIS scheme.

4.4 Evolution

The coefficient functions C_a in eq. (90) depend, beyond lowest order, on the momentum transfer Q^2 . This ‘‘scale breaking’’ is a refinement on the scaling behavior of the parton model. The

dependence of the coefficient functions, and hence of the structure functions themselves, on momentum transfer can be computed.

The factorization formulas eq. (90) depend, as we have seen, on a factorization scale μ , at which short and long distances are separated. μ may be interpreted, in turn, as the renormalization scale associated with the $\overline{\text{MS}}$ renormalized parton densities, matrix elements such as eq. (88). In a manner analogous to composite operators in the operator product expansion, the parton densities have calculable μ -dependence. This remarkable result is referred to as “evolution”. Because the coefficient functions depend on Q only through the ratio Q/μ , their evolution in μ determines their dependence on Q . This enables us to relate structure functions and parton densities measured at one scale to other scales, greatly extending the applicability of perturbative analysis.

It is simplest to illustrate evolution with a “nonsinglet” distribution. An example is the difference between proton and neutron structure functions,

$$F_a^{(NS)} = F_a^{(p)} - F_a^{(n)}, \quad (106)$$

which combines the contributions of the two nucleon states weighted by (twice) their isospin. In this combination, the contributions of gluons and “sea” quark pairs produced in virtual processes cancel, leaving factorized expressions for the $F_a^{(NS)}$ in terms of “valence” quark distributions $\phi^{(\text{val})}$. In this case, we have the difference between p and n valence distributions of each flavor, but for massless quarks the coefficient functions are all the same up to factors of Q_f^2 , and we may suppress partonic indices,

$$F_1^{(NS)} = \int_x^1 \frac{d\xi}{\xi} C_1^{(NS)} \left(x/\xi, Q^2/\mu^2, \alpha_s(\mu^2) \right) \phi^{(\text{val})}(\xi, \mu^2). \quad (107)$$

Under moments with respect to x , defined as

$$\bar{f}(n) \equiv \int_0^1 dx x^{n-1} f(x), \quad (108)$$

the nonsinglet structure function factors into a product of moments, one for the parton distribution and one for the coefficient function,

$$\bar{F}_1^{(NS)}(n, Q^2) = \bar{C}^{(NS)} \left(n, Q^2/\mu^2, \alpha_s(\mu^2) \right) \bar{\phi}^{(\text{val})}(n, \alpha_s(\mu^2)). \quad (109)$$

The essential ingredient in evolution is the independence of the physical structure functions from the factorization scale μ ,

$$\mu \frac{d}{d\mu} \bar{F}_1^{(NS)}(n, Q^2) = 0. \quad (110)$$

Given (107) and (110), ϕ and C obey the joint evolution equations,

$$\mu \frac{d}{d\mu} \ln \bar{\phi} \left(n, \alpha_s(\mu^2) \right) = -\gamma_n \left(\alpha_s(\mu^2) \right) = -\mu \frac{d}{d\mu} \ln \bar{C}_1^{(NS)} \left(n, Q^2/\mu^2, \alpha_s(\mu^2) \right). \quad (111)$$

The anomalous dimension γ_n is a function of α_s only, since this is the only variable which ϕ and C have in common.

Logarithmic Q^2 dependence in moments of F may conveniently be computed from (111) by setting $\mu = Q$, and solving for the μ dependence of $\bar{\phi}(n)$. Contributions from $\bar{C}(n)$ will then be a simple expansion in $\alpha_s(Q)$, since all logarithms of Q/μ will vanish. The relevant solution for $\bar{\phi}$ is

$$\begin{aligned}\bar{\phi}^{(\text{val})}(n, \mu^2) &= \bar{\phi}^{(\text{val})}(n, \mu_0^2) \exp \left\{ -\frac{1}{2} \int_0^{\ln \mu^2/\mu_0^2} dt \gamma_n(\alpha_s(\mu_0^2 e^t)) \right\} \\ &= \bar{\phi}^{(\text{val})}(n, \mu_0^2) \exp \left\{ -\frac{2\gamma_n^{(1)}}{b_2} \int_0^{\ln \mu^2/\mu_0^2} \frac{dt}{t + \ln(\mu_0^2/\Lambda^2)} + \dots \right\},\end{aligned}\quad (112)$$

where $\gamma_n(\alpha_s) = (\alpha_s/\pi)\gamma_N^{(1)} + \dots$. Using the asymptotically free running coupling eq. (21) in the second line of (112), we find that the resulting μ (and hence Q) dependence is logarithmic in QCD, which accounts for the mild nature of scale breaking. For a frozen coupling, or one that runs to a finite value, scale breaking is power-law in Q , in apparent contradiction to the successes of the parton model. This is a fundamental success of quantum chromodynamics, which played a central role in its acceptance. Indeed, the results described here meet the challenge set in Section 2 above, to use asymptotic freedom to account for the approximate scaling of DIS in the presence of multiple scales.

Although the analysis we have just described is particularly simple for moments, in most practical cases, it is best to work with the parton distributions themselves. The full set of moment evolution equations (111) are very conveniently summarized by the celebrated DGLAP (Dokshitzer-Gribov-Lipatov-Altarelli-Parisi) [7] integro-differential equation for the $\phi_{i/h}(x, \mu)$,

$$\mu \frac{d^2}{d\mu^2} \phi_{i/h}(x, \mu^2) = \sum_{j=f, \bar{f}, G} \int_x^1 \frac{d\xi}{\xi} P_{ij}(\frac{x}{\xi}, \alpha_s(\mu^2)) \phi_{j/h}(\xi, \mu^2), \quad (113)$$

where the distributions P_{ij} summarize a matrix of “singlet” anomalous dimensions as their moments,

$$\int_0^1 d\xi \xi^{n-1} P_{ij}(\xi, \alpha_s) = -\gamma_{ij}(n). \quad (114)$$

The $P_{ij}(x, \alpha_s)$ are power series in the strong coupling given to one loop by the distributions above, for instance,

$$P_{qq}(x, \alpha_s) = \frac{\alpha}{\pi} P_{q/q}^{(1)}(x) + \dots. \quad (115)$$

Eq. (113) is one of the most useful tools in perturbative QCD and in the search for new physics, since it enables us to connect experiments at widely differing momentum transfers, and to predict the outcomes of experiments even at very high energy.

4.5 The light-cone expansion

Before generalizing factorization beyond DIS, it is useful to acquire some insight into the field-theoretic content of evolution. Consider the moments of a nucleon quark distribution, taken

for simplicity in $A^+ = 0$ gauge⁵ (and supressing the spin average),

$$\begin{aligned}
\bar{\phi}_{a/N}(n, \alpha_s(\mu^2)) &= \frac{1}{2\pi} \int_0^1 dx x^{n-1} \int_{-\infty}^{\infty} dy^- e^{-iy^- x p^+} \langle N(p) | \bar{q}(y^-) \gamma^+ q(0) | N(p) \rangle \\
&= \frac{1}{2\pi} \sum_{m=0}^{\infty} \frac{1}{m!} \langle N(p) | \left[(\partial^+)^m \bar{q}(0) \right] \gamma^+ q(0) | N(p) \rangle \\
&\quad \times \int_0^1 dx x^{n-1} \int_{-\infty}^{\infty} dy^- (y^-)^m e^{-iy^- x p^+} \\
&= \frac{1}{(p^+)^n} \langle N(p) | \left[(-i\partial^+)^{n-1} \bar{q}(0) \right] \gamma^+ q(0) | N(p) \rangle. \tag{116}
\end{aligned}$$

In the second equality, we have formally expanded the \bar{q} field about $y^- = 0$, that is, on the light cone, and in the third we have done, first, the resulting y^- integrals to get delta functions, and then the x integrals (treating $\int_0^1 dx \delta(x) = 1$). We see that only a single term contributes to the sum, corresponding to the *local* product of the quark field with the $n - 1$ st derivative of its conjugate. Thus, moments of parton distributions are related to local operators, with dimensions that increase with the moment variable n .

This rough discussion can be carried out in an arbitrary gauge, and the full set of relevant gauge-invariant operators found in this manner is

$$\mathcal{O}_f^{\mu_1 \dots \mu_n} = \bar{q}(0) \left(\prod_{i=1}^{n-1} i D^{\mu_i} [A] \right) \gamma^{\mu_n} q(0) \tag{117}$$

for quarks and

$$\mathcal{O}_G^{\mu_1 \dots \mu_n} = F^{\mu_1}{}_{\alpha}(0) \left(\prod_{i=2}^{n-1} i D^{\mu_i} [A] \right) F^{\alpha \mu_n}(0) \tag{118}$$

for gluons, with $D_\mu = \partial_\mu + igA_\mu$ the covariant derivative (in covariant gauges, ghost operators may also contribute in general, but not to physical matrix elements).

These operators occur in the expansion of the product of electromagnetic currents at short distances,

$$J^\mu(\text{em})(x) J_\mu^{\text{(em)}}(0) = \sum_{n=0}^{\infty} \sum_I C_{n,I} \left(x^2, \mu^2, \alpha_s(\mu^2) \right) x_{\mu_1} \dots x_{\mu_n} \mathcal{O}_I^{\mu_1 \dots \mu_n}(0), \tag{119}$$

where they are distinguished by the behavior of their coefficient functions near the light-cone $x^2 = 0$,

$$C_{n,I} \left(x^2, \mu^2, \alpha_s(\mu^2) \right) \sim (x^2)^{-2} h_I(x^2 \mu^2, \alpha_s(\mu^2)). \tag{120}$$

This singularity is identified by dimensional counting: the product of two currents has (mass) dimension 6, while the operators in (117) and (118) have dimension $3 + (s - 1) = 2 + s$, with s the (maximum) spin (*i.e.*, number of vector indices), while the corresponding factors of x^μ contribute mass dimension $-s$. The power behavior of the coefficient function for any such

⁵Notice that $\partial/\partial y^- = \partial^+ = \partial_-$.

tensor operator of spin s and dimension D is thus $(x^2)^{-3+(D-s)/2}$. The short-distance expansion organized according to light-cone singularities is known as the *light-cone expansion* [42].

The quantity $D - s$ is called the “twist”. All operators in eqs. (117) and (118) have twist equal to two. Twist controls singularities on the light cone, and hence the high- q^2 behavior of the Fourier transforms of the products of currents, the DIS structure function. For DIS, then, the effect of Minkowski space is to elevate an infinite set of (twist-two) operators to leading behavior.

Note that the light-cone $x^2 = 0$ corresponds to the manifold $x^+ = 0$ when the momentum p is in the plus direction. It is thus not the light cone along which the target particle moves, but rather the opposite-moving light cone, corresponding to a light-like scattered parton in the “brick-wall” frame. Of course, the scattered parton is not always in the opposite direction, but all the details of final states are absorbed into the hard scattering function H of fig. 17 and eq. (86). This is another consequence of factorization. From the point of view of calculating long-distance behavior in the parton distribution, the entire scattering process may be replaced by a pair of Wilson lines, as in eq. (91). There is a strong similarity here to the effective field theory picture often used to discuss the dynamics of heavy quarks [43], and indeed, the symmetries of heavy-quark effective theory are closely related to the universality properties of parton distributions, to which we now turn.

4.6 Hard hadron-hadron scattering

Once we introduce the concept of factorization, it is natural to apply it beyond inclusive DIS [1, 44]. Of course, we must be careful to consider only inclusive hard-scattering processes, for which we may hope to find the necessary incoherence between the short-distance scattering and long-distance hadronic binding effects.

In an important example, we consider processes in which a quark from hadron h annihilates an antiquark from hadron h' , forming a virtual electroweak vector boson, which decays to a lepton pair. This reaction,

$$h(p) + h'(p') \rightarrow \ell\ell'(Q^\mu) + X, \quad (121)$$

with its characteristic signal of a lepton pair (momentum Q^μ), is known as the Drell-Yan process [45]. Its observation was one of the early successes of parton ideas, especially because it signals the presence of a sea of quark pairs within ordinary hadrons.

It is easy to write a factorization formula for such a cross section, by a straightforward generalization of the expressions for DIS structure functions, eq. (90). It is a convolution of two parton distributions, one for each hadron, with a hard-scattering function H . At lowest order, H is given by the Born cross section for quark pair annihilation to the relevant leptons.

At higher orders, gluon-quark scattering may also contribute,

$$\frac{d\sigma_{hh' \rightarrow Q^2}(s, Q^2)}{dQ^2} = \sum_{i,j=f,\bar{f},G} \int_0^1 d\xi d\xi' \phi_{i/h}(\xi, \mu^2) H_{ij} \left(\frac{Q^2}{\xi \xi' s}, \frac{Q^2}{\mu^2}, \alpha_s(\mu^2) \right) \phi_{j/h'}(\xi', \mu^2). \quad (122)$$

As in DIS, the hard-scattering function is a power series in $\alpha_s(\mu^2)$. H depends on the scheme chosen for the parton distributions. As an example, for $H_{f\bar{f}}$, we have, to one loop in DIS scheme [41],

$$H_{f\bar{f}} = \frac{d\sigma_{f\bar{f}}^{(\text{Born})}}{dQ^2} \left(\delta(1-z) + \frac{\alpha_s}{\pi} \left\{ C_F[(1+z^2) \left(\frac{\ln(1-z)}{1-z} \right)_+ + 3 \left[\frac{1}{1-z} \right]_+ - 6 - 4z - \ln z] + \left(\frac{4\pi^2}{3} + 1 \right) \delta(1-z) \right\} \right), \quad (123)$$

where $z = Q^2/\xi \xi' s$. Given phenomenological parton distributions in some scheme, the factorization formula gives an absolute prediction for the Drell-Yan cross section, which has been successfully applied to a wide range of experiments. The corrections in H are not always small, however, and as we shall see, we sometimes need information about contributions at arbitrarily high power.

Another application of parton model ideas, extended to perturbative QCD, involves single-particle inclusive cross sections, which count hadrons at fixed momenta, but are otherwise inclusive in the hadronic final state,

$$h(p) + h'(p') \rightarrow C(p_C) + X. \quad (124)$$

If the hadron (C) is observed, for instance, at large transverse momentum, we know that a hard scattering has taken place, and may hope that incoherence and hence factorization is relevant [46, 47]. In this case, the parton model suggests that the hadron C arises from the “hadronization”, or fragmentation, of some parton k . The process of hadronization should, following our discussion of Section 1, occur over time scales that are independent of the hard-scattering scale, and of the fragmentation of other partons, scattered in other directions. Hadron C is thus expected to be produced in a universal fashion from parton k , and to inherit a fraction $0 \leq z \leq 1$ of that parton’s momentum. The (incoherent) probability for this evolution is summarized in a “fragmentation function” $d_{C/k}(z, \mu^2)$, which describes the distribution of hadrons in the fragments of a parton, and is analogous to the parton distribution $\phi_{i/h}$, but with the roles of hadron and parton reversed. In perturbation theory, d must be renormalized, and thus it depends on the factorization scale μ . The corresponding factorization formula for single-particle inclusive cross sections is

$$\omega_C \frac{d\sigma_{hh' \rightarrow C(p_C)}(p, p', p_c)}{d^3 p_C} = \sum_{i,j,k=f,f,G} \int_0^1 d\xi d\xi' \frac{dz}{z^2} H_{ijk} \left(\frac{\mu^2}{\xi \xi' s}, \frac{p_C \cdot \xi p}{z \mu^2}, \frac{p_C \cdot \xi' p'}{z \mu^2}, \alpha_s(\mu^2) \right) \times \phi_{i/h}(\xi, \mu^2) \phi_{j/h'}(\xi', \mu^2) d_{C/k}(z, \mu^2). \quad (125)$$

The extra factor $1/z^2$ allows H to be normalized to the corresponding Born cross section for $i + j \rightarrow k + X$.

Like parton distributions, fragmentation functions are universal, within a given scheme to define them, and the same functions appear in hadron-hadron scattering, DIS and e^+e^- annihilation. Also like parton distributions, their μ -dependence may be analyzed, and summarized by evolution equations [39]. We shall not go into these applications here, however. Rather, we shall close this section with a few comments on how generalizations of DIS factorization are established in perturbation theory.

4.7 Jet-soft analysis

The proof of factorization theorems [1, 44, 48] like those described above is highly nontrivial in perturbation theory, and, indeed, has not reached the sophistication of technical treatments of the operator product expansion in Euclidean space. We may, however, briefly discuss a few relevant physical issues.

The essential complication in demonstrating the factorization of hadron-hadron cross sections is evident in the relevant pinch surfaces, shown in fig. 20. The jets of the two incoming

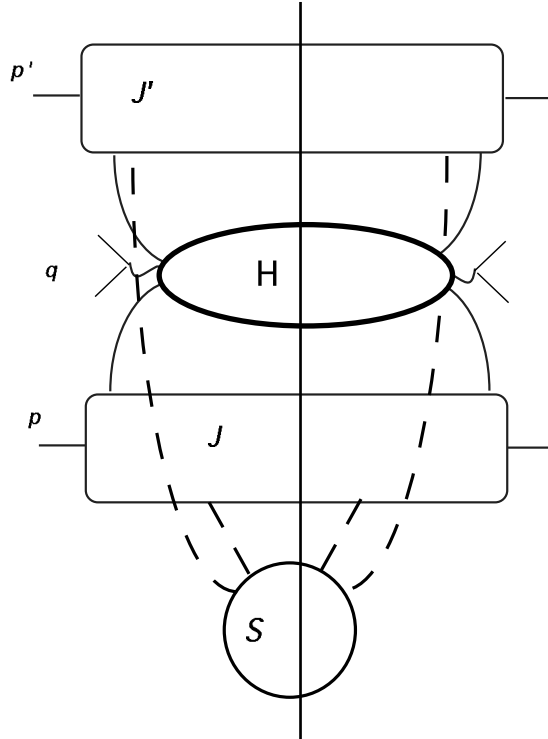


Figure 20: General reduced diagram for pinch surface of a Drell-Yan cross section. The subdiagram H includes possible final-state jets, and for lack of space the Drell-Yan pair is reversed in direction.

hadrons are connected by soft gluons, whose momenta vanish at the pinch surface. Roughly, this corresponds to the scattering of partons in each hadron from the Coulomb fields of partons in the other hadron before and/or after the hard scattering. Final-state interactions are present as well in DIS, and we expect them to cancel by unitarity arguments; initial-state interactions, however, are special to hadron-hadron scattering, and could, in principle, lead to a rearrangement of color, and even transverse momentum, of the partons in each hadron, due to the presence of the other hadron. Such a rearrangement could, in turn, affect the hard scattering, and break the universality necessary to identify the parton distributions of hadron-hadron collisions with those of DIS. This does not happen, however, for the following physical reasons.

We recognize that the quanta of perturbation theory are gauge fields A^μ , which include unphysical as well as physical degrees of freedom. Physical information is associated with field strengths, $F_{\mu\nu}$, and the latter behave very differently than the former under Lorentz boosts. In particular, the field strengths are strongly Lorentz contracted, while the unphysical polarization of A^μ , proportional to the momentum of each gluon, actually grows under Lorentz boosts. Thus, we expect the effects unphysical polarizations to contribute in individual diagrams in perturbation theory, but to cancel in a gauge invariant sum over diagrams.

Such an analysis requires, in addition to the identification of pinch surfaces and power counting, an application of the Ward identities of the theory that decouple unphysical gluons from physical processes. Let us sketch how this can be done, taking as an example connections of soft lines to a final-state jet, as shown in fig. 21.

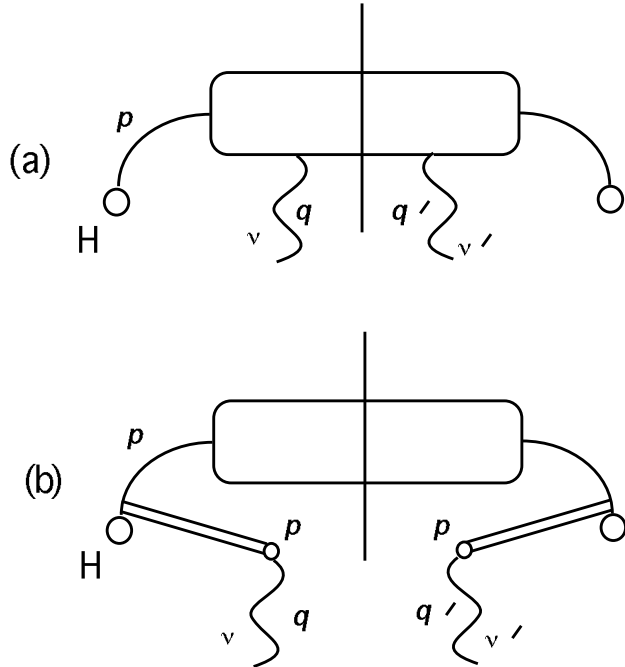


Figure 21: (a) Reduced diagram in which soft lines connect to a final-state jet. (b) Factorization of soft lines.

At a typical pinch surface, soft lines, q to the left of the cut, and q' to the right, are attached to the jet, which we may take in the plus direction, with large momentum component p^+ . We may define both soft momenta to flow into the jet, and then along jet lines away from the final state and toward the hard scattering functions H . For each jet line along which a soft momentum flows the momentum is then of the form $\ell - q$ for lines to the left of the cut (amplitude) and $\ell + q$ to the right (complex conjugate amplitude). Here ℓ is the momentum of a jet line in the absence of the extra soft momentum, and is hence naturally parameterized as

$$\ell = (xp^+, \ell^-, \ell_\perp), \quad (126)$$

with $0 < x \leq 1$. For ℓ a jet momentum, we can assume that xp^+ is its largest component. We can now make two approximations that will enable us to factor the soft gluons from the jet, replacing their couplings by an effective eikonal line. The first is that the coupling of the gluons' propagators $G_{\nu\lambda}(q)$ to the jet is always through the combination $p^\nu G_{\nu\lambda}(q)$, that is, that the soft gluons couple only to the large component of the current. The second is that propagator denominators $(\ell + q)^2$, depend only upon the minus component of the soft gluon's momenta, *i.e.* the components in the direction opposite to the jet direction,

$$(\ell \pm q)^2 \sim \pm 2xp^+q^- + \ell^2. \quad (127)$$

We shall return to this condition in a moment.

Once these approximations are made, the jet depends only on one component of each soft gluons' momentum, and on the same component of its polarization. Thus the coupling of soft gluons to a jet moving in the plus direction is equivalent to the coupling of a set of gluons with *only* minus momenta and *only* minus polarizations. Such gluons are unphysical, and are equivalent to a phase rotation on the external lines of the jet, which attach to the hard scatterings. In an abelian theory, for instance, an arbitrary jet with one vector (photon) attached to each side of the cut, is equivalent to a jet with no photons, multiplied by two linearized propagators (“eikonal lines”), one for each of the photons,

$$J_2^{\nu\nu'}(p, \hat{q}, \hat{q}') \sim J_2^{++}(p, \hat{q}, \hat{q}') = g^2 \frac{p^{\nu'}}{p^+q'^- - i\epsilon} \frac{p^\nu}{-p^+q^- + i\epsilon} J_0(p), \quad (128)$$

where $J_0(p)$ is the jet with no soft photon connections and where

$$\hat{q}^\mu = (0, q^-, \mathbf{0}). \quad (129)$$

The factors on the right of (128) are of the form of the propagator and vertex in eq. (92) with $n = p$. The eikonal lines here are illustrated in fig. 21b.

In a nonabelian theory, multiple gluons still factor, and their color interactions are summarized by connections to eikonal Wilson lines, which have the same perturbation theory rules for lines and vertices as those in eq. (91) for DIS parton distributions. Schematically, we write

$$J_n^{+\cdots+}(p, \hat{q}_i, \hat{q}'_j) = E^*(\{q'_j\}) E(\{q_i\}) J_0(p), \quad (130)$$

where the E 's are generated from the operators

$$U(A) = \exp \left[-ig \int_0^\infty d\lambda \, p \cdot A(\lambda p) \right]. \quad (131)$$

The soft divergences factorized in this manner cancel [47, 1], due to the unitarity of the Wilson lines,

$$U[A]^\dagger \, U[A] = I. \quad (132)$$

To realize this cancellation, it is necessary to sum over all final states that differ by soft gluon emission. This, of course, is exactly what we do in inclusive hard-scattering cross sections. Given this cancellation, the remaining jets are independent of each other, and may be factored from the hard scattering as in DIS.

The argument that we have given above is, of course, quite rough. In particular, the approximation (127), is highly nontrivial [1]. It is clearly not true for every soft momentum q^μ , since it fails whenever q^- vanishes compared to the other components of q^μ . The approximation will hold, however, if the q^- integral is not trapped at or very near zero. Arguments to this effect are relatively easy to give for many cross sections in e^+e^- annihilation, where we verify that all the poles in q^- from lines within the jet, $(\ell \pm q)^2 \mp i\epsilon$, are in the upper half-plane for soft gluon momenta routed as above. The situation is much more difficult when the jet originates from an incoming hadron, as in the Drell-Yan process. Here, pinches may occur on a diagram-by-diagram basis, as in fig. 22, where the lines $xp+q$ and $(1-x)p-q$ have q^- poles in opposite half-planes. These pinches cancel, however, in sufficiently inclusive cross sections,

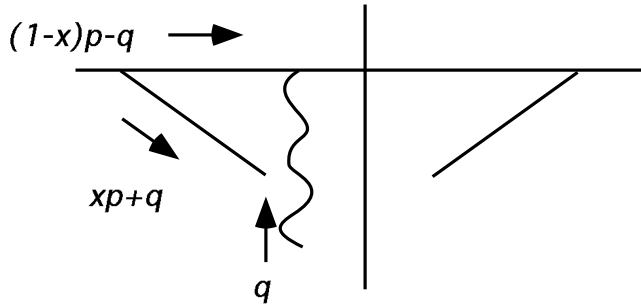


Figure 22: Reduced diagram for which q^- is pinched close to zero.

for the physical reasons that we have outlined above, and soft gluons that are not in the jet direction decouple from incoming as well as outgoing jets [1, 48].

We now ask when a soft gluon is close enough to a jet's direction to be part of that jet. Let us consider the case when the two momenta in eq. (127) are both on-shell, *i.e.*, $q^2 = \ell^2 = 0$. To factor q from the p -jet we require, in particular, that

$$xp^+q^- > |\ell_\perp \cdot q_\perp|. \quad (133)$$

This condition has a natural geometrical interpretation, which itself has important physical consequences. For a well-collimated jet, $\theta_\ell = |\ell_\perp|/(xp^+)$ is the angle of ℓ^μ to the overall jet

direction. Defining θ_q similarly, and parameterizing $q^+ = yp^+$, we have

$$|\ell_\perp| = \theta_\ell p^+, \quad |q_\perp| = \theta_q p^+, \quad q^- = \frac{q_\perp^2}{2p^+}. \quad (134)$$

Using these relations it is easy to show that the soft gluon q will factorize from the jet, *i.e.* eq. (127) will hold, *unless*

$$\theta_q < \theta_\ell, \quad (135)$$

that is, unless q is emitted closer to the jet axis than ℓ , the particle that emitted it. This “angular ordering” [49], limits the region of phase space into which soft gluons may be emitted late in jet evolution, and hence suppresses the multiplicity of very soft gluons, since gluons that factor from the jet do not get enhancements from pinch surfaces where jet lines are near the mass shell. This is one of the many consequences of the coherence of gluon emission in QCD [20].

5 Two-scale problems I: Sudakov resummation

The factorization theorems of the previous section go far toward connecting perturbative QCD to experiment. Their application, however, is limited somewhat by our assumption that there is only a single large scale in the problem, for instance, Q^2 in DIS. In this case, it is natural to choose the factorization scale to be of order of Q , and to use the evolution of the parton distributions discussed above. The coefficient function is then of the general form

$$C(x/\xi) = \sum_n d_n(x/\xi) \alpha_s^n, \quad (136)$$

where $d_n(z)$ is a distribution in z . Then, if $\alpha_s(Q^2)$ is small, we may hope that the effect of higher-order terms in C is small as well.

Unfortunately, this is not always the case even in DIS; the $d_n(z)$ will generally include factors like $\alpha_s^n \ln^n(z)/z$, or even $\alpha_s^n \ln^{2n-1}(1-z)/(1-z)$. When x is very small, or very close to unity, these logarithms may produce large corrections at every order. Recalling that $(p+q)^2/Q^2 = (1-x)/x$, we see that in both cases the arguments of the logarithms are ratios of kinematic invariants. There are many other such examples, all with two hard scales, Q_1^2 and Q_2^2 , which satisfy

$$Q_1^2 \gg Q_2^2 \gg \Lambda^2. \quad (137)$$

The first inequality ensures the presence of a large ratio in the hard scattering function. The second ensures that parton densities evolve perturbatively, and that the running coupling in the hard scattering function, $\alpha_s(Q_2^2)$ is small, even if the combination $\alpha_s(Q_2^2) \ln(Q_1^2/Q_2^2)$ is not. In this case, we may try to “resum” the series in $\ln(Q_1^2/Q_2^2)$ to all orders in perturbation theory.

We shall treat three representative cases: $T \rightarrow 1$, with T the thrust, eq. (80), in e^+e^- annihilation, $Q_T \ll Q$ for Drell-Yan production of pairs of mass Q , and $x \rightarrow 0$ in deeply

inelastic scattering. The first and second illustrate the resummation of so-called ‘‘Sudakov’’ double logarithms, and the second and third illustrate resummations based on an extension of factorization to fixed transverse momenta.

5.1 Sudakov double logarithms

Let us return for a moment to our dimensionally-regulated expression for one-loop corrections, eq. (44), to the electromagnetic form factor,

$$\Gamma_\mu(q^2, \epsilon) = -ie\mu^\epsilon \bar{u}(p_1)\gamma_\mu v(p_2) \rho(q^2, \epsilon). \quad (138)$$

At one loop, its momentum-dependence is contained in an overall factor $(-q^2)^{-\epsilon}$, which we may expand to order ϵ^2 to get an expansion in $\ln q^2$,

$$\rho(q^2, \epsilon) = 1 - \frac{\alpha_s}{4\pi} C_F \ln^2(q^2/\mu^2) + \dots \quad (139)$$

The double logarithms in momentum transfer are another reflection of the overlap of collinear and soft singularities in the vertex function, and are generally referred to as Sudakov double logarithms [8, 50, 51]. Although the electromagnetic vertex is not infrared safe, it is an important element in any process whose kinematics approaches those of elastic scattering.

Our first example [52] is the e^+e^- annihilation cross section near unit thrust, $T = 1$. Here the double logarithms appear not in Q^2 directly, but in $(1 - T)$. Consulting the definition of thrust, eq. (80), we see that at $T = 1$ the final state consists of two back-to-back massless jets. A little kinematics also shows that when both jet masses p_i^2 are small compared to Q^2 they are related to the thrust by

$$1 - T = \frac{p_1^2 + p_2^2}{Q^2}. \quad (140)$$

At order α_s^n the leading logarithm in $1 - T$ is given by an exponential of Sudakov logarithms,

$$\frac{1}{\sigma_{\text{tot}}} \frac{d\sigma}{dT} = -2C_F \frac{\alpha_s}{\pi} \frac{\ln(1 - T)}{1 - T} \exp \left\{ -C_F \frac{\alpha_s}{\pi} \ln^2(1 - T) \right\}. \quad (141)$$

As T approaches one, $\frac{d\sigma}{dT}$ vanishes. This is a quantum-mechanical reflection of the classical radiation field that must accompany any process in which a charged particle is accelerated (quark pair creation being an extreme example). Quantum field theory assembles this classical field out of many soft and collinear gluons (the correspondence principle). Cross sections in which gluon emission is forbidden in part of phase space are correspondingly suppressed.

5.2 Factorization for $T \rightarrow 1$

Our goal in the following is to rederive eq. (141), and to extend it to include nonleading logarithms and the effects of the running coupling. Our arguments apply to a large class of

cross sections. In fact, the resummation of Sudakov logarithms follows from the factorization properties of the cross section in the regions of momentum space that give rise to the logarithms. This factorization has already been illustrated by the physical picture of annihilation given in fig. 15, which shows a two-jet configuration. The infrared divergences associated with such configurations cancel, according to the arguments of Section 3.3, but for $T \sim 1$, the cancellation between diagrams with virtual and real gluons is constrained by the requirements that the real gluons be either very soft or emitted very close to the quark or antiquark directions. This leaves large finite remainders in the cancellation of divergences. These are the logarithms of $1 - T$.

Let us recall the power counting arguments of section 2.3. We saw there that in an axial gauge, $\xi \cdot A = 0$, all collinear divergences may be absorbed into the jets. As a result, in such gauges, double logarithms arise from collinear gluons in jets which become soft, while staying collinear. The form of fig. 15, combined with the factorization of soft gluons from jets, described in Section 4.7 above, suggests that the thrust cross section, like Drell-Yan, factorizes into functions that describe the two jets, the hard, and the soft subdiagrams. At double logarithmic accuracy in axial gauge, therefore, we may neglect soft gluons that connect the jets to each other. This approximation will simplify the arguments below, without changing the character of a more general treatment, which gives an essentially equivalent result, but is accurate to all logarithmic order. At fixed values of jet masses p_i^2 , we shall therefore begin with the factorized expression

$$\frac{d\sigma}{dp_1^2 dp_2^2} = J_1(p_1, \mu, \xi) J_2(p_2, \mu, \xi) H(p_1, p_2, \mu, \xi), \quad (142)$$

where the J 's represent the jets, and H the hard-scattering factor. We shall suppress particle labels, but it is relatively easy to show from power counting that to leading *power* in $1 - T$ the jets are connected to the hard scattering by a quark and antiquark only. Eq. (142) is enough to derive the exponentiated double logarithms of eq. (141) above, with corrections due to the running of the coupling.

In axial gauge the jets depend, not only on their invariant momenta, but also on their energies through the products $p_i \cdot \xi$. The jets and H are thus not individually Lorentz invariant. For a general gauge vector ξ^μ , the precise arguments are $p_i \cdot \xi / \sqrt{\xi^2}$ because the gluon propagator, and hence J is invariant under simple rescalings of ξ^μ . (In the following, we set $\xi^2 = 1$.)

In view of eqs. (140) and (142), the cross section at fixed $1 - T \sim 0$ is of a convolution form

$$\begin{aligned} \frac{1}{\sigma_0} \frac{d\sigma}{dT} &\simeq \int_0^{Q^2} dp_1^2 dp_2^2 \delta \left(1 - T - \frac{p_2^2}{Q^2} - \frac{p_2^2}{Q^2} \right) H \left(p_1 \cdot \xi / \mu, p_2 \cdot \xi / \mu, \alpha_s(\mu^2) \right) \\ &\quad \times J_1 \left(p_1^2 / \mu^2, p_1 \cdot \xi / \mu, \alpha_s(\mu^2) \right) J_2 \left(p_2^2 / \mu^2, p_2 \cdot \xi / \mu, \alpha_s(\mu^2) \right). \end{aligned} \quad (143)$$

Dividing by the Born cross section σ_0 gives $H = 1$ at lowest order. Because we are interested in the limit $p_i^2/Q^2 \rightarrow 0$, the p_i may be expanded about back-to-back lightlike momenta. We

choose axes so that p_1^μ is in the plus direction and p_2^μ is in the minus direction. Then p_1^+ and p_2^- are both nearly equal to $Q/\sqrt{2}$, while

$$p_1^- \sim \frac{p_1^2}{\sqrt{2}Q}, \quad p_2^+ \sim \frac{p_2^2}{\sqrt{2}Q}. \quad (144)$$

For ξ in an arbitrary direction, we may take $p_1 \cdot \xi \sim p_1^+ \xi^-$ and $p_2 \cdot \xi \sim p_2^- \xi^+$ to leading power in Q . Then to leading power in $1 - T$, the p_i^2 integrals are independent of $p_i \cdot \xi$.

We want to identify singular $\ln^m(1 - T)/(1 - T)$ behavior for $T \rightarrow 1$, and for this purpose moments with respect to T are particularly useful,

$$\tilde{\sigma}(n) = \frac{1}{\sigma_0} \int_0^1 dT T^n \frac{d\sigma}{dT}, \quad (145)$$

since the moments of any function that is finite at $T = 1$ falls off as $1/n$ for $n \rightarrow \infty$. In particular, logarithms of $1 - T$ are transformed into logarithms of n by

$$\int_0^1 dT \frac{T^n - 1}{1 - T} \ln^m(1 - T) = \frac{(-1)^m}{m+1} \ln^{m+1} n + \dots \quad (146)$$

Keeping only terms that are finite or grow as $n \rightarrow \infty$, and using the relation $T^n \sim e^{-n(1-T)}$, which holds in this approximation, we find that the convolution in (143) factors into a simple product under moments,

$$\begin{aligned} \tilde{\sigma}(n) = & \tilde{J}_1 \left(Q^2/n\mu^2, p_1 \cdot \xi/\mu, \alpha_s(\mu^2) \right) \tilde{J}_2 \left(Q^2/n\mu^2, p_2 \cdot \xi/\mu, \alpha_s(\mu^2) \right) \\ & \times H \left(p_1 \cdot \xi/\mu, p_2 \cdot \xi/\mu, \alpha_s(\mu^2) \right), \end{aligned}$$

up to corrections that vanish as $1/n$. Note that n now appears only in the combination $Q^2/n\mu^2$. By analogy to the derivation of evolution for DIS structure functions, we shall use this factorized expression, coupled with renormalization group arguments, to derive a resummed cross section. The new feature in our Sudakov factorization is the dependence on the axial gauge vector ξ . Although each of the factors that makes up $\tilde{\sigma}$ is ξ -dependent, the physical quantity $\tilde{\sigma}$ must be gauge-invariant. This invariance will drive the resummation [51].

5.3 Resummation for $T \rightarrow 1$

We start with the renormalization group behavior of J , which is simple, since it has only two external (quark or antiquark) lines,

$$\left[\mu \frac{\partial}{\partial \mu} + \beta \frac{\partial}{\partial g} \right] \ln \tilde{J} = -2\gamma_q, \quad (147)$$

with γ_q the quark anomalous dimension. Since the cross section is independent of the renormalization scale μ , H must behave in a corresponding fashion

$$\left[\mu \frac{\partial}{\partial \mu} + \beta \frac{\partial}{\partial g} \right] \ln H = 4\gamma_q. \quad (148)$$

We now observe that very similar reasoning may be applied to the gauge-fixing vector ξ .

Let us change (boost) ξ^+ and ξ^- in a manner that leaves $\xi^2 = 1$. Using the discussion after eq. (142), the independence of $\tilde{\sigma}(n)$ from ξ^μ may be expressed as $\partial\tilde{\sigma}/\partial\ln\xi^- = -\partial\tilde{\sigma}/\partial\ln\xi^+$. The chain rule then gives

$$\frac{\partial\ln\tilde{J}_2(Q^2/n\mu^2, p_2^-/\mu)}{\partial\ln p_2^-} + \frac{\partial\ln H(p_1^+/\mu, p_2^-/\mu)}{\partial\ln p_2^-} = -\frac{\partial\ln\tilde{J}_1(Q^2/n\mu^2, p_1^+/\mu)}{\partial\ln p_1^+} - \frac{\partial\ln H(p_1^+/\mu, p_2^-/\mu)}{\partial\ln p_1^+}, \quad (149)$$

where we have made components explicit and have suppressed α_s . This relation is surprisingly powerful, because J_1 , J_2 and H depend on different sets of arguments. J_2 , for instance, depends on both p_2^- and $Q^2/n\mu^2$. Its derivative with respect to p_2^- may depend upon either of these arguments, but must be cancelled in (149) by the derivatives of H and J_1 , which contribute additively. Thus, its dependence on p_2^- and $Q^2/n\mu^2$ can only be additive after the derivative,

$$\frac{\partial}{\partial\ln p_2^-}\ln\tilde{J}_2\left(\frac{Q^2}{n\mu^2}, \frac{p_2^-}{\mu}, \alpha_s(\mu^2)\right) = K\left(\frac{Q^2}{n\mu^2}, \alpha_s(\mu^2)\right) + G\left(\frac{p_2^-}{\mu}, \alpha_s(\mu^2)\right). \quad (150)$$

The function K cancels a corresponding term from J_1 while G cancels the contribution from H , whose derivatives must satisfy,

$$\frac{\partial\ln H}{\partial\ln p_1^+} + \frac{\partial\ln H}{\partial\ln p_1^+} = -G\left(\frac{p_2^-}{\mu}\right) - G\left(\frac{p_1^+}{\mu}\right). \quad (151)$$

This separation of short-distance and long-distance dependence in jets is characteristic of Sudakov factorization. As the gauge changes, the jets exchange contributions with each other (via K) and with the hard part (via G). Here we find a strong analogy to the “matching conditions” of effective field theory.

We now have at our disposal two evolution equations, the first relying on invariance under renormalization group rescalings, the other on gauge invariance, but both based on factorization. Combining the two, we shall find enough information to determine all logarithmic n -dependence.

By eq. (147), $(d\ln J_i/d\mu)$ is independent of momenta, so, for instance

$$\frac{d^2}{d\mu dp_1^+}\ln J_1 = 0. \quad (152)$$

Applying this result to (150), we conclude that the combination $K+G$ is itself a renormalization group invariant

$$\mu\frac{d}{d\mu}(K+G) = 0, \quad (153)$$

which implies that yet another anomalous dimension relates K and G [50, 51, 53],

$$\mu\frac{d}{d\mu}K = -\gamma_k(\alpha_s) = -\mu\frac{d}{d\mu}G. \quad (154)$$

Now we can relate the moment-dependence of K and G through

$$\begin{aligned} K\left(\frac{Q^2}{n\mu^2}, \alpha_s(\mu^2)\right) + G\left(\frac{Q}{\mu}, \alpha_s(\mu^2)\right) &= K\left(1, \alpha_s(Q^2/n)\right) + G\left(1, \alpha_s(Q^2)\right) \\ &\quad - \frac{1}{2} \int_{Q^2/n}^{Q^2} \frac{d\mu'^2}{\mu'^2} \gamma_K\left(\alpha_s(\mu'^2)\right), \end{aligned} \quad (155)$$

in which all logarithms of n are generated either through the running coupling and/or the explicit μ' integral. There are only two steps left, to solve for the n -dependence of the J 's and to combine everything together in the cross section.

Combining eqs. (150) and (155), we derive the full evolution of J_2 in terms of p_2^- , an exactly similar equation holding for J_1 in terms of p_1^+ ,

$$\frac{\partial}{\partial \ln p_2^-} \ln J_2 = K(1, \alpha_s(Q^2)) + G(1, \alpha_s(Q^2)) - \frac{1}{2} \int_{Q^2/n}^{Q^2} \frac{d\lambda^2}{\lambda^2} \Gamma_J(\alpha_s(\lambda^2)). \quad (156)$$

Here Γ_J combines γ_K with a term that allow us to have the same running coupling in K and G ,

$$\begin{aligned} \Gamma_J(\alpha_s) &= \gamma_K(\alpha_s) + \beta(g) \frac{\partial}{\partial g} K(1, \alpha_s) \\ &= \left(\frac{\alpha_s}{\pi}\right) 2C_F + \left(\frac{\alpha_s}{\pi}\right)^2 \left[\left(\frac{67}{18} - \frac{\pi^2}{6}\right) C_F C_A - \left(\frac{5}{9}\right) n_f C_F \right]. \end{aligned} \quad (157)$$

In the second line, we have given the two-loop expression for Γ_J , where as usual n_f is the number of quark flavors.

It is now a simple applications of the chain rule to derive a differential equation for the n -dependence of both jets,

$$\left[\frac{\partial}{\partial \ln n} + \frac{1}{2} \beta \frac{\partial}{\partial g} \right] \ln J\left(\frac{Q^2}{n\mu^2}, \frac{Q}{\mu}, \alpha_s(\mu^2)\right) = \frac{1}{2} \Gamma'_J\left(\alpha_s(\mu^2)\right) - \frac{1}{2} \int_{Q^2/n}^{Q^2} \frac{d\lambda^2}{\lambda^2} \Gamma_J\left(\alpha_s(\lambda^2)\right), \quad (158)$$

where we have set $p_i \cdot \xi = Q$ and where

$$\Gamma'_J\left(\alpha_s(\mu^2)\right) \equiv G_J\left(1, \alpha_s(Q^2)\right) + K_J\left(1, \alpha_s(Q^2)\right) - 2\gamma_q\left(\alpha_s(\mu^2)\right). \quad (159)$$

The solution of eq. (158) relates J at large n to J at $n = 1$ ⁶,

$$\begin{aligned} \ln J\left(\frac{Q^2}{n\mu^2}, \frac{p'^-}{\mu}, \alpha_s(\mu^2)\right) &= \ln J\left(\frac{Q^2}{\mu^2}, \frac{p'^-}{\mu}, \alpha_s(\mu^2/n)\right) \\ &\quad - \frac{1}{2} \int_{Q^2/n}^{Q^2} \frac{d\lambda^2}{\lambda^2} \left[\ln \frac{\mu}{\lambda} \Gamma_J\left(\alpha_s(\lambda^2)\right) - \Gamma'_J\left(\alpha_s(\lambda^2)\right) \right]. \end{aligned} \quad (160)$$

If we now set $\mu = Q$, all logarithms of n are generated by the integrals of the two anomalous dimensions Γ and Γ' and the expansion of $\alpha_s(Q^2/n)$, and, as promised, exponentiate in the moments of J .

⁶One way to verify this result is to observe that $\beta(g)\partial\Gamma(\alpha_s(\lambda^2))/\partial g = \lambda\partial\Gamma(\alpha_s(\lambda^2))/\partial\lambda$.

The resummed expression (160) for the jets organizes all logarithms of n in the moments of the cross section, since the hard function H has no $\ln n$ -dependence. The inverse transform of $\tilde{J}(n)$ then gives the singular $1 - T$ -dependence. To be explicit, the inverse Mellin transform of \tilde{J} in (160) is given by [52, 54]

$$J\left((1-x)\frac{Q^2}{\mu^2}, \frac{Q}{\mu}, \alpha_s(\mu^2)\right) |_{\mu=Q} = \left[\frac{e^{E(1-x, \alpha_s(Q^2))} \left[\frac{1}{\pi} \sin(\pi_1 P_1) \Gamma(1 + P_1) + \dots \right]}{1-x} \right]_+, \quad (161)$$

where $1 - x \equiv p^2/Q^2$, and where the exponent E is given by the right-hand side of (160) with $\mu = Q$,

$$E = -\frac{1}{2} \int_{(1-x)Q^2}^{Q^2} \frac{d\lambda^2}{\lambda^2} \left[\ln\left(\frac{\mu}{\lambda^2}\right) \Gamma_J(\alpha_s(\lambda^2)) - \Gamma'_J(\alpha_s(\lambda^2)) \right] + \ln \tilde{J}(1, 1, \alpha_s((1-x)Q^2)), \quad (162)$$

while P_1 is related to the exponent by

$$P_1 \equiv -\frac{dE(1-x, \alpha_s(Q^2))}{d\ln(1-x)}. \quad (163)$$

Terms omitted in eq. (161) are suppressed by powers of p^2/Q^2 . It is a straightforward matter to verify that the leading logarithms in $1 - T$ in eq. (141) are indeed generated by this form. Here, however, we see the essential role of the running coupling for nonleading logarithms. In particular, because of asymptotic freedom, the exponent receives relatively larger contributions from long distances, and relatively smaller contributions from short distances than in the case of a fixed coupling. We shall return to the consequences of this observation in the final section below.

5.4 k_T -factorization for the Drell-Yan cross section

As another example of the variety of interesting cross sections to which a variant of (142) applies, consider Drell-Yan cross sections at measured pair mass squared Q^2 and transverse momentum, Q_T . (The discussion below follows the extraordinary analysis of Collins and Soper for transverse momentum distributions in e^+e^- annihilation [51].) Here again a factorization holds in convolution form, but now the convolution is in terms of the transverse momenta of gluons emitted from jet functions associated with the incoming hadrons, along with “central” soft gluons from the soft subdiagram of fig. 20. For the Sudakov resummation of logarithms of Q_T in the Drell-Yan cross section, a convolution in transverse momentum will play the role of the convolution in jet mass for the thrust distribution. Otherwise, the reasoning is quite similar.

Explicitly, the convolution is [55]

$$\begin{aligned} \frac{d\sigma_{hh'}}{dQ^2 d^2 Q_T} &= \sum_f \int d\xi d\xi' \int \frac{d^2 k_T d^2 k'_T d^2 k_{T,s}}{(2\pi)^6} \\ &\times P_{f/h}(\xi, k_T) P_{\bar{f}/h'}(\xi', k'_T) H_{f\bar{f}}(Q^2) S(k_{T,s}) \delta^2(\mathbf{Q}_T - \mathbf{k}_T - \mathbf{k}'_T - \mathbf{k}_{s,T}), \end{aligned} \quad (164)$$

which factorizes under a Fourier transform,

$$\begin{aligned}\tilde{W}(bQ, Q^2) &= \sigma_0^{-1} \int d^2 Q_T e^{-i \mathbf{Q}_T \cdot \mathbf{b}} \frac{d\sigma_{hh'}}{dQ^2 d^2 Q_T} \\ &\cong \sum_f \int \frac{d\xi}{\xi} \frac{d\xi'}{\xi'} \tilde{P}_{f/h}(\xi, b\mu, Q/\mu) \tilde{P}_{\bar{f}/h'}(\xi', b\mu, Q/\mu) S(b\mu),\end{aligned}\quad (165)$$

where $\sigma_0 = 4\pi\alpha^2/9Q^2s$, the Born cross section, summarizes the hard part H to leading order in α_s . The jet functions are defined as matrix elements of quark fields separated by a spacelike vector $(0^+ y^-, \mathbf{b})$,

$$\tilde{P}_{\delta/h}(\xi, b\mu, p^+/\mu) = \int \frac{dy^-}{4\pi} e^{-i\xi p^+ y^-} \langle h(p) | \bar{q}_f(0^+, y^-, \mathbf{b}) \gamma^+ q_f(0) | h(p) \rangle, \quad (166)$$

where we suppress an average over spin. These matrix elements are gauge-dependent, but in any axial gauge they absorb all double logarithms of b (or Q_T in momentum space). At $b = 0$, they are normalized to the quark distributions eq. (88). The gauge vector plays the same role as in the case of thrust, and the jet matrix elements obey a noncovariant evolution equation that separates their dependence on hard and soft scales,

$$\frac{\partial}{\partial \ln Q} \ln \tilde{P} = K_P(b\mu, \alpha_s(\mu^2)) + G_P\left(\frac{Q}{\mu}, \alpha_s(\mu^2)\right), \quad (167)$$

where the combination $K_P + G_P$ is renormalization scale invariant,

$$\mu \frac{d}{d\mu} (K_P + G_P) = 0. \quad (168)$$

Following essentially the same reasoning as for the n dependence of the jets in the thrust cross section, the logarithmic dependence of the jets exponentiates in the transform (b) space,

$$\tilde{P}_{f/h} \approx \exp \left\{ -\frac{1}{2} \int_{1/b^2}^{Q^2} \frac{d\lambda^2}{\lambda^2} \left[\ln \left(\frac{Q^2}{\lambda^2} \right) \Gamma_J(\alpha_s(\lambda^2)) + B(\alpha_s(\lambda^2)) \right] \right\} \phi_{f/h}(\xi, 1/b^2)(1 + \alpha_s(1/b^2)), \quad (169)$$

with Γ_J as in eq. (157) and B a power series in α_s . This approximation holds in the range of b for which $Q \gg 1/b \gg \Lambda$, and organizes all perturbative logarithms of Q_T/Q in the cross section.

Sudakov resummation may be relevant to any cross section with an underlying hard-soft-jet factorization. The exponentiation of logarithms requires a convolution in phase space, like (164) or (143). Applications include threshold corrections (where the relevant variable is $1-z = 1-Q^2/\xi\xi' s$) for the inclusive Drell-Yan cross section [54, 56] (122) as well as other, purely QCD cross sections such as top or jet production [57]. Another important case involves transverse momentum distributions in e^+e^- annihilation (where the first really complete analysis of such a process was carried out [51]). Yet another example is semileptonic B meson decay at the endpoint of the lepton energy spectrum [58], where the lepton recoils against a jet of hadrons. Undoubtedly, there are others as well.

We now turn to another classic resummation of large logarithms, organized by the BFKL equation.

6 Two-Scale Problems II: Small x and the BFKL equation

The small- x limit of deeply inelastic scattering is one of many cross sections that show a set of enhancements organized by the BFKL (Balitskii-Fadin-Kuraev-Lipatov) equation [9, 59]. Here again a transverse momentum factorization may be used as a starting point, although in a rather different kinematic region from the Drell-Yan cross section just discussed. In DIS, these enhancements appear as logarithms in x at fixed Q^2 . For Q^2 not very large, the quantity $\alpha_s(Q^2) \ln(1/x)$ can be large, and we may be tempted to resum corrections of this sort to all orders. We begin with a brief review of the origin of logs of x in the evolution formalism developed in Section 4 above.

6.1 $x \rightarrow 0$ for DGLAP evolution

Referring to eq. (101) above, the kernel $P_{G/G}^{(1)}$ which describes gluon-to-gluon evolution is singular as $x \rightarrow 0$, so that in the notation of (115) (and using $C_A = N$),

$$P_{GG}(x) = \frac{2N\alpha_s}{\pi} \frac{1}{x} + \dots \quad (170)$$

This behavior produces a pole at $n = 1$ in the corresponding diagonal element of the singlet anomalous dimension matrix, eq. (114),

$$\gamma_{GG}(n) = \frac{2N\alpha_s}{\pi} \frac{1}{n-1} + \dots \quad (171)$$

We now recall the solution to the renormalization group equation for the moment of a DIS structure function $\bar{F}(n, Q^2)$, which follows from eq. (112),

$$\bar{F}(n, Q^2) = \bar{F}(n, Q_0^2) e^{(2\gamma_n^{(1)}/b_2) \ln t}, \quad (172)$$

where $\gamma_n(\alpha_s) = \gamma_n^{(1)} (\alpha_s/\pi) + \dots$, and $t \equiv \ln(Q^2/\Lambda^2)/\ln(Q_0^2/\Lambda^2)$.

For $x \rightarrow 0$, the (inverse) transform from $\bar{F}(n, Q^2)$ to $F(x, Q^2)$,

$$F(x, Q^2) = \int_{-i\infty}^{i\infty} \frac{dn}{2\pi i} e^{-n \ln x + 4N/(b_2(n-1)) \ln t}, \quad (173)$$

has a sharp saddle point at $(n-1) = \sqrt{4N \ln t / (b_2 \ln(1/x))}$, which gives the x behavior

$$F(x, Q^2) \sim e^{4\sqrt{(N/b_2) \ln(1/x) \ln t}}. \quad (174)$$

This striking result shows a rapid increase as $x \rightarrow 0$. It relies, however, on DGLAP evolution, which assumes that $\ln Q^2$ is relatively large. It is natural to ask what happens if x is so small that, for instance, $\ln(1/x) \gg \ln(Q^2/\Lambda^2)$, and to treat the resummation of logarithms of x self-consistently.

6.2 k_T -factorization for DIS; the BFKL equation

The standard DIS factorization, eq. (90), assumes an ordering in transverse momenta, which allows us to decouple the transverse momenta of the partons from the hard scattering. Now, however, we do not wish to treat Q^2 as arbitrarily large, so we generalize (90) to a convolution in *both* ξ and k_T . The k_T -factorized form of a DIS structure function $F(x, Q^2)$ is [60, 61]

$$F(x, Q^2) = \int d^2 k_T \int_x^1 \frac{d\xi}{\xi} C\left(\frac{x}{\xi}, Q, k_T\right) \mathcal{F}(\xi, k_T), \quad (175)$$

with $\mathcal{F}(\xi, k_T)$ a generalized parton distribution at measured x and k_T , and $C(x/\xi, Q, k_T)$ the corresponding coefficient function. Since leading logarithms of x are generated by purely gluonic evolution, we shall restrict ourselves to gluon distributions, neglect mixing, and suppress parton indices. This factorization is illustrated in fig. 23. It is appropriate for the limit Q^2 fixed, $x \rightarrow 0$.

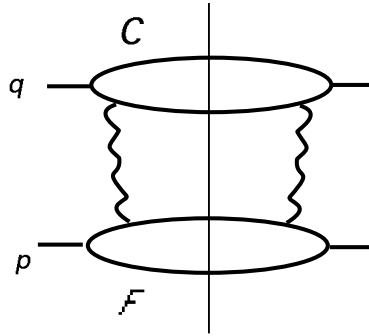


Figure 23: k_T -factorization in DIS.

The leading logarithms of x in (175) are generated by a large set of diagrams. The diagrams that show the relevant mechanism most clearly are the ladders, illustrated by fig. 24. To understand how logarithms of x are produced, we parameterize the momenta flowing on the sides (vertical lines in the figure) in components parallel to the incoming momenta p and q and transverse components,

$$k_i = \alpha_i p + \beta_i q + k_{iT}. \quad (176)$$

Here q is approximated by a lightlike vector, because as $x \rightarrow 0$ the ratio of the photon invariant mass to the center of mass energy vanishes. Logarithms of x result from configurations in which the “light-cone” fractions α_i and β_j are strongly ordered, but the transverse momenta are all of the same order,

$$\begin{aligned} \alpha_1 &\gg \alpha_2 \gg \dots \gg \alpha_{n-1} \\ \beta_1 &\ll \beta_2 \ll \dots \ll \beta_{n-1} \\ k_{iT} &\sim k_{jT}. \end{aligned} \quad (177)$$

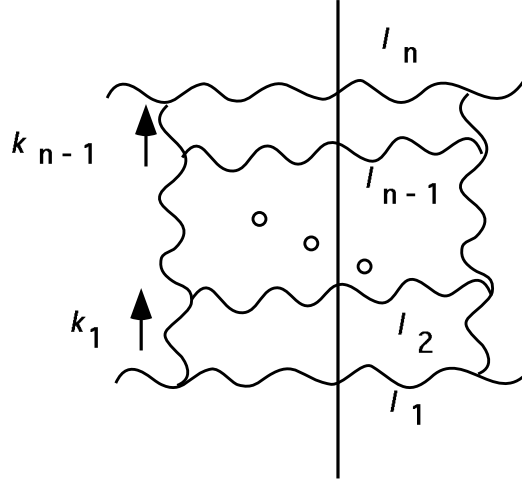


Figure 24: n -gluon cut ladder. In DIS, the photon would attach to a quark loop at the top.

It is the lack of ordering in transverse momentum that distinguishes BFKL evolution. Useful approximations that follow from (177) are

$$\begin{aligned} \sum_{i=1}^j \beta_i &\sim \beta_j, \\ \sum_{i=j}^{n-1} \alpha_i &\sim \alpha_j, \end{aligned} \quad (178)$$

for the lightcone fractions and

$$k_i^2 \sim -k_{i,T}^2, \quad (179)$$

for the invariant masses of lines on the sides of the ladder. The emitted “rungs” of the ladder carry momenta

$$\ell_i = k_{i-1} - k_i, \quad (180)$$

with $k_0 = p$ and $k_n = -q$.

A diagram like fig. 24 with n rungs generates $n - 2$ logarithms of x , which come from ordered logarithmic integrals over the α_i , or equivalently rapidities y_i of the i th rung,

$$y_i = \frac{1}{2} \ln \frac{\alpha_{i-1}}{\beta_i}. \quad (181)$$

It is relatively easy to identify the leading behavior of the ladder diagrams. There are n mass-shell delta functions from the cut rungs, $\delta(\ell_i^2)$. The top-most mass-shell condition fixes $\alpha_{n-1} \sim x$, while the remaining $\delta(\ell_i^2)$ fix $n - 1$ fractions β_i , $i = 1 \dots n - 1$. The leading numerator factor comes from the terms that contract the incoming momenta of the top and bottom vertices to give $(p \cdot q)^2$, while the vertices to which i th rung connects produce a factor of order $|(k_{T,i-1} + k_{T,i}) \cdot \epsilon_i(\ell_i)|^2$, with $\epsilon_i(\ell_i)$ the polarization of the i th emitted gluon. The resulting term is logarithmic in the remaining, ordered α_i integrals, which are each of the form,

$$\int_{\alpha_{i-1}} d\alpha_i / \alpha_i = \int_{y_{i-1}} dy_i, \quad (182)$$

with a minimum value $\alpha_{n-2,\min} = x$. Transverse integrals also give logarithmic power counting on a graph-by-graph basis. The resulting logarithms, however, cancel in the sum over diagrams. This cancellation will be evident in the equation we derive below.

Consider what happens when we insert yet another gluon into an arbitrary diagram, as illustrated in fig. 25. The diagram has been factorized because all of its gluons are already ordered as in (177). To get an additional logarithm from this gluon, it should fit into the

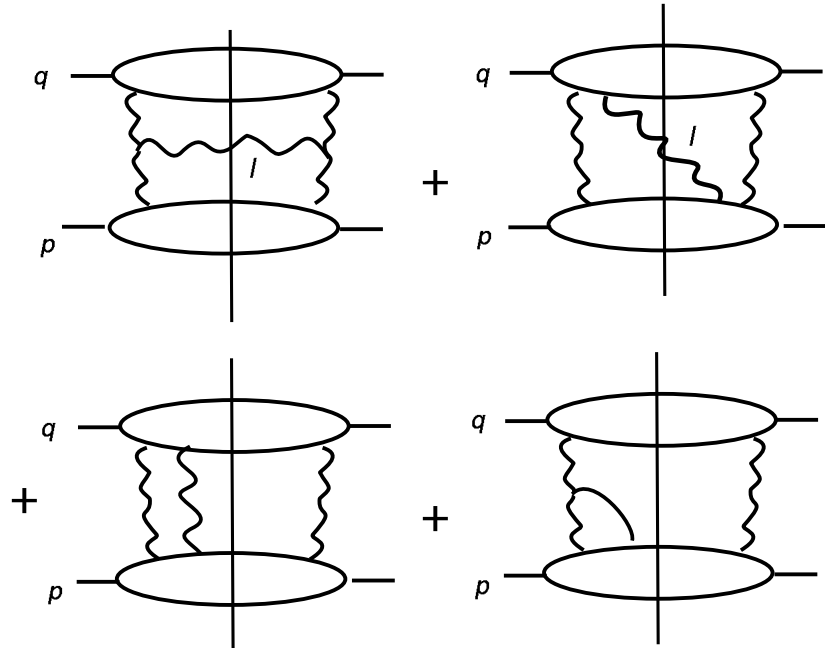


Figure 25: Adding an extra strongly ordered gluon.

rapidity gap between C and \mathcal{F} , and should have a transverse momentum comparable to those of the other gluons. To get the logarithm, however, the “new” gluon, of momentum ℓ , need not itself be inserted as a ladder. The ladder insertion, the first in fig. 25, works, but so do many insertions that connect the vertical gluon and *either* the top or bottom, or even some that connect the top and bottom directly. Similarly, there are additional possibilities for the insertion of a virtual gluon, also illustrated in fig. 25.

To determine when each of these diagrammatic insertions can give logarithms we use strong ordering (177). Because of strong ordering, whenever the momentum ℓ flows along a line of momentum $\ell' + \ell$, say, in C , $(\ell' + \ell)^2 \sim 2\ell' \cdot \ell^+ = 2\alpha_\ell \beta_{\ell'} s$, and analogously for attachments to \mathcal{F} , but with the roles of the fractions α and β reversed.

Luckily, however, it is not really necessary to worry about each diagram individually. Instead, we appeal to the jet-soft analysis of Section 4.7 above. Strong ordering implies that C is sensitive to ℓ^+ only, and \mathcal{F} is sensitive to ℓ^- only. At the same time, it is clear that the + component of the polarization of ℓ is also dominant in its coupling to C , and the minus to \mathcal{F} . We are thus in the situation of eq. (128), fig. 21, and as in that case, the sum of all attachments

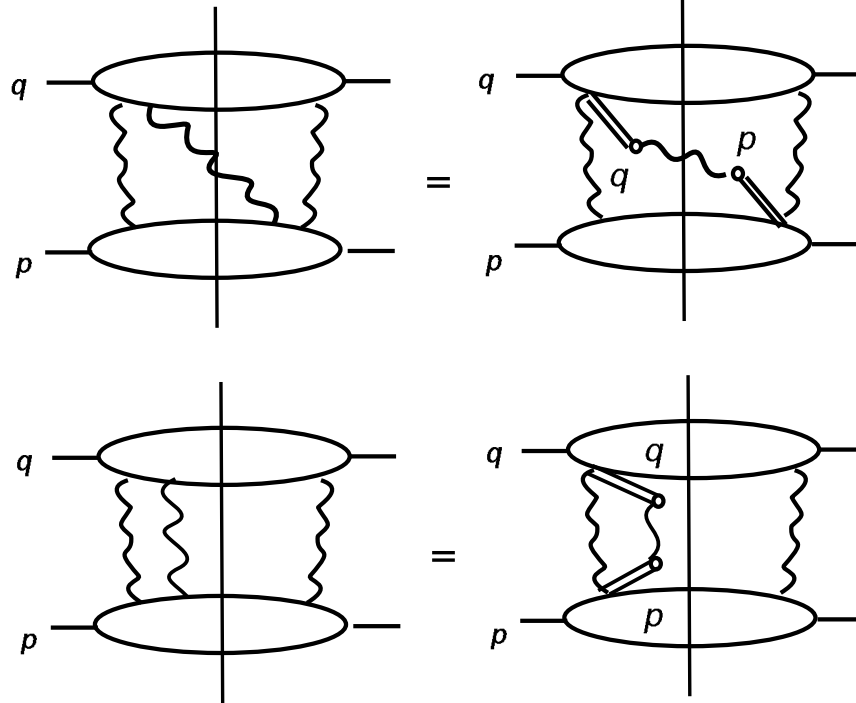


Figure 26: Eikonal factorization of additional strongly ordered gluon.

of the gluon ℓ to either of the subdiagrams C and \mathcal{F} factors from it as in fig. 26, with an eikonal factor

$$\frac{q^\nu(-gC_{abd})}{q \cdot \ell}, \quad (183)$$

for C , and similarly for its connection to \mathcal{F} .

The result of attaching our extra gluon is then summarized by a kernel $\bar{K}(k', k)$, which we illustrate with a cut gluon in fig. 27. The new gluon attaches at either end to a vertex represented by a circle. The eikonal factors themselves (183) are as usual represented by double lines.

Because the α_i integrals are ordered, the separation between \mathcal{F} and C in eq. (175) is at a definite value of α , or equivalently of plus momentum $\ell^+ = \alpha p^+$. We may thus identify the combination of $\mathcal{F}(k)$ and $\bar{K}(k', k)$ in fig. 27 with $\mathcal{F}(k')$, now evaluated at external momentum $k' = k - \ell$. This gives an integral equation for the k_T -dependent jet function \mathcal{F} . Since we know there is a logarithmic integral in ℓ^+ , we write

$$\mathcal{F}(k') = \int_{\alpha p^+} \frac{d\ell^+}{\ell^+} \int d^2 k_T \bar{K}(k'_T, k_T) \mathcal{F}(\ell^+, k_T). \quad (184)$$

Here α plays the role of a factorization scale, separating C and \mathcal{F} . Thinking back to DGLAP evolution for ordered transverse momenta, we derive a new equation by taking a derivative with respect to α ,

$$\alpha \frac{\partial}{\partial \alpha} \bar{\mathcal{F}}(\alpha, k'_T) = \int d^2 k_T K(k'_T, k_T) \bar{\mathcal{F}}(\alpha, k_T)$$

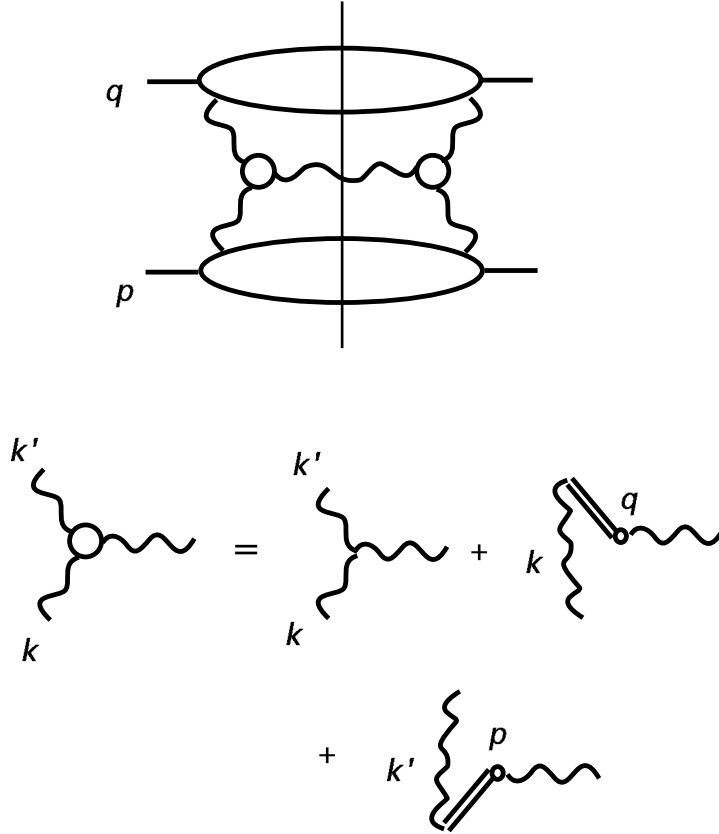


Figure 27: Graphical representation of the BFKL kernel for a cut gluon.

$$= -\frac{\alpha_s N}{\pi^2} \int \frac{d^2 k_T}{(k_T - k'_T)^2} \left\{ \bar{\mathcal{F}}(\alpha, k_T) - \frac{k'^2}{2k_T^2} \bar{\mathcal{F}}(\alpha, k'_T) \right\}, \quad (185)$$

where we have defined

$$\bar{\mathcal{F}}(\alpha, k_T) \equiv \frac{1}{k_T^2} \mathcal{F}(\alpha, k_T). \quad (186)$$

This is the BFKL equation, as it appears in DIS, and $K(k'_T, k_T)$ is called the BFKL kernel. In the second line the kernel has been evaluated explicitly for the diagrams of fig. 27. Details of the evaluation are given in Appendix C. This is only one of many forms in which the kernel is expressed, but it is one of the simplest. Clearly, the first term comes from real-gluon diagrams, for which k'_T is not identically equal to k_T , while the second term comes from virtual gluons.

6.3 Solution of the BFKL equation

Because the BFKL equation (185) is a convolution in k_T , and first order in the derivative with respect to $\ln \alpha$, it is natural to express its solution as an expansion in functions that are powers in α and k_T ,

$$\mathcal{F}_{\omega, \nu}(\alpha, k_T) = c_{\omega, \nu} \alpha^{-\omega} \left(\frac{k_T^2}{\mu^2} \right)^{i\nu - \frac{1}{2}}, \quad (187)$$

where $c_{\omega,\nu}$ and μ^2 are constants. We want to solve for ω , which determines the power-law α -dependence, and the associated power ν for transverse momenta. ν is to be considered as a complex number, so that $i\nu$ is not necessarily imaginary. The extra $-1/2$ in the power of k_T^2 is a matter of convenience. Together, $i\nu - 1/2$ serve as an anomalous dimension appropriate to evolution with a *fixed* coupling (see eq. (112)). From the discussion of DGLAP evolution in Sec. 4.4 above, we recall that logarithms, and hence evolution, in parton distributions arise from transverse momentum integrals. The argument of the running coupling is thus naturally chosen as k_T^2 , which is effectively fixed in our case, because of the strong-ordered kinematics of eq. (177).

Substituting the ansatz (187) into the BFKL equation (185), we readily find an implicit expression that relates ω and ν (see Appendix C),

$$\omega(\nu) \left(\frac{k_T'^2}{\mu^2} \right)^{i\nu - \frac{1}{2}} = \frac{\alpha_s N}{\pi^2} \int d^2 k_T \left\{ \left(\frac{k_T'^2}{\mu^2} \right)^{i\nu - \frac{1}{2}} \frac{1}{(k_T - k_T')^2} - \left(\frac{k_T'^2}{\mu^2} \right)^{i\nu - \frac{1}{2}} \frac{(k_T'^2)}{2k_T^2(k_T - k_T')^2} \right\}. \quad (188)$$

The infrared divergences of each term on the right-hand side of this expression cancel, as may be seen by carrying out the integrals via dimensional regularization, and the explicit relation between ω and ν is

$$\omega(\nu) = -\frac{2\alpha_s N}{\pi} \left(\text{Re } \psi \left(i\nu + \frac{1}{2} \right) - \psi(1) \right), \quad (189)$$

where the special function ψ is the logarithmic derivative of the gamma function,

$$\begin{aligned} \psi(x) &= \frac{d}{dx} \ln \Gamma(x), \\ \psi(1) &= -\gamma_E. \end{aligned} \quad (190)$$

Another common form for the relation (189) is found by defining

$$\gamma \equiv i\nu + \frac{1}{2}, \quad (191)$$

in terms of which

$$\omega(\gamma) = -\frac{\alpha_s N}{\pi} (\psi(\gamma) + \psi(1 - \gamma) - 2\psi(1)). \quad (192)$$

A general solution to the BFKL equation for DIS may be written as a superposition of power-law solutions,

$$\mathcal{F}(x, k_T) = \int_{-\infty}^{\infty} d\nu x^{-\omega(\nu)} \left(\frac{k_T^2}{\mu^2} \right)^{i\nu - \frac{1}{2}}. \quad (193)$$

The small- x limit is dominated by a saddle-point of ω as a function of ν , in much the same way as the small- x behavior from DGLAP evolution in eq. (173) above. In this case there is a saddle point at $\nu = 0$, as may be seen from the series found by expanding the ψ functions,

$$\omega(\nu) = \frac{2\alpha_s N}{\pi} \left(2 \ln 2 + \sum_{k=1}^{\infty} (-1)^k (2^{2k+1} - 1) \zeta(2k+1) \nu^{2k} \right), \quad (194)$$

with $\zeta(2k+1)$ the zeta function $\zeta(x) = \sum_n (1/n^x)$. This leads to the (famous) asymptotic behavior [9]

$$\mathcal{F}(x, q_T) \sim x^{-4N \ln 2(\alpha_s/\pi)} (q_T^2)^{-1/2}, \quad (195)$$

in which we see a power-law enhancement as x vanishes, much stronger than in DGLAP evolution, eq. (174).

The BFKL formalism was originally developed [9] to describe hadron-hadron scattering in QCD, both the total cross section and the closely-related Regge limit [62], t fixed, $s \rightarrow \infty$. The $t = 0$ Regge limit is related to the $x \rightarrow 0$ limit in DIS by the following “translation”,

$$\begin{aligned} (p+q)^2 &= \frac{1-x}{x} Q^2 \rightarrow s \\ x^{-\omega_0} &\rightarrow s^{\omega_0} \\ F(x) &\rightarrow \sigma_{\text{tot}} \sim s^{\omega_0}. \end{aligned} \quad (196)$$

Thus, at $t = 0$, σ_{tot} grows as a power of s in this approximation. In fact, the total cross section for hadron-hadron scattering does increase at high energy, although an uninterrupted power-law rise would violate unitarity, as embodied in the Froissart bound [62]. The BFKL behavior that we have just derived therefore cannot be the final answer.

Although the dominant BFKL power (195) is infrared finite, in most applications, such as the total cross section, there is no natural perturbative scale at which to evaluate α_s . The scale of k_T introduced above is, after all, quite arbitrary. There are, however, two-jet correlations [63] for which BFKL resummation is naturally infrared safe, with a coupling fixed at a perturbative scale of the order of the transverse momenta of the jets. The dominance of resummed leading logarithms in such cross sections may require very high energy [64]. Another infrared safe application of the BFKL formalism is to hypothetical heavy-quark onium-onium scattering, in which the inverse size of the onium wave function serves as an infrared cutoff [65]. This model is serving as a valuable laboratory for the study of forward scattering in a self-consistent perturbative context.

At least two sets of corrections can lead to a softening of the BFKL or “bare” pomeron, nonleading logarithms and nonleading powers (higher twist). “Nonleading logarithms” refers to higher powers of α_s at a fixed power of $\ln s$. One approach is to derive nonleading terms in the expansion of the kernel $K(k, k')$ [67]. Another is to compute exchanges of multiple ladders [66]. Indeed, a multiladder generalization of the BFKL equation [68] may be used as an inspiration for a picture of forward scattering in terms of two-dimensional field theories. In these investigations, QCD comes into contact with conformal field theory and the theory of exactly soluble models.

In addition, ladders may interact with each other, a process that produces “shadowing”, the softening of parton distributions due to the spatial overlap of partons with small momentum fractions [69]. If shadowing is a small correction, it is a higher-twist effect. Higher-twist need

not mean small, however, because when the overlap large, it destroys the incoherence at the basis of the partonic formulation, and all twists become equally important.

The field of small- x dynamics is especially compelling because at very small x , but large Q^2 , the density of partons is high, even while the coupling $\alpha_s(Q^2)$ remains small [69]. Such a dense, but weakly coupled system promises a new testing ground for field theory, with a close relation to the physics of nonabelian plasmas. Even before such an asymptotic condition is understood, however, there are many plausible applications of small- x resummation and k_T -factorization [61] to current phenomenology, whenever a hard scattering occurs at scale Q^2 , with $Q^2 \ll s$. For example, much attention has been given to the production of jets and heavy quarks in this regime. Discussions of some of these developments are found elsewhere in this volume.

We have barely scratched the surface of the physics of two-scale problems here. The representative examples described above, however, may give a sense of how far it is possible, and necessary, to go beyond low-order perturbation theory in QCD. In the next section, we shall encounter another extension of the formalism, in which long- and short-distances mix, even in cross sections with a single hard scale.

7 High Orders in Perturbation Theory

Throughout these lectures, we have used the singularities of perturbation theory as a diagnostic for long-distance behavior, and as a guide for organizing the relation of short to long distances. In this section, we shall briefly discuss yet another aspect of perturbation theory that gives hints of nonperturbative structure, its behavior at high orders [70, 71].

Recall the relation between the total e^+e^- annihilation cross section and the imaginary part of the two-current correlation function, eqs. (75) and (76),

$$\sigma_{e^+e^-}^{(\text{tot})} \sim \int d^4x e^{iqx} \langle 0 | J^\mu(x) J_\mu(0) | 0 \rangle, \quad (197)$$

with J_μ an electromagnetic current. As in eq. (119), we can apply the operator product expansion, but now, because there is no “external” momentum in the matrix element, only the expectation values of scalar operators can contribute, and only a few operators appear with singularities at $x^2 = 0$ in the operator product expansion,

$$J^\mu(x) J_\mu(0) \sim \frac{1}{x^6} C_0(x^2 \mu^2) I + \frac{m}{x^2} C_q(x^2 \mu^2) \bar{q}q(0) + \frac{1}{x^2} C_F(x^2 \mu^2) F_{\mu\nu} F^{\mu\nu}(0) + \dots, \quad (198)$$

with I the identity operator, which does not contribute to DIS. Perturbation theory with all masses set to zero contributes at any finite order to $C_0(x^2 \mu^2)$ only. Yet, as we shall now see, there is a problem with C_0 from high orders, which suggests the presence of the higher terms in the operator product expansion, even in the absence of explicit quark masses.

Our reasoning begins with the pinch surfaces of C_0 , which we have already identified in Sec. 3.2, fig. 13, in which a purely soft subdiagram S , consisting entirely of zero-momentum lines, is attached to a single hard subdiagram H . Near the pinch surface, all soft momenta may be neglected in H , which may therefore be treated effectively as a gauge-invariant local vertex. Consider any single gluon internal to subdiagram S , whose momentum we label k . S may formally be written as

$$S = \int d^4k \frac{g^{\alpha\beta}}{k^2} T_{\alpha\beta}(k, \mu, \alpha_s(\mu)), \quad (199)$$

where we have isolated the k propagator (in Feynman gauge) and where $T_{\alpha\beta}$ is the remainder of the subdiagram, as in fig. 28. Dimensional counting and gauge invariance then require $T_{\alpha\beta}$

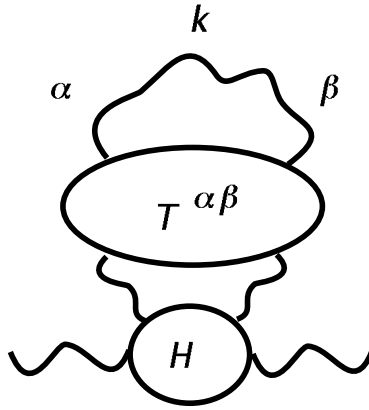


Figure 28: Reduced diagram for a soft pinch surface.

to have the form

$$T_{\alpha\beta}(k, \mu, \alpha_s(\mu)) = \left(k^2 G_2(k^2) \right) (k_\alpha k_\beta - k^2 g_{\alpha\beta}) t \left(k^2/\mu^2, \alpha_s(\mu^2) \right), \quad (200)$$

where $G_2(k)$ is the normalized trace of the full gluon propagator. Neglecting for simplicity any renormalization of the vertex H , the function t is renormalization-group invariant,

$$\mu \frac{d}{d\mu} t(k^2/\mu^2, \alpha_s(\mu^2)) = 0, \quad (201)$$

from which we conclude that we may choose $\mu^2 = k^2$ as we integrate over k , at the cost of running the coupling to the scale k^2 ,

$$\begin{aligned} t \left(k^2/\mu^2, \alpha_s(\mu^2) \right) &= t \left(1, \alpha_s(k^2) \right) \\ &= \sum_i a_i \alpha_s^i(k^2), \end{aligned} \quad (202)$$

with the a_i numbers. We can already see something funny by looking at the resulting a_1 term for S . Using the one-loop running coupling, we find

$$S^{(1)} = -3 \int_0^Q d^4k k^2 \frac{\alpha_s(k^2)}{k^2}$$

$$\begin{aligned}
&= -12\pi \int_0^{Q^2} dk^2 k^2 \frac{\alpha_s(Q^2)}{1 + \frac{\alpha_s(Q^2)}{4\pi} b_2 \ln \frac{k^2}{Q^2}} \\
&= -12\pi Q^4 \alpha_s \sum_n \left(\alpha_s \frac{b_2}{4\pi} \right)^n \int_0^1 dx x \ln^n \frac{1}{x} \\
&= -6\pi Q^4 \alpha_s \sum_n \left(\alpha_s \frac{b_2}{8\pi} \right)^n \Gamma(n+1),
\end{aligned} \tag{203}$$

where in the last two lines we have reexpanded the running coupling in terms of $\alpha_s(Q^2) \equiv \alpha_s$. As a result, the n th order in α_s has a coefficient that grows like $\Gamma(n+1) = n!$. This is despite the infrared safety of the matrix element. Evidently, this uncontrolled growth in perturbative coefficients is a direct reflection of the singularity in the running coupling. All is not lost, however, although this behavior will require us to reevaluate how we regard the perturbative expansion in QCD.

A very useful conceptual tool for treating high orders in a perturbative series is the Borel transform. Consider a general power series in an expansion variable, in this case α_s ,

$$\Pi(\alpha_s) = \sum_{n=0}^{\infty} c_n \alpha_s^n, \tag{204}$$

with the c_n constants. If $\Pi(\alpha_s)$ is analytic at $\alpha_s = 0$, the c_n are coefficients in a Taylor series expansion. This need not always be the case, however. We are interested in the case when the c_n grow, and Π may possess no radius of convergence at all about $\alpha_s = 0$. Nevertheless, there is a good deal of information in the expansion (204). To see why, we define the Borel transform of $\Pi(\alpha_s)$ by

$$\tilde{\pi}(b) = \sum_{n=0}^{\infty} \frac{c_n}{n!} b^n. \tag{205}$$

It is an expansion in a conjugate variable b , whose expansion coefficients are simply $c_n/n!$. $\tilde{\pi}(b)$ is thus much more convergent than $\Pi(\alpha_s)$ is, and has a finite radius of convergence about $b = 0$ even when the c_n grow as fast as $n!$. Formally, the inverse transform from $\tilde{\pi}$ back to Π is

$$\Pi(\alpha_s) = \alpha_s^{-1} \int_0^{\infty} db e^{-b/\alpha_s} \tilde{\pi}(b), \tag{206}$$

since the integral over b precisely generates $n! \alpha_s^{n+1}$ from the b^n term. Factorial growth in the expansion coefficients of Π now shows up as a singularity in $\tilde{\pi}$. If this singularity is on the real axis, the inverse transform is an ambiguous integral even if $\tilde{\pi}$ is known as a function. Even if the singularity is off the real axis, its presence indicates contributions to Π that cannot be described fully by the series (204), *i.e.*, nonperturbative contributions.

Returning to our example $S^{(1)}$ above, we observe that a simple change of variables,

$$b' = \frac{\alpha_s(Q^2)}{4\pi} \ln(Q^2/k^2), \tag{207}$$

in the second line of eq. (203) leads to an expression for $S^{(1)}$ that is precisely of the inverse Borel form,

$$S^{(1)}(Q^2) = -48\pi^2 \alpha_s^{-1} Q^4 \int_0^{\infty} db' \frac{e^{-8\pi b'/\alpha_s(Q^2)}}{(1 - b_2 b')} . \tag{208}$$

Here $1/(1 - b_2 b')$ plays the role of the Borel transform of $S^{(1)}$, and its singularity is a direct reflection of the singularity in the perturbative running coupling at $k^2 = \Lambda^2$. Any such singularity in the plane of the Borel variable due to the infrared behavior of the running coupling is called an infrared renormalon.

Although (208) is ill-defined, we have gained something by reexpressing the integral in this fashion, if we regard the singularity as an ambiguity in the inverse Borel transform, which is well-defined in the full theory, although not in perturbation theory alone. We imagine that the Borel transform is well approximated by perturbation theory up to $b' = 1/b_2$. Although the perturbative integral is not well-defined beyond this point, the integrand is already suppressed at $b' = 1/b_2$ by a factor $\exp[-8\pi/b_2\alpha_s(Q^2)] = (\Lambda^2/Q^2)^2$. Thinking back to the operator product expansion, eq. (198), we recognize that this is the power corresponding to the gluon condensate, the vacuum expectation of the operator F^2 . Perturbation theory itself thus signals its own incompleteness by generating an infrared renormalon ambiguity at precisely the leading nonperturbative power of the operator product expansion (at zero quark mass, in this approximation).

It is a widely accepted viewpoint that the correct way to treat the perturbative expansion is to *define* perturbation theory by regulating the inverse Borel transform in such a way that it introduces a new nonperturbative parameter that may be associated with the vacuum expectation value $\langle 0|F^2|0 \rangle$. The theory in principle then gives a consistent picture of the function Π up to corrections of order Q^{-6} relative to the leading power, and up to the next uncalculated order in perturbation theory [71].

The above discussion has brought us to the threshold of nonperturbative physics, which we cannot expect to cross without nonperturbative methods. In closing, we may note that infrared renormalons appear not only in the total cross section for e^+e^- annihilation, but in many other cross sections as well. They are particularly interesting in resummed cross sections, where we have seen integrals over running couplings, analogous to those just encountered, appear in the organization of large corrections [72]. It is natural to ask whether here, as above, perturbation theory is signalling a new set of nonperturbative parameters, which probably cannot be reduced to the operator product expansion. The full answer to this intriguing question is not, to my knowledge, available at present.

Acknowledgements

It is a pleasure to express my appreciation to the TASI 95 Organizing Committee, and to its General Director K.T. Mahhanthapa and Program Director, Dave Soper. I would like to thank as well the TASI Scientific Advisory Committee, for their choice of quantum chromodynamics as the central theme of the 1995 school, which made it possible to explore the topics presented

here at a depth that would not otherwise have been possible. I am truly indepted to Ms. Linda Freuh for her expert assistance at Boulder.

The treatment above on Sudakov resummation grew out of discussions with Harry Contopanagos and Eric Laenen, and of small- x resummation out of discussions with Michael Sotiropoulos. To Gregory Korchemsky, I would like to express my appreciation for many conversations during the months leading to the school, which profoundly influenced my presentations there. Many other insights expressed above are due, directly or indirectly, to exchanges in recent years with Lyndon Alvero, Stan Brodsky and Anatoly Radyushkin, and with my colleagues in the CTEQ Collaboration, especially John Collins, Jianwei Qiu, Jack Smith and Dave Soper.

Finally, I wish to thank the students of TASI 95, for their interest and challenging questions, and for bringing their own research experience to bear on these lectures, which acquired as a result a sense of dialogue.

This work was supported in part by the National Science Foundation under grant PHY-9309888.

Appendix A. Color Matrix Identities and Invariants

I will review in this appendix a few of the group identities useful for elementary perturbative calculations in QCD. The “defining” generators $T_a^{(F)}$ are $N^2 - 1$ $N \times N$ traceless hermitian matrices, while the generators $T_a^{(A)}$ are defined by the $SU(N)$ structure constants C_{abc} , through

$$(T_a^{(A)})_{bc} = -iC_{abc} . \quad (209)$$

In representation R , the generators satisfy the trace normalization

$$\text{Tr} [T_a^{(R)} T_b^{(R)}] = T_R \delta_{ab} , \quad (210)$$

where for the defining (quark) and adjoint (gluonic) representations

$$\begin{aligned} T_F &= \frac{1}{2} \\ T_A &= N . \end{aligned} \quad (211)$$

The generators also give rise to invariants C_R ,

$$\sum_{a=1}^{N^2-1} (T_a^{(R)})^2 = C_R I, \quad (212)$$

with I the identity matrix. For the defining and adjoint representations, these are

$$\begin{aligned} C_F &= \frac{N^2 - 1}{2N} \\ C_A &= N . \end{aligned} \quad (213)$$

For the defining representation, products of the generators in $SU(3)$ are given by

$$T_a^{(F)} T_b^{(F)} = \frac{1}{2} [i C_{abc} T_c^{(F)} + d_{abc} T_c^{(F)}] + \frac{1}{6} \delta_{ab} I, \quad (214)$$

with I the 3×3 identity, and the d_{abc} real and totally symmetric.

Appendix B. Time Ordered Perturbation Theory, Generalized Unitarity and the Landau Equations

Time-ordered perturbation theory (TOPT) allows a simple proof of the generalized unitarity discussed in Sec. 3.1.

Time-ordered (“old-fashioned”) perturbation theory is equivalent to the more familiar expansion in covariant “Feynman” diagrams. Schematically, for any Green function,

$$\text{Green function} = \sum_{\text{cov. graphs}} G = \sum_{\text{TO graphs}} \Gamma. \quad (215)$$

Time-ordered (TO) diagrams are topologically identical to covariant diagrams, but their vertices are ordered in time. Thus, a covariant diagram with V vertices corresponds to as many as $V!$ TO diagrams. (When a subset of these $V!$ permutations are identical, they are counted only once [11].) A TO diagram Γ consists of the integral of a product of factors, “energy denominators”, that measure the virtuality of a set of states,

$$\Gamma(p) = -i \prod_{\text{loops}} \int \frac{d^3 \ell_i}{(2\pi)^3} \prod_{\text{lines}} \frac{1}{2\omega_j(p, \ell_i)} \prod_{\text{states}} \frac{1}{E_a - S_a + i\epsilon} N(p, \ell_i). \quad (216)$$

Here the set of lines between the a th and $(a+1)$ st vertices define the “state” a . E_a is the “energy of state a ”, the total energy that has flowed into the diagram up to the a th vertex. S_a is the “on-shell” energy of state a , which is the sum of the mass-shell energies of each of the lines in a ,

$$S_a = \sum_{\substack{\text{lines } j \\ \text{in } a}} \omega_j = \sum_{j \text{ in } a} \sqrt{|\mathbf{p}_j|^2 + m_j^2}. \quad (217)$$

The factor N represents “numerator” factors from, for instance, fermion propagators and three-gluon vertices, computed with on-shell line momenta. In gauge theories, there are further technicalities and modifications associated with extra gauge propagators and self-energy diagrams, but we shall not need these subtleties here. The general form of eq. (216) is, hopefully, familiar from TOPT in nonrelativistic quantum mechanics.

The expression (216) is relatively easy to prove directly from covariant perturbation theory. The example of a scalar self-energy diagram, fig. 29 already illustrates the general pattern. In this context, TOPT emerges as the result of carrying out the energy integral(s) of the diagram

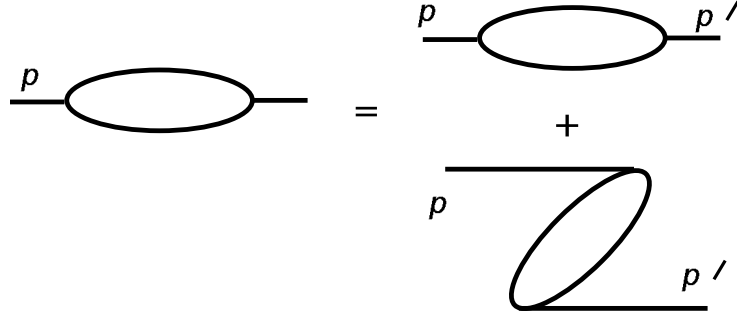


Figure 29: The two TO diagrams corresponding to the scalar self-energy.

according to a particular prescription. This consists of (i) reexpressing the energy conservation delta function at each vertex as a (time) integral of a phase, (ii) ordering the times of each vertex, and (iii) carrying out the energy integrals of each line. For the scalar self-energy, these three steps are illustrated by the following:

$$\begin{aligned}
I(p, p') &= \int_{-\infty}^{\infty} \frac{dk_0}{2\pi} \frac{1}{k_0^2 - \mathbf{k}^2 - m^2 + i\epsilon} \int_{-\infty}^{\infty} \frac{dk'_0}{2\pi} \frac{1}{k'_0{}^2 - (\mathbf{p} - \mathbf{k})^2 - m^2 + i\epsilon} \\
&\quad \times (2\pi)^2 \delta(p_0 - k_0 - k'_0) \delta(k_0 + k'_0 - p'_0), \\
&= \int_{-\infty}^{\infty} \frac{dk_0}{2\pi} \frac{1}{k_0^2 - \mathbf{k}^2 - m^2 + i\epsilon} \int_{-\infty}^{\infty} \frac{dk'_0}{2\pi} \frac{1}{k'_0{}^2 - (\mathbf{p} - \mathbf{k})^2 - m^2 + i\epsilon} \\
&\quad \times \int_{-\infty}^{\infty} d\tau_1 e^{-i\tau_1(p_0 - k_0 - k'_0)} \int_{-\infty}^{\infty} d\tau_2 e^{-i\tau_2(k_0 + k'_0 - p'_0)} \\
&= -\frac{1}{2\omega 2\omega'} \int_{-\infty}^{\infty} d\tau_1 \int_{-\infty}^{\infty} d\tau_2 e^{-i(p_0\tau_1 - p'_0\tau_2)} \left[\theta(\tau_2 - \tau_1) e^{-i(\omega + \omega')(\tau_2 - \tau_1)} \right. \\
&\quad \left. + \theta(\tau_1 - \tau_2) e^{-i(\omega + \omega')(\tau_1 - \tau_2)} \right], \tag{218}
\end{aligned}$$

where $\omega = \omega_k$ and $\omega' = \omega_{p-k}$. The expressions corresponding to the time-ordered scalar diagrams shown in fig. 29 result by carrying out the τ integrals in (218),

$$I = -i(2\pi)\delta(p_0 - p'_0) \left[\frac{1}{p_0 - \omega - \omega'} + \frac{1}{-\omega - \omega' - p_0} \right]. \tag{219}$$

It is clear that this pattern extends to all orders.

Within the TOPT formalism, generalized unitarity, represented by fig. 11 and eq. (73), is straightforward. To demonstrate fig. 11, consider the cuts of a diagram Γ with $A + 1$ vertices. Applying the energy integration procedure outlined above to the cut diagram, we generate a set of cut TOPT diagrams, in each of which a state m is on-shell, with energy denominator replaced by $\delta(E_m - S_m)$, which separates a subdiagram (states 1 to $m-1$, denoted Γ_m) computed according to eq. (216) and a subdiagram (states $m+1$ to A , denoted Γ_m^*) computed according to the complex conjugate rules. The sum over m , for a fixed relative ordering within Γ is, suppressing loop integrals and overall factors,

$$\sum_m \Gamma_m^* \Gamma_m = \sum_{m=1}^A \prod_{j=m+1}^A \frac{1}{E_j - S_j - i\epsilon} (2\pi)\delta(E_m - S_m) \prod_{i=1}^{m-1} \frac{1}{E_i - S_i + i\epsilon}, \tag{220}$$

where we have suppressed overall factors and integrals. At the same time, the imaginary part of ($-i$ times) Γ , suppressing the same factors and integrals, is

$$2\text{Im}(-i\Gamma) = -i \left[- \prod_{j=1}^A \frac{1}{E_j - S_j + i\epsilon} + \prod_{j=1}^A \frac{1}{E_j - S_j - i\epsilon} \right]. \quad (221)$$

The expressions (220) and (221) are equal, as may easily be verified by repeated use of the distribution identity

$$i \left(\frac{1}{x + i\epsilon} - \frac{1}{x - i\epsilon} \right) = 2\pi\delta(x). \quad (222)$$

The equality of (220) and (221) is equivalent to fig. 11, and holds at the level of the integrands of TOPT. The unitarity relation thus holds, as promised, for fixed spatial momentum integrals. Only the energies need be integrated.

New insights into many other theorems of perturbation theory may be found by reconsidering them in TOPT. An example is the Landau equations (51). An arbitrary TOPT diagram may, following the procedure of eq. (218) above, be written as an ordered time integral,

$$\begin{aligned} \Gamma(p) = & \int_{-\infty}^{\infty} d\tau_n \dots \int_{-\infty}^{\tau_3} d\tau_2 \int_{-\infty}^{\tau_2} d\tau_1 \prod_{\text{loops } i} \int \frac{d^3\ell_i}{(2\pi)^3} \prod_{\text{lines } j} \frac{1}{2\omega_j} \\ & \times \exp \left[-i \sum_{\text{states } a=1}^{n-1} (S_a(\ell_i) - E_a - i\epsilon)(\tau_{a+1} - \tau_a) - i(E_{\text{in}} - E_{\text{out}})\tau_n \right], \end{aligned} \quad (223)$$

where we have made the $i\epsilon$ prescription consistent with Wick rotation explicit, and have exhibited the loop integrals. The Landau equations emerge as the conditions of *stationary phase* with respect to the loop momentum variables,

$$\frac{\partial}{\partial \ell_i^\mu} \sum_a S_a(\ell_i)(\tau_{a+1} - \tau_a) = 0, \quad (224)$$

or,

$$\sum_a \sum_{\text{lines } j \text{ in } a} v_j^\mu (\tau_{a+1} - \tau_a) \epsilon_{ij}^{(a)} = 0, \quad (225)$$

where v_j is the usual relativistic velocity,

$$v_j^\mu = \frac{p_j^\mu}{\omega_j}. \quad (226)$$

$\epsilon_{ij}^{(a)}$ = +1 for ℓ_i flowing in the same sense as the momentum p_j in state a ; it equals -1 when the sense of flow is opposite with p_j in state a , and it is zero for p_j independent of ℓ_i and/or p_j not in state a . We recognize eq. (225) as the Landau equations in terms of Feynman parameters α_j , by identifying

$$\sum_{a(j \text{ in } a)} \left(\frac{\tau_{a+1} - \tau_a}{\omega_j} \right) = \alpha_j, \quad (227)$$

that is, the ratio of the total time of the states in which a particle propagates to its energy. Thus the Coleman-Norton physical process interpretation appears naturally in the context of TOPT.

Appendix C. The BFKL Kernel and Power Behavior

In this appendix, I will sketch the derivations of the BFKL kernel in eq. (185), and of the power $\omega(\nu)$ in eq. (188).

The vertex in fig. 27 is given by the combination of three-point vertex and eikonal diagrams,

$$\begin{aligned}
V_{a'ab;\nu} &= \frac{-gC_{a'ab}}{k_T^2 k_T'^2} \left[-(k' + k)_\nu g_{\mu\mu'} + (k + \ell)_{\mu'} g_{\mu\nu} - (\ell - k')_\mu g_{\mu'\nu} \right. \\
&\quad \left. + k_T'^2 \frac{q_\nu g_{\mu\mu'}}{q \cdot \ell} - k_T^2 \frac{p_\nu}{p \cdot \ell} g_{\mu\mu'} \right] \frac{q^{\mu'} p^\mu}{(s/2)}, \\
&= \frac{-gC_{a'ab}}{k_T^2 k_T'^2} \left[-(k' + k)_\nu + \frac{4\ell \cdot q}{s} p_\nu - \frac{4\ell \cdot p}{s} q_\nu \right. \\
&\quad \left. + \frac{k_T'^2}{q \cdot \ell} q_\nu - \frac{k_T^2}{p \cdot \ell} p_\nu \right] \\
&= \frac{gC_{a'ab}}{k_T^2 k_T'^2} \left[(k' + k)_{T\nu} - \left(\frac{2\ell \cdot q}{s} - \frac{k_T^2}{p \cdot \ell} \right) p_\nu \right. \\
&\quad \left. + \left(\frac{2\ell \cdot p}{s} - \frac{k_T'^2}{q \cdot \ell} \right) q_\nu \right], \tag{228}
\end{aligned}$$

where in the second equality we have used $q \cdot k \ll q \cdot \ell$ and $p \cdot k' \ll p \cdot \ell$, and in the third

$$(k + k')_\nu \sim (k + k')_{T\nu} + \frac{2\ell \cdot p}{s} q_\nu - \frac{2\ell \cdot q}{s} p_\nu. \tag{229}$$

All of these identities follow from the strong ordering assumption, eq. (177).

In the square of the real diagrams, the color factor is easily seen to give $-N$. The square of the momentum factors requires some algebra, and use of

$$\frac{4\ell \cdot q \ell \cdot p}{s} = (k - k')_T^2, \tag{230}$$

which results in the surprisingly simple relation

$$\left[(k' + k)_{T\nu} - \left(\frac{2\ell \cdot q}{s} - \frac{k_T^2}{p \cdot \ell} \right) p_\nu + \left(\frac{2\ell \cdot p}{s} - \frac{k_T'^2}{q \cdot \ell} \right) q_\nu \right]^2 = -\frac{4k_T^2 k_T'^2}{\ell_T^2}. \tag{231}$$

The real-gluon contribution to $\mathcal{F}(k')$ is then

$$\begin{aligned}
\frac{\mathcal{F}_{\text{real}}(k')}{(k_T'^2)^2} &= -Ng^2 \int \frac{d^4 \ell}{(2\pi)^4} (2\pi) \delta_+(\ell^2) \left(-\frac{4k_T^2 k_T'^2}{\ell_T^2} \right) \frac{\mathcal{F}(k)}{(k_T^2)^2 (k_T'^2)^2} \\
&= \frac{\alpha_s N}{\pi^2} \int_{k'^+}^{p^+} \frac{dk^+}{k^+} \frac{1}{k_T'^2} \int \frac{d^2 k_T}{(k_T - k_T')^2 k_T^2} \mathcal{F}(k), \tag{232}
\end{aligned}$$

which, after the redefinition $\bar{\mathcal{F}}(k) = \mathcal{F}(k)/k_T^2$, and a logarithmic derivative with respect to k'^+ , gives the first (“real gluon”) term in the kernel of eq. (185).

The virtual gluon contribution comes only from the two-eikonal diagrams of the type shown in fig. 27. In these diagrams, the eikonals play the role of the jets, and the k^- loop

integral may be closed on the pole of the lower (p) eikonal to give the logarithmic integral in k^+ . The color factor is again $-N$. The contribution to $\bar{\mathcal{F}}$ is

$$\bar{\mathcal{F}}_{\text{virtual}}(k') = -\frac{1}{2} \frac{\alpha_s N}{\pi} \int_{k'^+}^{p^+} \frac{dk^+}{k^+} \int \frac{d^2 k_T k_T'^2}{(k_T - k_T')^2 k_T^2} \bar{\mathcal{F}}(k), \quad (233)$$

which corresponds to the second term in (185).

The computation of the power $\omega(\nu)$ is reasonably straightforward in dimensional regularization. Substituting the ansatz (187) into the BFKL equation (185), we get

$$\begin{aligned} \omega(\nu) = & \frac{\alpha_s N}{\pi^2} \left[(k_T'^2)^{-i\nu+1/2} \int d^{2-2\epsilon} k_T \frac{1}{(k_T^2)^{-i\nu+1/2} (k_T - k_T')^2} \right. \\ & \left. - \frac{1}{2} k_T'^2 \int d^{2-2\epsilon} k_T \frac{1}{k_T^2 (k_T - k_T')^2} \right], \end{aligned} \quad (234)$$

in which $\epsilon = 2 - n/2$ for n dimensions. Both of these integrals have infrared divergences when the infrared regularization is removed, but their combination is finite.

We now use the identity for generalized Feynman parameterization,

$$\frac{1}{A^\alpha B^\beta} = \frac{\Gamma(\alpha + \beta)}{\Gamma(\alpha)\Gamma(\beta)} \int_0^1 dy \frac{y^{\alpha-1} (1-y)^{\beta-1}}{[yA + (1-y)B]^{\alpha+\beta}}, \quad (235)$$

which holds for complex α and β . This enables us to perform the transverse integrals by standard methods to get

$$\begin{aligned} \omega(\nu) = & \frac{\alpha_s N}{2\pi} (\pi k'^2)^{-\epsilon} \left[\frac{\Gamma(-i\nu + 1/2 + \epsilon)}{\Gamma(-i\nu + 1/2)} \int_0^1 \frac{dy y^{-i\nu-1/2}}{[y(1-y)]^{-i\nu+1/2+\epsilon}} \right. \\ & \left. - \frac{1}{2} \Gamma(1 + \epsilon) \int_0^1 \frac{dy}{[y(1-y)]^{1-\epsilon}} \right]. \end{aligned} \quad (236)$$

The y integrals now give beta functions, in which the infrared poles manifestly cancel,

$$\begin{aligned} \omega(\nu) = & \frac{\alpha_s N}{\pi} (\pi k'^2)^{-\epsilon} \left[\frac{\Gamma(-i\nu + 1/2 + \epsilon)}{\Gamma(-i\nu + 1/2)} B(-\epsilon, i\nu + 1/2 - \epsilon) \right. \\ & \left. - \frac{1}{2} \Gamma(1 + \epsilon) B(-\epsilon, -\epsilon) \right] \\ = & \frac{\alpha_s N}{\pi} (\pi k'^2)^{-\epsilon} \Gamma(-\epsilon) \left[\frac{\Gamma(-i\nu + 1/2 + \epsilon)}{\Gamma(-i\nu + 1/2)} \frac{\Gamma(i\nu + 1/2 - \epsilon)}{\Gamma(i\nu + 1/2 - 2\epsilon)} \right. \\ & \left. - \frac{1}{2} \frac{\Gamma(1 + \epsilon) \Gamma(-\epsilon)}{\Gamma(-2\epsilon)} \right]. \end{aligned} \quad (237)$$

(The factor $(k'^2)^{-\epsilon}$ is an artifact of dimensional regularization, which does not contribute to the final answer, since in $n \neq 4$ dimensions the kernel is not dimensionless.) Expanding about $\epsilon = 0$ by using

$$\Gamma(1 + \delta) = 1 + \delta\psi(1) + \dots, \quad (238)$$

we readily derive the explicit expression for $\omega(\nu)$ in eq. (188).

References

References

- [1] J.C. Collins, D.E. Soper and G. Sterman, in *Perturbative Quantum Chromodynamics*, ed. A.H. Mueller (World Scientific, Singapore, 1989), p. 1.
- [2] K.G. Wilson, Phys. Rev. **179**, 1499 (1969).
- [3] K.G. Wilson and J. Kogut, Phys. Rep. **12**, 75 (1974).
- [4] G. Sterman, and S. Weinberg, Phys. Rev. Lett. **39**, 1436 (1977).
- [5] R.P. Feynman, Phys. Rev. Lett. **23** (1969) 1415; J.D. Bjorken and E.A. Paschos, Phys. Rev. **185**, 1975 (1969).
- [6] P. Roy, *Theory of Lepton-Hadron Processes at High Energy* (Oxford University Press, Oxford, 1975); F.E. Close, *An Introduction to Quarks and Partons* (Academic Press, London, 1979).
- [7] G. Altarelli and G. Parisi, Nucl. Phys. **B126**, 298 (1977); V.N. Gribov and L.N. Lipatov, Sov. J. Nucl. Phys. **15**, 438, 675 (1972); Yu.L. Dokshitser, Sov. Phys. JETP **46**, 641 (1977).
- [8] J.C. Collins, in *Perturbative Quantum Chromodynamics*, ed. A.H. Mueller (World Scientific, Singapore, 1989), p. 573.
- [9] É.A. Kuraev, L.N. Lipatov, V.S. Fadin, Sov. Phys. JETP **45**, 199 (1977); Ya.Ya. Balitskii and L.N. Lipatov, Sov. J. Nucl. Phys. **28**, 822 (1978).
- [10] J.D. Bjorken and S.D. Drell, *Relativistic Quantum Fields* (McGraw Hill, New York, 1965); C. Itzykson and J.B. Zuber, *Quantum Field Theory* (McGraw Hill, New York, 1980); P. Ramond, *Field Theory* (Benjamin-Cummings, Reading, Mass., 1981); L.S. Brown, *Quantum Field Theory* (Cambridge University Press, Cambridge, 1992); S. Weinberg, *Quantum Theory of Fields, Vol. 1* (Cambridge University Press, Cambridge, 1995).
- [11] G. Sterman, *An Introduction to Quantum Field Theory* (Cambridge University Press, Cambridge, 1993).
- [12] F.J. Ynduráin, *Quantum Chromodynamics* (Springer-Verlag, New York, 1982). T. Muta, *Foundations of Quantum Chromodynamics* (World Scientific, Singapore, 1987).
- [13] G. Sterman, Phys. Rev. **D17**, 2773, 2789 (1978).

- [14] R.J. Eden, P.V. Landshoff, D.I. Olive and J.C. Polkinghorne, *The Analytic S-matrix* (Cambridge University Press, Cambridge, 1966).
- [15] G. Sterman, in *Perspectives in the Standard Model*, proceedings of the 1991 Theoretical Advanced Study Institute, ed. R.K. Ellis, C.T. Hill and J.D. Lykken (World Scientific, Singapore, 1992), p. 475.
- [16] R.K. Ellis, lectures at TASI 94, FERMILAB-CONF-94-410-T, Dec 1994.
- [17] G. Sterman *et al.* (CTEQ Collaboration), Rev. Mod. Phys. **67**, 157 (1995).
- [18] A.H. Mueller, ed., *Perturbative Quantum Chromodynamics*, (World Scientific, Singapore, 1989).
- [19] S.J. Brodsky and G.P. Lepage, in *Perturbative Quantum Chromodynamics*, ed. A.H. Mueller (World Scientific, Singapore, 1989), p. 93.
- [20] Yu.L. Dokshitzer, V.A. Khoze, S.I. Troian and A.H. Mueller, Rev. Mod. Phys. **60**, 373 (1988); M. Ciafaloni, Nucl. Phys. B296, **49** (1988); Yu.L. Dokshitzer, V.A. Khoze, S.I. Troian, in *Perturbative Quantum Chromodynamics*, ed. A.H. Mueller (World Scientific, Singapore, 1989), p. 241; S. Catani, F. Fiorani, G. Marchesini and G. Oriani, Nucl. Phys. **B361**, 645 (1991).
- [21] M. Ciafaloni in *Perturbative Quantum Chromodynamics*, ed. A.H. Mueller (World Scientific, Singapore, 1989), p. 491.
- [22] Yu.L. Dokshitzer, V.A. Khoze, S.I. Troian and A.H. Mueller, *Basics of Perturbative Quantum Chromodynamics* (Editions Frontières, Gif-sur-Yvette, 1991).
- [23] A. Pais, *Inward Bound* (Oxford University Press, New York, 1986).
- [24] T.-P. Cheng and L.-P. Li, *Gauge Theory of Elementary Particle Physics* (Oxford University Press, New York, 1984).
- [25] F. Halzen and A.D. Martin, *Quarks & Leptons* (John Wiley, New York, 1984).
- [26] C.N. Yang and R.L. Mills, Phys. Rev. **96**, 191 (1954).
- [27] H. Fritzsch, M. Gell-Mann and H. Leutwyler, Phys. Lett. **B47**, 365 (1973); D.J. Gross and F. Wilczek, Phys. Rev. **D8**, 3633 (1973) 3633, S. Weinberg, Phys. Rev. Lett. **31**, 494 (1973).
- [28] H.D. Politzer, Phys. Rev. Lett. **30**, 1346 (1973); D.J. Gross and F. Wilczek, Phys. Rev. Lett. **30**, 1343 (1973).

- [29] E.D. Bloom *et al.*, Phys. Rev. Lett. **23**, 930 (1969); M. Breidenbach *et al.*, Phys. Rev. Lett. **23**, 935 (1969).
- [30] J.I. Friedman and H.W. Kendall, Ann. Rev. Nucl. Part. Sci. **22**, 203 (1972).
- [31] C.G. Callan and D.G. Gross, Phys. Rev. Lett. **22**, 156 (1969).
- [32] J. Gasser and H. Leutwyler, Phys. Rep. **87**, 77 (1982).
- [33] L. Landau, Nucl. Phys. **13**, 181 (1959).
- [34] S. Coleman and R.E. Norton, Nuovo Cimento **38**, 438 (1965).
- [35] T. Kinoshita, J. Math. Phys. **3**, 650 (1962). T.D. Lee and M. Nauenberg, Phys. Rev. **133**, B1549 (1964).
- [36] G. Sterman, Phys. Rev. **D19**, 3135 (1979); G. Tiktopoulos, Nucl. Phys. **B147**, 371 (1979).
- [37] E. Farhi, Phys. Rev. Lett. **39**, 1587 (1977).
- [38] D. Catani, Yu.L. Dokshitzer, M. Olsson, G. Turnok and B.R. Webber, Phys. Lett. **B269**, 432 (1991).
- [39] J.C. Collins and D.E. Soper, Nucl. Phys. **B194**, 445 (1982).
- [40] J.F. Owens and W.-K. Tung, Ann. Rev. Nucl. Part. Sci. **42**, 291 (1992).
- [41] G. Altarelli, R.K. Ellis and G. Martinelli, Nucl. Phys. **B157**, 451 (1979); B. Humpert and W.L. van Neerven, Phys. Lett. **B84**, 327 (1979); J. Kubar-Andre and F.E. Paige, Phys. Rev. **D19**, 221 (1979); K. Harada, T. Kaneko and N. Sakai, Nucl. Phys. **B155**, 169 (1980); (E) **B165** 545.
- [42] Y. Frishman, Phys. Rep. **13**, 1 (1974).
- [43] H. Georgi, in *Perspectives in the Standard Model*, Proceedings of the 1991 Theoretical Advanced Study Institute, ed. R.K. Ellis, C.T. Hill and J.D. Lykken (World Scientific, Singapore, 1992), p. 589.
- [44] H.D. Politzer, Nucl. Phys. **B129**, 301 (1977); D. Amati, R. Petronzio and G. Veneziano, Nucl. Phys. **B140**, 54 (1978); **B146**, 29 (1978); S. Libby and G. Sterman, Phys. Rev. **D18**, 3252 (1978), *ibid* 4737 (1978); C.T. Sachrajda, Phys. Lett. **B73**, 185 (1978); R.K. Ellis, H. Georgi, M. Machacek, H.D. Politzer and G.G. Ross, Nucl. Phys. **B152**, 285 (1979); A.V. Efremov and A.V. Radyushkin, Theor. Math. Phys. **44**, 327 (1980), **44**, 664 (1981).

- [45] S.D. Drell and T.M. Yan, Ann. Phys. **66**, 578 (1971).
- [46] A.H. Mueller, Phys. Rev. **D18**, 3705 (1978).
- [47] J.C. Collins and G. Sterman, Nucl. Phys. **B185**, 172 (1981).
- [48] G.T. Bodwin, Phys. Rev. **D31**, 2616 (1985); J.C. Collins, D.E. Soper and G. Sterman, Nucl. Phys. **B261**, 104 (1985); **B308**, 833 (1988).
- [49] A.H. Mueller, Phys. Lett. **B104**, 161 (1981); B.I. Ermolaev and V.S. Fadin, JETP. Lett. **33**, 269 (1981); A. Bassetto, M. Ciafaloni, G. Marchesini and A.H. Mueller, Nucl. Phys. **B207**, 189 (1982).
- [50] A. Sen, Phys. Rev. **D24**, 3281 (1981); G.P. Korchemsky and A.V. Radyushkin, Phys. Lett. **B171**, 459 (1986).
- [51] J.C. Collins and D.E. Soper, Nucl. Phys. **B193**, 381 (1981); **B197**, 446 (1982).
- [52] S. Catani, L. Trentadue, G. Turnock and B.R. Webber, Nucl. Phys. **B407**, 3 (1993).
- [53] A.H. Mueller, Phys. Rev. **D20**, 2037 (1979); J. Kodaira and L. Trentadue, Phys. Lett. **112B**, 66 (1982); **123B**, 335 (1983).
- [54] H. Contopanagos and G. Sterman, Nucl. Phys. **B400**, 211 (1993).
- [55] J.C. Collins, D.E. Soper and G. Sterman, Nucl. Phys. **B250**, 199 (1985); G. Altarelli, R.K. Ellis, M. Greco and G. Martinelli, Nucl. Phys. **B246**, 12 (1984); C.T.H. Davies and W.J. Stirling, Nucl. Phys. **B244**, 337 (1984); C.T.H. Davies, B.R. Webber and W.J. Stirling, Nucl. Phys. **B256**, 413 (1984); P.B. Arnold and R.P. Kauffman, Nucl. Phys. **B349**, 381 (1991); G.A. Ladinsky and C.P. Yuan, Phys. Rev. **D50**, R4239 (1994).
- [56] G. Sterman, Nucl. Phys. **B281**, 310 (1987); S. Catani and L. Trentadue, Nucl. Phys. **B327**, 323 (1989); **B353**, 183 (1991).
- [57] E. Laenen, J. Smith and W.L. van Neerven, Nucl. Phys. **B369**, 543 (1992); Phys. Lett. **B321**, 254 (1994); H. Contopanagos and E.L. Berger, Phys. Lett. **B361**, 115 (1995).
- [58] G. Altarelli, N. Cabibbo, G. Corbo, L. Maiani and G. Martinelli, Nucl. Phys. **B208**, 365 (1982); A.F. Falk, E. Jenkins, A.V. Manohar and M.B. Wise, Phys. Rev. **D49**, 4553 (1994); I.I. Bigi, M.A. Shifman, N.G. Uraltsev, A.I. Vainstein, Int. J. Mod. Phys. **A9**, 2467 (1994); M. Neubert, Phys. Rev. **D49**, 3392, 4623 (1994). G.P. Korchemsky and G. Sterman, Phys. Lett. **B340**, 96 (1994); R.D. Dikeman, M. Shifman, N.G. Uraltsev, Minnesota preprint, TPI-MINN-95-9-T, May 1995, e-Print Archive: hep-ph/9505397
- [59] V. Del Duca, DESY preprint DESY 95-023, Feb. 1995, Scientifica Acta, INFN Pavia, **X**, 91 (1995), hep-ph/9503226.

- [60] A. Sen, Phys. Rev. **D27**, 2997 (1983).
- [61] S. Catani, M. Ciafaloni and F. Hautmann, Phys. Lett. **B242**, 97 (1990); Nucl. Phys. **B366**, 135 (1991); Phys. Lett. **B307**, 147 (1993); J.C. Collins and R.K. Ellis, Nucl. Phys. **B360**, 3 (1991).
- [62] P.D.B. Collins and E.J. Squires, *Regge Poles in Particle Physics*, Springer Tracts in Modern Physics, Vol. 45 (Springer-Verlag, Berlin, 1968).
- [63] A.H. Mueller and H. Navelet, Nucl. Phys. **B282**, 727 (1987).
- [64] V. Del Duca and C.R. Schmidt, Phys. Rev. **D49**, 177, 4510 (1994); W.J. Stirling, Nucl. Phys. **B423**, 56 (1994).
- [65] A.H. Mueller, Nucl. Phys. **B415**, 373 (1994); Z. Chen and A.H. Mueller, Nucl. Phys. **B451**, 579 (1995); Nikolaev, B.G. Zakharov and V.R. Zoller, Phys. Lett. **B328**, 486 (1994).
- [66] A.H. Mueller and B. Patel, Nucl. Phys. **B425**, 471 (1994).
- [67] V.S. Fadin and L.N. Lipatov, Nucl. Phys. **B406**, 259 (1993); A.R. White, Phys. Lett. **B334**, 87 (1994), C. Coriano and A.R. White, Nucl. Phys. **B451**, 231 (1995).
- [68] L.N. Lipatov, in *Perturbative Quantum Chromodynamics*, ed. A.H. Mueller (World Scientific, Singapore, 1989), p. 411; L. Lipatov, JETP Lett. **59**, 596 (1994); L.D. Faddeev and G.P. Korchemsky, Phys. Lett. **B342**, 311 (1995).
- [69] L.V. Gribov, E.M. Levin and M.G. Ryskin, Phys. Rep. **100**, 1 (1983); E.M. Levin and M.G. Ryskin, Phys. Rep. **189**, 267 (1990); J. Qiu and A.H. Mueller, Nucl. Phys. **B268**, 427 (1986); J. Qiu, Nucl. Phys. **B291**, 746 (1987); E. Laenen, E. Levin and A.G. Shuvaev, Nucl. Phys. **B419**, 39 (1994); J. Bartels, Z. Phys. **C60**, 471 (1993).
- [70] G. 't Hooft, in *The Whys Of Subnuclear Physics*, Erice 1977, ed. A. Zichichi (Plenum, New York, 1977), p. 943; B. Lautrup, Phys. Lett. **69B**, 109 (1977); G. Parisi, Phys. Lett. **76B**, 65 (1978); Nucl. Phys. **B150**, 163 (1979); Phys. Rep. **49**, 215 (1979); F. David, Nucl. Phys. **B234**, 237 (1984); Nucl. Phys. **B263**, 637 (1986); V.I. Zakharov, Nucl. Phys. **B385**, 452 (1992); M. Beneke and V.I. Zakharov, Phys. Rev. Lett. **69**, 2472 (1992).
- [71] A.H. Mueller, Nucl. Phys. **B250**, 327 (1985); in *QCD 20 Years Later*, Aachen, 1992, ed. P.M. Zerwas and H.A. Kastrup (World Scientific, Singapore, 1993) v.1, p.162.
- [72] D. Appell, P. Mackenzie and G. Sterman in *Proceedings of the Storrs Meeting*, Fourth Meeting of the Division of Particles and Fields, Storrs, CT, August 15-18, 1988, p. 567; B.R. Webber, Phys. Lett. **B339**, 148 (1994); A.V. Manohar and M.B. Wise, Phys. Lett.

B344, 407 (1995); G.P. Korchemsky and G. Sterman, Nucl. Phys. **B437**, 415 (1995); Yu.L. Dokshitzer and B.R. Webber, Phys. Lett. **B352**, 451 (1995); R. Akhoury and V.I. Zakharov, Phys. Lett. **B357**, 646 (1995); P. Nason and M.H. Seymour, Nucl. Phys. **B454**, 291 (1995); M. Beneke and V.M. Braun, Nucl. Phys. **B454**, 253 (1995).